A NMR spectroscopic study of hepatic metabolism in *Meriones unguiculatus* infected with *Echinococcus multilocularis*

By

Jodi Schoen

A thesis
submitted to the Faculty of Graduate Studies
in partial fulfillment of the requirements
for the Degree of

Master of Science

Department of Human Anatomy and Cell Science
University of Manitoba
Winnipeg, Manitoba

July, 1997

THE UNIVERSITY OF MANITOBA

FACULTY OF GRADUATE STUDIES

*****

COPYRIGHT PERMISSION PAGE

A NMR SPECTROSCOPIC STUDY OF HEPATIC METABOLISM IN *Meriones unguiculatus* INFECTED WITH *Echinococcus multilocularis*

BY

JODI SCHOEN

A Thesis/Practicum submitted to the Faculty of Graduate Studies of The University of Manitoba in partial fulfillment of the requirements of the degree of

MASTER OF SCIENCE

Abstract

Hepatic carbohydrate and lipid metabolism were studied in alveolar echinococcosis using the *Meriones unguiculatus/Echinococcus multilocularis* host/parasite model system. Carbon-13 decoupled ^{1}H spin echo NMR spectroscopy, with and without population inversion, was used to monitor [2-^{13}C]acetate metabolism in the liver of jirds infected with *Echinococcus multilocularis*. Thirty minutes after injection of labeled acetate solution into the portal vein, ^{13}C enrichment was observed in hepatic acetate, β-hydroxybutyrate, succinate, alanine, lactate and glucose. At 120 min. there was a significant decrease in the amount of label present in all these metabolites. For *E. multilocularis* cysts, 30 min. post injection of [2-^{13}C]acetate, ^{13}C enrichment was observed in the same metabolites as in the host livers and, in addition, citrate. More label was present after 120 min. in cyst glycogen, glucose, succinate, alanine and lactate, but less in acetate and β-hydroxybutyrate, than in the corresponding metabolites in the 30 min. group. The presence of ^{13}C enriched glucose in the cyst and its increase in enrichment with time strongly suggests that the parasite is siphoning off glucose that is newly synthesized by the host. Even though acetate is not normally thought of as a gluconeogenic precursor, it can end up in glucose after passing through a portion of the Kreb's cycle; this biosynthetic route is not available to the parasite. The presence of other labeled metabolites in the cysts could result from metabolism of this labeled glucose by the parasite and/or by uptake from the host.

^{1}H NMR spectroscopy was used to investigate changes in composition of hepatic lipids. It was found that livers from infected jirds had less total glycerophospholipids (GPL), phosphatidylinositol (PTI), phosphatidylcholine (PTC) and cholesterol (CTL) but more phosphatidylethanolamine (PTE) than

those of uninfected controls. Also, in infected jirds, the ratios of the $C\underline{H_2}CH=CHHC=CHC\underline{H_2}$, arachidonic acid and linoleic acid to total fatty acid all increased. The parasite contained the same lipids as the host liver, except for the absence of PTI. In general, concentrations of lipid in the cysts were lower than in the livers. Furthermore, the ratios of their unsaturated and saturated components to total FA, the degree of unsaturation (DU) of FA chains and the average FA chain length were also lower than those in the liver.

Acknowledgements

One of the many things I have learned during this degree is that no man (or woman) is an island. Scientific research is certainly no exception to this rule. There were numerous people who helped me throughout the preparation of my thesis, and I would like to thank them for their help during the research and writing processes.

First, I would like to sincerely thank Dr. Marie Novak and Dr. Barry J. Blackburn for their patience and encouragement, for giving me the opportunity to learn from them, and for never settling for second best. From you, I have learned much about science and research, and about myself.

Thank you to Ian Corbin, for your technical assistance and support for the duration of this research. I enjoyed all of our discussions, and want to thank you for being a good friend.

To Terry Wolowiec I would like to say thank you for your technical assistance, for all those discussions on NMR and for your friendship.

Also, thank you to Ashok Modha, Kenny Maslow, Rachael Simcoff and Charis Kepron for your assistance throughout this research. All of you have contributed to the positive experience that this degree has been for me.

I would like to thank my evaluation committee members Dr. Jim Peeling and Dr. Judy Anderson for their valuable suggestions and for their patience throughout the entire thesis.

To the Department of Anatomy and Cell Sciences, I would like to say thank you for the financial support which enabled me to attend out of town conferences and for the teaching opportunities in the Gross Human Anatomy (Medicine and Pharmacy) labs.

I must also thank my Mom and Dad for their love, support and patience over the last three years. Without it, this time would have been much more difficult for me.

Last, but centainly not least, thank you to my friends, especially Laura McIntosh, Sheryl Hnylycia and Lori Wazny, for your assistance and support throughout this degree. I am very fortunate to have had your input, and would like to thank you for your friendship.

Every one of you has contributed to the invaluable knowledge and experience I have gained over the last three years. I deeply appreciate all that everyone has done for me throughout the research and writing of this thesis.

Table of Contents

	Page
Abstract	i
Acknowledgements	iii
Table of Contents	v
List of Figures	vi
List of Tables	vii
List of Abbreviations	viii
Hypothesis	xi
Introduction	
I. Parasite	1
II. Host carbohydrate metabolism	10
III. Host lipid metabolism	17
Materials and Methods	
I. Carbohydrate metabolism	32
II. Lipid metabolism	35
Results	
I. Carbohydrate metabolism	39
II. Lipid metabolism	48
Discussion	
I. Carbohydrate metabolism	58
II. Lipid metabolism	78
III. Future research	90
References	94

List of Figures

	Page
Figure 1: Life cycle of *Echinococcus multilocularis*.	3
Figure 2: Pulse sequence for ^{13}C decoupled ^{1}H spin echo NMR spectroscopy.	15
Figure 3: Structure of some common fatty acid.	19
Figure 4: Structure of membrane glycerophospholipids.	24
Figure 5: Pathways of glycerophospholipid metabolism in mammals.	26
Figure 6: ^{13}C decoupled ^{1}H spin echo NMR spectrum of a PCA extract of uninfected *M. unguiculatus* liver, 30 minutes after injection of [2-^{13}C]acetate.	40
Figure 7: ^{13}C decoupled ^{1}H spin echo NMR spectrum of a PCA extract of *E. multilocularis* cyst, 30 minutes after injection of [2-^{13}C]acetate into the host.	43
Figure 8: ^{1}H NMR spectrum of a C:M extract of uninfected *Meriones unguiculatus* liver.	49
Figure 9: ^{1}H NMR spectrum of a C:M extract of *Echinococcus multilocularis* cyst.	55
Figure 10: The fate of carbon-13 label from [2-^{13}C]acetate in intermediates of the Kreb's cycle.	59
Figure 11: The fate of carbon-13 label from [2-13C]acetate in metabolites of gluconeogenesis.	63
Figure 12: Metabolism of labeled glucose in *Echinococcus multilocularis* cysts.	67
Figure 13: Pathways of phosphatidylcholine synthesis in mammals.	74
Figure 14: Peroxidation of fatty acids.	87

List of Tables

Page

Table 1: Concentrations of metabolites from livers of uninfected and infected *Meriones unguiculatus*, and from *Echinococcus multilocularis* cysts, 30 minutes after introduction of [2-^{13}C]acetate into the host. 42

Table 2: Concentrations of metabolites from livers of uninfected and infected *Meriones unguiculatus*, and from *Echinococcus multilocularis* cysts, 120 minutes after introduction of [2-^{13}C]acetate into the host. 46

Table 3: Percent carbon-13 in metabolites from livers of uninfected and infected *Meriones unguiculatus*, and from *Echinococcus multilocularis* cysts, after introduction of [2-^{13}C]acetate into the host. 47

Table 4: Concentrations of lipid from livers of uninfected and infected *Meriones unguiculatus*, and from *Echinococcus multilocularis* cysts. 52

Table 5: Analysis of fatty acid components in livers from uninfected and infected *Meriones unguiculatus*, and from *Echinococcus multilocularis* cysts. 53

List of Abbreviations

ATP = adenosine triphosphate

β-HB = β-hydroxybutyrate

cAMP = cyclic adenosine monophosphate

CDP = cytidine diphosphate

CFT = complement fixation test

C:M = chloroform:methanol

CMP = cytidine monophosphate

CoA = coenzyme A

CT = computerized tomography

CTL = cholesterol

CTP = cytidine triphosphate

DG = diacylglycerol

DHAP = dihydroxyacetone phosphate

DU = degree of unsaturation

E. multilocularis = *Echinococcus multilocularis*

ELISA = enzyme-linked immunosorbent assay

ER = endoplasmic reticulum

F-1,6-BP = fructose-1,6-bisphosphate

F-6-P = fructose-6-phosphate

FA = fatty acid

G-3-P = glycerol-3-phosphate

G-6-P = glucose-6-phosphate

GAP = glyceraldehyde -3-phosphate

GPC = glycerophosphocholine

GPE = glycerophosphoethanolamine

GPL = glycerophospholipid

GSH = glutathione, oxidized form

GSL = glycosphingolipid

GSSH = glutathione, reduced form

GTP = guanosine triphosphate

HMG CoA = β-hydroxy-β-methylglutaryl CoA

IDL = intermediate density lipoprotein

IHA = indirect hemagglutination test

IIF = indirect immunofluorescence test

LDL = low density lipoprotein

LPA = lysophosphatidic acid

LPC = lysophosphatidylcholine

LPE = lysophosphatidylethanolamine

LT = leukotrienes

M. unguiculatus = *Meriones unguiculatus*

M. vogae = *Mesocestoides vogae*

MDH = malate dehydrogenase

MRI = magnetic resonance imaging

$NAD^+/NADH + H^+$ = nicotinamide adenine dinucleotide

$NADP^+/NADPH + H^+$ = nicotinamide adenine dinucleotide phosphate

NMR = nuclear magnetic resonance

PC = phosphocholine

PCA = perchloric acid

PCr/Cr = phosphocreatine/creatine

PE = phosphoethanolamine

PEMT = phosphatidylethanolamine *N*-methyltransferase

PEP = phosphoenolpyruvate

PEPCK = phosphoenolpyruvate carboxykinase

PG = prostaglandin

p.i. = post infection

PS = prostacyclin

PTA = phosphatidic acid

PTC = phosphatidylcholine

PTE = phosphatidylethanolamine

PTI = phosphatidylinositol

PTS = phosphatidylserine

rf = radiofrequency

TG = triacylglycerol

TX = thromboxanes

US = ultrasonography

VLDL = very low density lipoprotein

Hypothesis

Infection of *Meriones unguiculatus* with *Echinococcus multilocularis* alters carbohydrate and lipid metabolism in the host liver.

Introduction

I. Parasite

Echinococcus multilocularis is an obligate endoparasite of the class Cestoda. First described in 1863 by Leuckart, the larval stage of *E. multilocularis* was thought to be an adapted variation of the metacestode of the well known parasite *Echinococcus granulosus*. However, morphological and biological studies by Vogel in 1955 and 1957 investigating the complete life cycle of *E. granulosus* and *E. multilocularis*, respectively, confirmed the existence of two individual parasitic species (Gottstein, 1993; Tornieporth and Disko, 1994). Of these two species, *E. granulosus* is cosmopolitan, while *E. multilocularis* is endemic to the northern hemisphere only. Incidences of *E. multilocularis* infection have been reported in areas such as Austria, France, Switzerland, Germany, the United Kingdom, China, Japan, Russia, Canada and the United States - including Alaska (Lukashenko, 1971; Rausch *et al.*, 1986; Stehr-Green *et al.*, 1988; Deblock *et al.*, 1989; Petavy *et al.*, 1990; Cook, 1991; Craig *et al.*, 1992; Okamoto *et al.*, 1992; Gottstein, 1993; Lee *et al.*, 1993; Storandt and Kazacos, 1993; Tornieporth and Disko, 1994). In North America *E. multilocularis* infection in animals has been mainly detected in North and South Dakota, Minnesota, Wyoming, Montana, Iowa, Illinois, Wisconsin, Nebraska, Indiana, Ohio, Alberta, Saskatchewan and Manitoba (Bartel *et al.*, 1992; Schantz, 1993; Storandt and Kazacos, 1993) while cases of human infection have been reported only in Alaska (Wilson and Rausch, 1980; Gottstein, 1993). The parasite survives in these regions as appropriate hosts co-habitate in an existing predator-prey relationship essential for the *E. multilocularis* life cycle.

The complete life cycle of *E. multilocularis* (Figure 1) involves two mammalian hosts (Kamya and Sato, 1990). The adult tapeworm is found in the small intestine of the definitive host, usually a fox or domestic dog or cat. However, the larval form, or cyst, primarily invades the liver of the intermediate host, usually a small rodent or vole. Infection of the definitive host occurs when this host ingests an intermediate host containing infective cysts. These contain many protoscolices which, in the stomach of the definitive host, are liberated from cyst tissue. In the small intestine each protoscolex attaches to the intestinal wall and develops into a hermaphroditic adult tapeworm. The mature worm is 1.2 to 3.7 mm in length and possesses 3 to 5 segments, or proglottids (Schmidt and Roberts, 1989; Tornieporth and Disko, 1994). Egg production usually starts after 28 to 35 days. They are released in gravid proglottids into the environment in the faeces of the definitive host (Thompson, 1986; 1995). These eggs, each containing an embryo called an oncosphere, are extremely resistant to variable environmental conditions. When a suitable intermediate host ingests viable eggs, the shell and the protective covering, called an embryophore, are digested away enzymatically in the stomach and small intestine, liberating and activating the oncosphere (Thompson, 1986; 1995; Tornieporth and Disko, 1994). The activated oncosphere penetrates the gut wall and reaches the liver via mesenteric blood vessels. Once in the liver, the oncosphere develops into a hydatid cyst, the larval form of this parasite. The cyst, at first unilocular, soon develops a multilocular vesicular structure characteristic to *E. multilocularis* (Ohbayashi, 1993). The vesicular wall contains two layers of tissue: an inner cellular germinative layer and an outer non-cellular laminated layer. Unlike *E. granulosus*, vesicles of *E. multilocularis* have no adventitial layer external to the laminated layer to act as a limiting host-tissue barrier (Thompson, 1986, 1995). As these vesicles grow, the germinal layer

Figure 1

Life cycle of *Echinococcus multilocularis*

I. Adult worm in the small intestine of a fox.

II. Eggs passed with faeces and eaten by rodent intermediate host.

III. In liver, the oncosphere develops into a multilocular cyst.

The life cycle is completed when a fox eats the infected rodent.

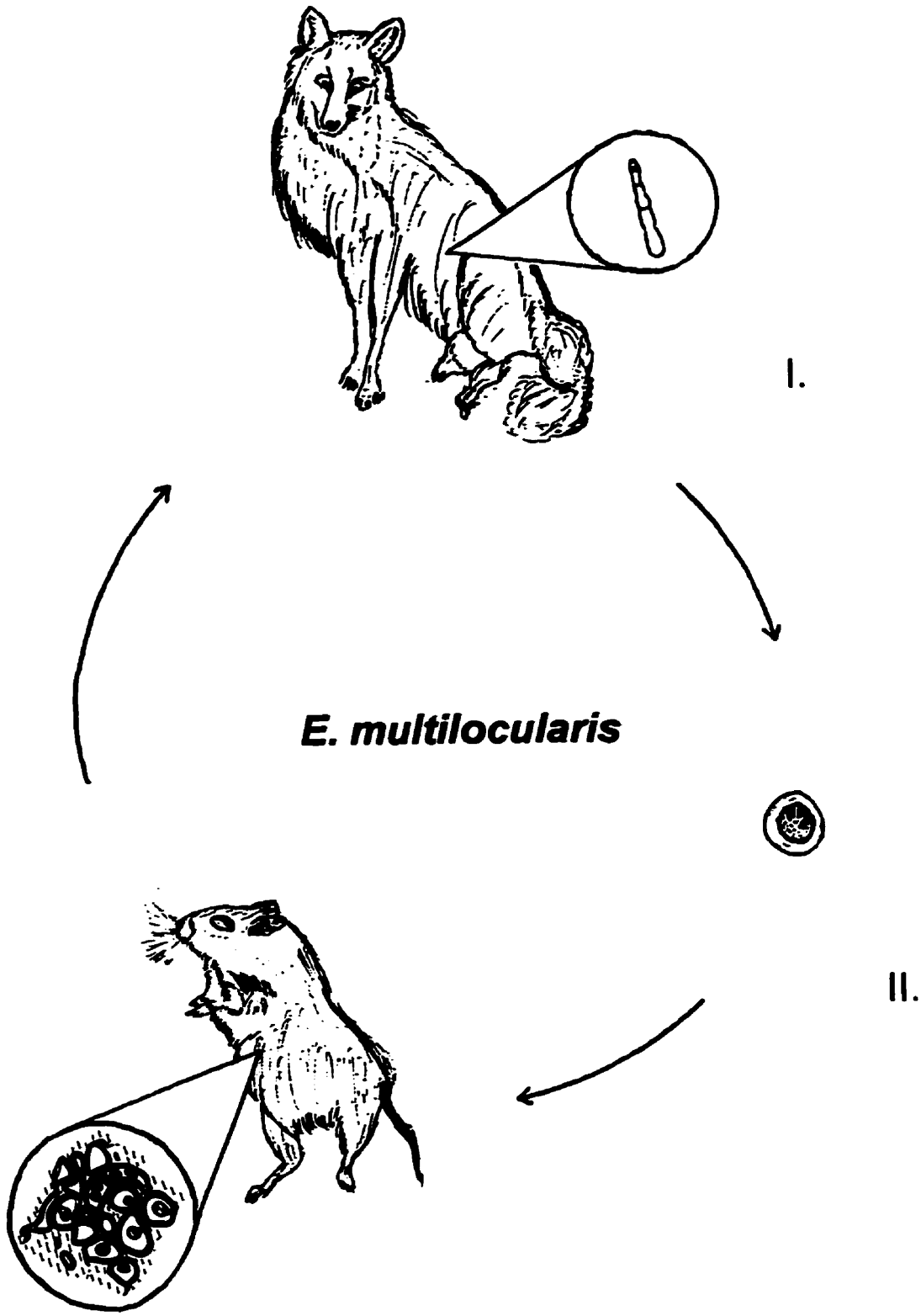
I.
E. multilocularis
II.
III.

invaginates into the central matrix, creating a stalked vesicular protrusion. From undifferentiated germinal cells in the wall of the protruding vesicle, protoscolices, the precursors of infective *E. multilocularis* scolices, begin to develop. This production of protoscolices usually takes place 2 to 5 months after infection, depending on the type of the intermediate host (Gottstein, 1993; Tornieporth and Disko, 1994). When fully developed, each protoscolex is equipped with two rows of hooks and four suckers. The invaginated vesicles, containing numerous protoscolices, are called brood capsules (Thompson, 1986, 1995; Leduq and Gabrion, 1992).

Protoscolex development, however, does not occur in all infections. In humans, for example, growth of the larval mass occurs as described above, but protoscolices rarely develop (Rausch and Wilson, 1973; Fujioka *et al.*, 1993; Ammann and Eckert, 1995). This is because humans are not a natural intermediate host of this parasite, but are abnormal, accidentally infected hosts. It is suspected that a major source of infection for humans may be domestic dogs (Lukashenko, 1971; Stehr-Green *et al.*, 1988; Rausch *et al.*, 1990) or foxes. Mature *E. multilocularis* eggs passed in the faeces of the definitive host can contaminate vegetables or berries, and be accidentally ingested by an unsuspecting human. The infection usually goes unnoticed for some time, as the initial stage of alveolar hydatid disease is slow and asymptomatic. This asymptomatic stage can last as long as 10 years after infection (Kasai *et al.*, 1980; Stehr-Green *et al.*, 1988; Sato *et al.*, 1993a). However, when symptoms do develop, correct diagnosis is difficult. Symptoms of alveolar hydatid disease, initially mild and vague, can be attributed to numerous other maladies. They usually include upper right quadrant abdominal pain and an intermittent low grade fever. As the disease progresses, the patient may experience a palpable abdominal mass, gradual distention of the abdomen, increasing weight loss and

shortness of breath. In severe cases, there is often massive hepatomegaly, ascites, jaundice and portal hypertension (Kasai *et al.*, 1980; Wilson and Rausch, 1980; Taneja *et al.*, 1990). The disease can be further complicated, as the parasitic cyst, which grossly resembles a hepatic carcinoma, is also capable of metastasis. As the cyst grows, the thin outer laminar layer breaks and the surrounding host tissue is invaded by tiny protrusions of the parasitic germinal layer. Detachment of germinal cells from these infiltrating cellular protrusions and their subsequent distribution by lymph or blood can give rise to distant metastatic foci (Ali-Khan *et al.*, 1983; Thompson, 1986; 1995). These secondary foci of infection are often found in the lungs, brain, diaphragm, mediastinum, adjacent mesenteries and organs, and even bone (Miskovitz and Javitt, 1980; Wilson and Rausch, 1980; Taneja *et al.*, 1990; Gottstein, 1993).

From initial infection, through metastasis of the cyst, the host's immune system attempts to overcome the parasitic invasion. As in other helminthic infections, in human alveolar echinococcosis there is an elevation in the level of IgE antibody (Vuitton *et al.*, 1988; Gottstein, 1993). In addition, Playford and co-workers (1992) demonstrated that interaction between the parasite and host T-lymphocytes, macrophages, and possibly granulocytes, plays a role in host resistance to *E. multilocularis* metacestode infection. Some more resistant hosts are able to overcome the parasitic infection, while others are not as successful (Playford *et al.*, 1993). In the susceptible intermediate host, neither inflammatory reaction, involving neutrophils, macrophages and eosinophils, nor production of antibodies have a direct role in limiting the growth of the cyst mass (Ali-Khan and Siboo, 1980; Treves and Ali-Khan, 1981; Alkarmi and Behbehani, 1989; Gottstein, 1993). During the initial (or restrictive) phase, cyst growth is slow suggesting that the host immune system is able to control the growth of the parasite. However, the larval cestode slowly overcomes host defenses and

enters the invasive (or progressive) growth phase which is characterized by a rapid, exponential increase in cyst size and metastasis of the cyst mass (Alkarmi and Behbehani, 1989; Kizaki *et al.*, 1991). The parasite accomplishes this through the functional modification of host T-lymphocytes and macrophages, thereby successfully avoiding the host's immune defenses (Rakha *et al.*, 1991; Gottstein *et al.*, 1993).

Modern methods used in the detection of *E. multilocularis* infection are most frequently a combination of imaging and immunodiagnostic techniques. Imaging methods, which are rather unspecific, include ultrasonography (US) and computerized tomography (CT). In addition, preoperative evaluation of hepatic vascular status, as well as future diagnoses, may be made by magnetic resonance imaging (MRI) (Ogasawara *et al.*, 1993; Tornieporth and Disko, 1994; Thompson, 1995). More precise immunodiagnostic tests include the complement fixation test (CFT), the indirect hemagglutination (IHA) test, the indirect immunofluorescence (IIF) test and the enzyme-linked immunosorbent assay (ELISA) test. These tests are based on the detection of humoral or cellular immune responses of the host against the parasite. The most widely used diagnostic test is the ELISA one, which can differentiate between *E. multilocularis* and other larval echinococcal infections. The ELISA test uses the host antibody to the *E. multilocularis*-specific antigen Em2 in initial and recurrent diagnoses of alveolar hydatid disease (Gottstein *et al.*, 1989; Tornieporth and Disko, 1994; Thompson, 1995). However, it is not known how soon after infection antibodies first appear (Kumagai, 1993).

Once alveolar echinococcosis has been diagnosed, treatment of this infection can begin. Preferred treatment of alveolar echinococcosis is complete surgical resection, usually in conjunction with chemotherapy (Wilson and Rausch, 1980; Uchino *et al.*, 1993). If the cyst is inoperable, chemotherapy may

be utilized in an attempt to slow or arrest the growth of the parasite. At present, benzimidazole carbamates are preferred drugs for treatment of hydatid disease (Ersahin *et al.*, 1993; Uchino and Sato, 1993; Thompson, 1995). These compounds block glucose absorption by the parasite, and, if given at appropriate concentrations, inhibit growth of the cyst (Sato *et al.*, 1993b; Erzurumlu *et al.*, 1995). Of all benzimidazole carbamates tested, albendazole is the most effective. The drug arrests cell proliferation of the parasite (Morris and Smith, 1987; Rolin *et al.*, 1989; Wilson *et al.*, 1992; Sato *et al.*, 1993b), and modifies its metabolism (Modha *et al.*, 1997). Experiments showed that the cysts from albendazole treated jirds contained less glycogen, glycine, succinate, acetate and alanine, but more taurine, GPC and PCr/Cr than those from untreated animals. It was hypothesized that these albendazole-induced changes were probably due to inhibition of key metabolic enzymes and ATP-ases, dissipation of the mitochondrial transmembrane proton gradient and changes in intracellular osmolarity in the tissue of the parasite.

The *E. multilocularis* metacestode is capable of both anaerobic and aerobic metabolism. The parasite catabolizes glucose to pyruvate via glycolysis in the classical ten step pathway observed in mammals. There are two types of anaerobic energy metabolism in tapeworms: homolactic fermentation and malate dismutation, both of which occur in *E. multilocularis* (Smyth and McManus, 1989). In homolactic fermentation, glucose is dissimilated to phosphoenolpyruvate (PEP) and then dephosphorylated to pyruvate by pyruvate kinase (PK), as in glycolysis. However, the pyruvate is then anaerobically reduced to lactate by lactate dehydrogenase. The lactate is then excreted (Smyth and McManus, 1989). Also, for malate dismutation, malate is formed either from pyruvate, which enters the mitochondrion and is converted first to oxaloacetate and then malate by malic enzyme and malate dehydrogenase

respectively, or from PEP which is converted to oxaloacetate by PEPCK and then to malate via cytosolic malate dehydrogenase. This malate is then transported across the inner mitochondrial membrane. In the mitochondrial matrix, the malate is either converted back to pyruvate by malic enzyme or into fumarate by fumarase. Once pyruvate has been formed, the pyruvate dehydrogenase complex catalyzes its transformation to acetyl CoA. This acetyl CoA is then hydrolyzed to acetate, with concomitant production of ATP, and the acetate is excreted (Kohler, 1985; Smyth and McManus, 1989). Fumarate reductase accepts reducing equivalents, either NADH or NADPH, and catalyzes the reaction of fumarate to succinate, also producing ATP (Smyth and McManus, 1989). The succinate is then excreted. Alanine, another end product of glucose dissimilation, is thought to be formed from the transamination of pyruvate (Prescott and Campbell, 1965; Blackburn *et al.*, 1986; McManus and Bryant, 1995). Energy may also be generated by substrate level phosphorylation using the electron transport chain (McManus and Bryant, 1995). Although evidence for all Kreb's cycle enzymes in *E. multilocularis* has been reported (McManus and Smyth, 1982), it is not clear to what extent the cycle functions. Also, mammals use β-oxidation of lipids, stored as fat, in energy metabolism, whereas cestodes do not have a functioning β-oxidation pathway. Instead, lipids are used mostly as major cell membrane components and in enzyme regulation, cell surface recognition, cell interaction and in membrane transport. Some lipids are also used in the electron transport chain while others are highly antigenic (Smyth and McManus, 1989; McManus and Bryant, 1995). Cestodes obtain all lipid moieties from their hosts, through a mixture of diffusion and mediated transport, and are restricted to modification only of these molecules through a chain lengthening process involving the sequential addition of acetyl CoA (Smyth and McManus, 1989).

II. Host carbohydrate metabolism

As alveolar hydatid disease progresses, *E. multilocularis* successfully competes with its host for essential nutrients, inducing starvation conditions in the host (Novak *et al.*, 1989; 1993). Normally, glycogen stored in the liver and in muscle tissue can only supply body functions for half a day (Guyton, 1991). Therefore, in an effort to maintain host blood glucose levels, the gluconeogenic precursors lactate, alanine and other amino acids, and glycerol are used to synthesize glucose during prolonged starvation. Lactate, alanine and some amino acids such as glycine, serine, threonine and tryptophan, are converted to pyruvate which then enters the gluconeogenic pathway, while other amino acids including glutamate, glutamine, arginine, histidine and proline can enter the pathway at oxaloacetate (Mathews and van Holde, 1990; Voet and Voet, 1995). Generated glucose is then either used in host energy metabolism via glycolysis, the Kreb's cycle and substrate level phosphorylation, or siphoned off by the parasite for use in its own energy generating pathways. It has been hypothesized (Novak *et al.* 1995) that, in an effort to compensate for glucose loss to the parasite, gluconeogenesis is increased in infected hosts, and that gluconeogenic precursors of both host and parasite origin are utilized for glucose synthesis. Precursors of parasite origin include the metabolic end products alanine, lactate, succinate and acetate, which are excreted into the host. Alanine and lactate enter directly into the gluconeogenic pathway via conversion to pyruvate, while succinate and acetate, compounds not normally considered to be substrates for gluconeogenesis, can be used "indirectly" in this process through initial entry into the Kreb's cycle, and exit at malate or oxaloacetate.

To follow up on this information, I became interested in studying the metabolic fate of acetate in the liver of a host infected with *E. multilocularis*. In mammalian metabolism, under normal conditions, acetate is present as the product of β-oxidation of fatty acids (FAs) and from exogenous dietary sources (Pethick *et al.*, 1981). Free acetate, which is initially converted to acetyl CoA through the action of acetyl CoA synthase (Crabtree *et al.*, 1990), is then metabolized in the liver and in extrahepatic tissues such as muscle, heart and brain (Lundquist, 1962; Karlsson *et al.*, 1975; Pethick *et al.*, 1981; Malloy *et al.*, 1988; Badar-Goffer *et al.*, 1990; Petersen and Grunnet, 1993). This acetyl CoA has three metabolic fates: utilization in hepatic lipid synthesis, aerobic oxidation by Kreb's cycle in the liver and extrahepatic tissues or participation in ketogenesis in the liver only. It is unlikely that a significant amount of acetyl CoA will be incorporated into lipids in a starving host. Instead, the metabolism will most probably be oriented toward energy generation through oxidation of acetyl CoA in the Kreb's cycle and through ketogenesis.

Oxidation of acetyl CoA in the Kreb's cycle takes place in the mitochondria. Acetyl CoA enters the Kreb's cycle by combining with oxaloacetate via citrate synthase to form citrate. Isocitrate is then formed from this citrate through the action of aconitase. Carbon-6 of isocitrate is lost as CO_2 when isocitrate dehydrogenase converts this metabolite to α-ketoglutarate. A second CO_2 is released by decarboxylation of α-ketoglutarate by α-ketoglutarate dehydrogenase to produce succinyl CoA. When succinyl CoA synthetase converts succinyl CoA to succinate, CoA is lost and one molecule of GTP is generated. Succinate dehydrogenase then converts succinate to fumarate, which is then converted to malate via fumarase. Malate dehydrogenase then catalyzes the reaction interconverting malate and oxaloacetate in the mitochondria. With regeneration of oxaloacetate, the Kreb's cycle can undergo

another turn. The reducing equivalents NADH + H^+ are generated at the isocitrate to α-ketoglutarate and α-ketoglutarate to succinyl CoA steps while $FADH_2$ is generated at the succinate to fumarate step. Both NADH + H^+ and $FADH_2$ are then used in the electron transport chain to produce additional high energy phosphate compounds (Alberts *et al.*, 1989; Mathews and van Holde, 1990; Voet and Voet, 1995).

Under normal nutritional conditions, small quantities of the ketone bodies acetoacetate and β-hydroxybutyrate (β-HB) are produced primarily in the liver mitochondria via ketogenesis (Guyton, 1991). First, two acetyl CoA molecules condense to form acetoacetyl CoA, catalyzed by acetyl CoA acetyltransferase. An additional acetyl CoA is then required for the conversion of acetoacetyl CoA to β-hydroxy-β-methylglutaryl CoA (HMG CoA) via hydroxymethylglutaryl CoA synthase (HMG CoA synthase). This enzyme is present only in liver (Mathews and van Holde, 1990). The HMG CoA is then converted to acetoacetate and acetyl CoA by HMG CoA lyase. This acetoacetate may then be either reduced to β-HB by β-HB dehydrogenase or undergo spontaneous decarboxylation to form small amounts of acetone, which is mostly blown off with expired air (Guyton, 1991; Voet and Voet, 1995). However, when acetyl CoA accumulates beyond its capacity to be either oxidized in the Kreb's cycle or used in fatty acid synthesis, or under conditions associated with a high rate of fatty acid oxidation such as starvation, the liver mitochondria produce considerable quantities of these ketone bodies. Eventually, ketone bodies accumulate, and their concentration becomes greater than that of available glucose. Under these conditions, ketone bodies begin to be used in metabolism, reducing the need for gluconeogenesis and sparing muscle protein which would otherwise be mobilized (Murray *et al.*, 1988; Mathews and van Holde, 1990).

These ketone bodies are subsequently transported by the blood to cells in the rest of the body, where they are used in energy synthesis (Mathews and van Holde, 1990; Guyton, 1991). Although ketone bodies are synthesized in the liver, they may not be used in hepatic energy generating pathways. This is because the liver lacks 3-ketoacyl CoA transferase, an essential enzyme for conversion of acetoacetate to acetoacetyl CoA. This enzyme is present, however, in extrahepatic tissues. Thus, acetoacetate and β-HB are released by the liver and used as alternative fuels in peripheral tissues such as heart and skeletal muscle, and in the brain during starvation (Mathews and van Holde, 1990; Guyton, 1991). Oxidation of ketone bodies begins by conversion of β-HB to acetoacetate by β-HB dehydrogenase. Coenzyme A is donated to acetoacetate by succinyl CoA, a reaction catalyzed by 3-ketoacyl CoA transferase, producing succinate and acetoacetyl CoA. The acetoacetyl CoA is catabolized, via thiolase, to two molecules of acetyl CoA which can then be oxidized through entry into the Kreb's cycle, generating energy for the cell (Mathews and van Holde, 1990; Voet and Voet, 1995).

In order to monitor the utilization of acetate in biochemical pathways of glucose synthesis, I introduced carbon-13 labeled acetate into the infected host and followed the movement of labeled atoms through intermediate metabolites in gluconeogenic pathways by employing nuclear magnetic resonance (NMR) techniques. In general, NMR is concerned with the interaction between an oscillating magnetic field and the net magnetization of a sample. This net magnetization originates from the arrangement of its constituent nuclei and is brought about by the application of a static magnetic field (Derome, 1987). Single radiofrequency (rf) pulse ^{1}H NMR is routinely used to determine structure and conformation of molecules and quantitatively analyze mixtures. In addition, this technique can non-invasively measure the reaction rates of chemical

systems *in vivo*, in intact living organisms, and *in vitro* in a NMR tube (Petroff, 1988). Although relatively insensitive compared to other analytical techniques, NMR has the advantage of being non-invasive and non-destructive (Liebfritz, 1996). In order to detect and measure the conversion of ^{13}C labeled acetate into labeled products, I used ^{13}C decoupled ^{1}H NMR spin echo spectroscopy acquired with, and without, ^{13}C population inversion. This technique is a modification of the standard ^{1}H single pulse NMR experiment, and is useful because it combines the greater sensitivity of ^{1}H, relative to ^{13}C, NMR in doing carbon-13 labeled tracer studies (Derome, 1987).

The phenomenon of spin echoes was first discovered by Hahn (1950). He found that when one rf pulse was applied at time 0 followed by a second at time τ, a "spin echo" pulse was generated at time 2τ even though the signal had decayed to zero during the intervening period. Hahn described this phenomenon only for a 90^{o} pulse system, while Carr and Purcell later developed a pulse sequence involving a combination of 90^{o} and 180^{o} pulses (Derome, 1987). A modified Carr-Purcell pulse sequence was used in my research as follows:

$$90^{o} \text{ --- } \tau \text{ --- } 180^{o} \text{ --- } \tau \text{ --- acquire}$$

$$\text{where } \tau = 1 / 2J_{CH}$$

This pulse sequence, pictured in Figure 2, represents one of the two spin echo experiments carried out on all carbohydrate samples. The 90^{o} rf pulse displaces the proton net magnetization in the sample 90^{o} from the direction of the external magnetic field, which is in the direction of the z axis. A delay, τ, allows the proton spin vectors to relax and fan out through 90^{o} in the y plane until they are precessing along the x axis. The 180^{o} pulse then inverts the

Figure 2

Pulse sequence for ^{13}C decoupled ^{1}H spin echo NMR spectroscopy

1. At time = 0, a pulse is applied to the sample displacing the proton net magnetization, represented by the arrow, 90^0 from the direction of the external magnetic field, which is in the direction of the z axis. The net magnetization will now be aligned along the y-axis.

2. There is a delay equal to τ, or $1/2J_{CH}$, where J_{CH} is the coupling constant between carbon and hydrogen. This delay allows the proton spin vectors, precessing in the y-plane, to relax toward the x-axis.

3. A 180^0 pulse is applied, inverting the orientation of the relaxing protons.

4. There is a second delay also equal to τ. This delay allows the protons to refocus along the y axis.

5. Acquisition.

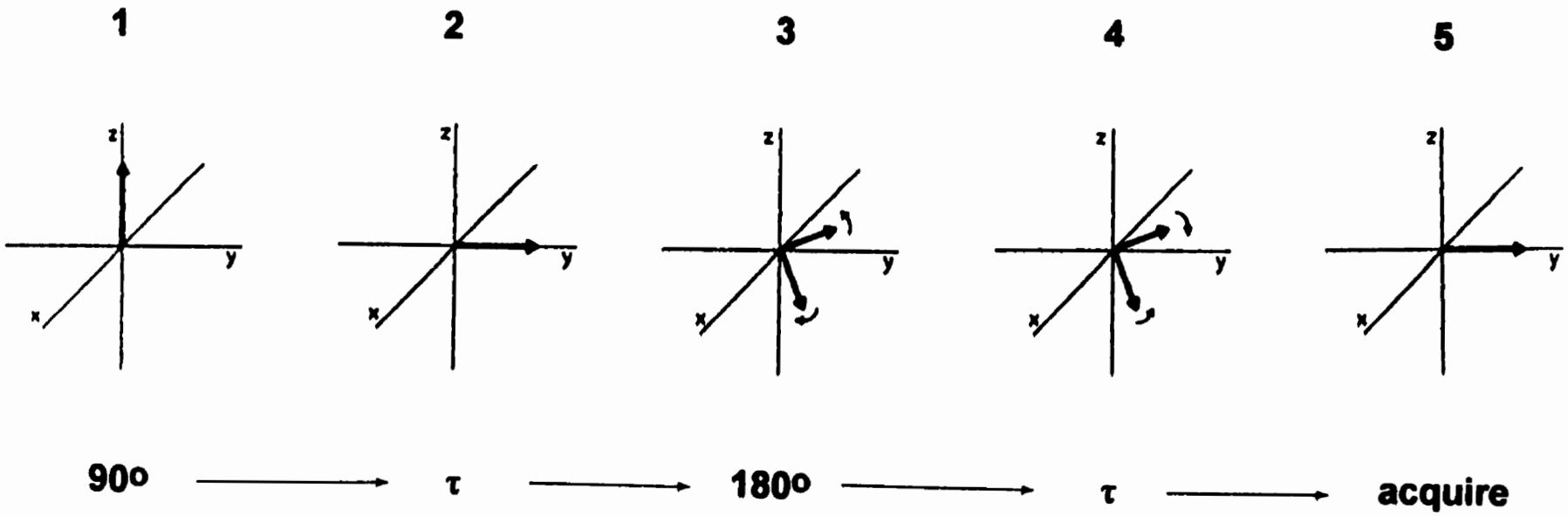
1
2
3
4
5
z
y
x
90o
τ
180o
τ
acquire

orientation of the relaxing protons, so that they are now moving in the opposite direction, i.e.: back towards the positive y axis. The second delay, τ, allows the protons to refocus along the y axis where the receiver coil is located, and is followed by data acquisition. The resulting spectrum includes contributions from all protons in the sample. In the other experiment, the pulse sequence is the same as in the first experiment, except that the 180° pulse is at the rf frequency specific for carbon-13 atoms. This "carbon-13" pulse reverses the inversion of direction for the relaxing protons attached to ^{13}C atoms, effectively eliminating the positive spectral contribution from these protons only. A spectrum acquired in this manner therefore includes peaks of protons attached to carbon-12 and other atoms, and negative resonances of protons attached to carbon-13. When spectra acquired in both manners are added, resonances of protons attached to carbon-13 cancel leaving resonances of protons attached to carbon-12. The difference in the area under the peaks between this sum spectrum and the (^{12}C + ^{13}C) spectrum indicates the amount of carbon-13 label present in each metabolite. In this way, I was able to observe and quantitatively evaluate how the host, and parasite, used atoms from [2-^{13}C]acetate in their energy generating metabolic pathways.

III. Host lipid metabolism

In addition to carbohydrate depletion observed in the infected host (Novak *et al.*, 1993; 1995), it can be expected that host lipid reserves are also depleted due to energy generation from lipid mobilization. Lipids are stored mainly in adipose tissue as triacylglycerols (TGs), which are composed of three fatty acid (FA) chains esterfied to a glycerol backbone. Some FAs commonly found as

their esters in TGs and other lipids are illustrated in Figure 3. These include the saturated FAs palmitic (16:0) and stearic (18:0), along with the unsaturated FAs oleic ($18:1^{\Delta 9}$), linoleic ($18:3^{\Delta 9,12,15}$), arachidonic ($20:4^{\Delta 5,8,11,14}$) and docosahexaenoic ($22:6^{\Delta 4,7,10,13,16,19}$) acid. (The numbers after the Δ indicate the position of the carbon-carbon double bonds, with the numbering beginning from the carboxyl carbon.) Hydrolysis of TG by triacyl lipase liberates glycerol and FAs which may then be further metabolized (Voet and Voet, 1995). Glycerol is converted first to glycerol-3-phosphate (G-3-P) by glycerol kinase and then to dihydroxyacetone phosphate (DHAP) via glycerol phosphate dehydrogenase. This DHAP may then participate in gluconeogenesis or glycolysis. The free FAs liberated from triacylglycerol are further metabolized via β-oxidation. Although initially activated for β-oxidation in the cytosol, oxidation takes place in the mitochondria. FAs are transported across the mitochondrial membrane by a carnitine protein carrier. Once in the mitochondria, the acyl chain separates from the carnitine carrier by reacting with coenzyme A to form fatty acyl coenzyme A (acyl CoA). The saturated FAs are then oxidized by a series of four reactions, yielding acetyl CoA and fatty acyl CoA, two carbon atoms shorter. The acetyl CoA can then enter the Kreb's cycle, while the new fatty acyl CoA can once again undergo β-oxidation. Unsaturated FAs are oxidized in much the same way, but require three extra steps to complete β-oxidation (Voet and Voet, 1995). While some of the acetyl CoA from FA oxidation is further metabolized via the Kreb's cycle, some of this acetyl CoA is also used in ketogenesis (the production of ketone bodies). As starvation continues, carbohydrates are metabolized less and less due to their reduced availability. Fat therefore becomes the main metabolic source of energy in this situation. Ketogenesis is an adaption to stressful starvation conditions increases survival time over that of

Figure 3

Structure of some common fatty acids

Saturated FAs

palmitic acid

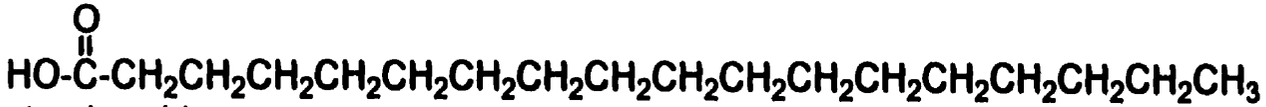

stearic acid

Unsaturated FAs

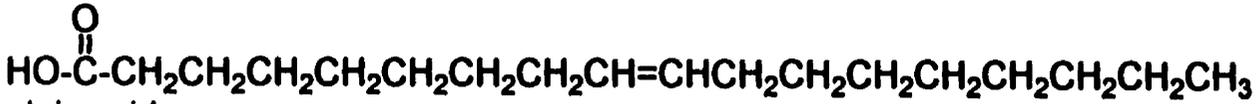

oleic acid

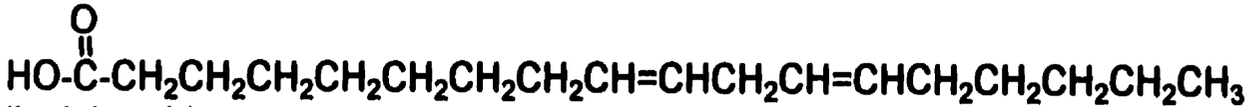

linoleic acid

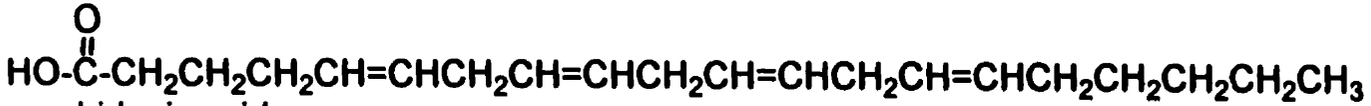

arachidonic acid

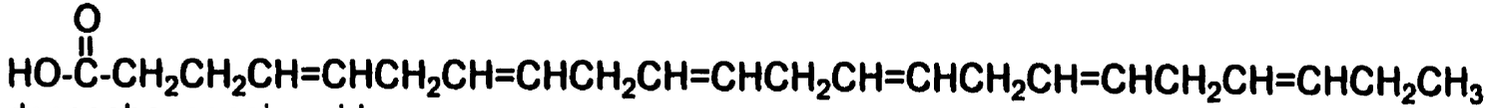

docosahexaenoic acid

continued "normal" glucose metabolism. This continues for the duration of starvation (Guyton, 1991; Alberti *et al.*, 1992).

In mammalian metabolism, FAs can be synthesized *de novo* and existing FAs can be modified into new moieties (Voet and Voet, 1995). *De novo* FA synthesis begins with the conversion of acetyl CoA to malonyl CoA by acetyl CoA carboxylase in the cytosol (Mathews and van Holde, 1990). This malonyl CoA is then transferred, by malonyl CoA-ACP transacylase, to a multifunctional enzyme complex known as acyl-carrier protein (ACP). A second acetyl CoA molecule is also transferred to ACP by acetyl CoA-ACP transacylase, forming acetyl ACP. Malonyl ACP and acetyl ACP then condense to form β-ketoacyl ACP via β-ketoacyl ACP synthase. This β-ketoacyl ACP synthase along with the remaining enzymes involved in the subsequent steps of FA synthesis are part of the ACP enzyme complex. β-Ketoacyl ACP reductase then catalyzes the conversion of β-ketoacyl ACP to D-3-hydroxyacyl ACP, which in turn forms *trans*-Δ^2-enoyl ACP via 3-hydroxyacyl ACP dehydrogenase. Enoyl CoA reductase converts *trans*-Δ^2-enoyl ACP to butyryl ACP, which then condenses with another malonyl CoA to form a FA chain two carbons longer. This cycle is repeated seven times, until the 16-carbon palmitoyl ACP is formed. Palmitoyl thioesterase then hydrolyzes palmitate (16:0), the primary product of this FA synthesis pathway, from the ACP enzyme complex (Mathews and van Holde, 1990; Voet and Voet, 1995). Palmitic acid may then be modified by elongases and desaturases to form other FAs. FA chain elongation takes place in the mitochondria and endoplasmic reticulum by sequential addition of acetyl CoA to an existing FA chain at the carboxyl end (Voet and Voet, 1995). For example, a common saturated FA synthesized from palmitic acid by addition of one two-carbon group from acetyl CoA is stearic acid (18:0). FA chains may also be modified by desaturation to produce cis double bonds. Desaturation occurs via

desaturase enzymes termed Δ^9, Δ^6, Δ^5 and Δ^4, which introduce double bonds at positions 9, 6, 5 and 4 from the carboxyl end of the FA moiety (Longmuir, 1987). Since mammalian cells do not possess desaturase enzymes which introduce double bonds beyond position 9 from the carboxyl group, fatty acids with double bonds at further positions must be either obtained through dietary means or modified first by desaturation and then elongation (Longmuir, 1987).

Fatty acids can also serve in other important roles. Arachidonic acid, (5,8,11,14-eicosatetraenoic acid) a C_{20} polyunsaturated FA that has four nonconjugated double bonds, is synthesized from dietary linoleic acid by elongation and desaturation (Hagmann and Keppler, 1988; Voet and Voet, 1995). Stored in cell membranes as the FA chain at C_2 of glycerol in phospholipids, arachidonic acid is a precursor of a group of biologically active compounds called the eicosanoids. These compounds include prostaglandins (PGs), prostacyclins (PSs), thromboxanes (TXs) and leukotrienes (LTs) which have roles in inflammatory response, pain and fever production, regulation of blood pressure, induction of blood clotting and control of reproductive functions (Hagmann and Keppler, 1988; Tao *et al.*, 1989; Voet and Voet, 1995; Woldseth *et al.*, 1995; Pageaux *et al.*, 1996). The role of LTs in inflammatory response includes stimulation of eosinophils, macrophages, monocytes and T-lymphocytes as well as augmentation of natural cytotoxic cell activities and T-lymphocyte proliferation (Hagmann and Keppler, 1988). The eicosanoids function similar to hormones but are not transported by the blood. They instead act in the same environment in which they are synthesized (Voet and Voet, 1995).

FAs are also important components of membrane phospholipids. One major class of phospholipids is the glycerophospholipids (GPLs) which are typically composed of FA chains attached at C_1 and C_2 of glycerol with a head

group containing phosphate attached at C_3. The FA moieties at C_1 are predominantly unsaturated while those at C_2 are usually saturated (Figure 4). The head group substituent attached to the phosphate is either a hydroxyl group (OH), choline, ethanolamine, serine or inositol, forming phosphatidic acid (PTA), PTC, PTE, PTS or PTI, respectively (Longmuir, 1987; Mathews and van Holde, 1990; Voet and Voet, 1995). GPLs are synthesized primarily in the endoplasmic reticulum (ER) and transported to other membrane sites by contact with, or via vesicles derived from, the ER, although *in situ* modification of GPLs is known to occur (Vance and Ridgeway, 1988; Vance, 1990). PTA, present in only small amounts in the inner and outer mitochondrial, nuclear and plasma membranes, is synthesized from glycerol or DHAP (Longmuir, 1987). Glycerol is first phosphorylated by glycerokinase (3), forming G-3-P (Figure 5). Then a FA chain, most often palmitic or stearic acid, is added to the G-3-P by glycerophosphate acyltransferase (4), forming lysophosphatidic acid (LPA). A second unsaturated FA chain, usually either oleic, linoleic, arachidonic or docosahexaenoic acid, is then added to C_2 of LPA by 1-acylglycerophosphate acyltransferase (5), forming PTA (Longmuir, 1987). Also, DHAP may be acylated by DHAP acyltransferase (1) to form 1-acyl-DHAP. A NADPH-dependent oxidoreductase (2) then catalyzes conversion of the 1-acyl-DHAP to LPA, followed by acylation of LPA to PTA via 1-acylglycerophosphate acyltransferase (5) (Longmuir, 1987; Mathews and van Holde, 1990). Hydrolysis of PTA forms 1,2-diacylglycerol (1,2-DG), which can then participate in the formation of other GPLs.

PTC is the most abundant GPL membrane constituent (Ansell and Spanner, 1982). Although this GPL is present in the plasma membrane, and all subcellular membranes, the greatest proportion of PTC occurs in nuclear membranes and in the endoplasmic reticulum (Longmuir, 1987). The major

Figure 4

Structure of membrane glycerophospholipids

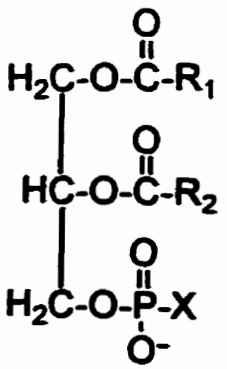

phosphatidic acid, X = OH

phosphatidylcholine, X = $O\text{-}CH_2CH_2N^+(CH_3)_3$

phosphatidylethanolamine, X = $O\text{-}CH_2CH_2N^+H_3$

phosphatidylserine, X = $O\text{-}CH_2\underset{\displaystyle N^+H_3}{\overset{\displaystyle COO^-}{CH}}$

phosphatidylinositol, X = 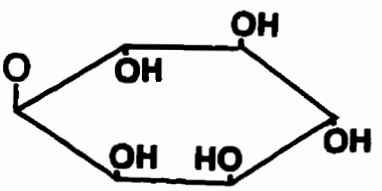

R_1 = predominantly saturated FAs

R_2 = predominantly unsaturated FAs

Figure 5

Pathways of glycerophospholipid metabolism in mammals

Enzymes include:

1, DHAP acyltransferase; 2, NADPH-dependent oxidoreductase; 3, glycerokinase; 4, glycerophosphate acyltransferase; 5, 1-acylglycerophosphate acyltransferase; 6, phosphatidate phosphohydrolase; 7, phosphatidate cytidylyltransferase; 8, CDP-DG-inositol phosphatidyltransferase; 9, PTE *N*-methyltransferase; 10, CDP-choline:1,2-DG choline phosphotransferase; 11, CTP:PC cytidylyltransferase; 12, choline kinase; 13, phospholipase A_2; 14, acyl CoA:LPA acyltransferase; 15, 2-LPC acylhydrolase; 16, acyltransferase; 17, glycero-3-PC cholinephosphohydrolase; 18, PTC cholinephosphohydrolase; 19, PTC phosphatidohydrolase; 20, CDP-ethanolamine:1,2-DG ethanolaminephosphotransferase; 21, CTP:PE cytidylyltransferase; 22, ethanolamine kinase; 23, phospholipase A_2; 24, acyl-(2-acyl *sn*-glycero-3-phosoho)ethanolamine acyltransferase; 25, LPE acylhydrolase; 26, acyltransferase; 27, unknown; 28, PTE ethanolaminephosphohydrolase; 29, PTE phosphatidohydrolase; 30, PTE serine transferase; 31, PTS decarboxylase.

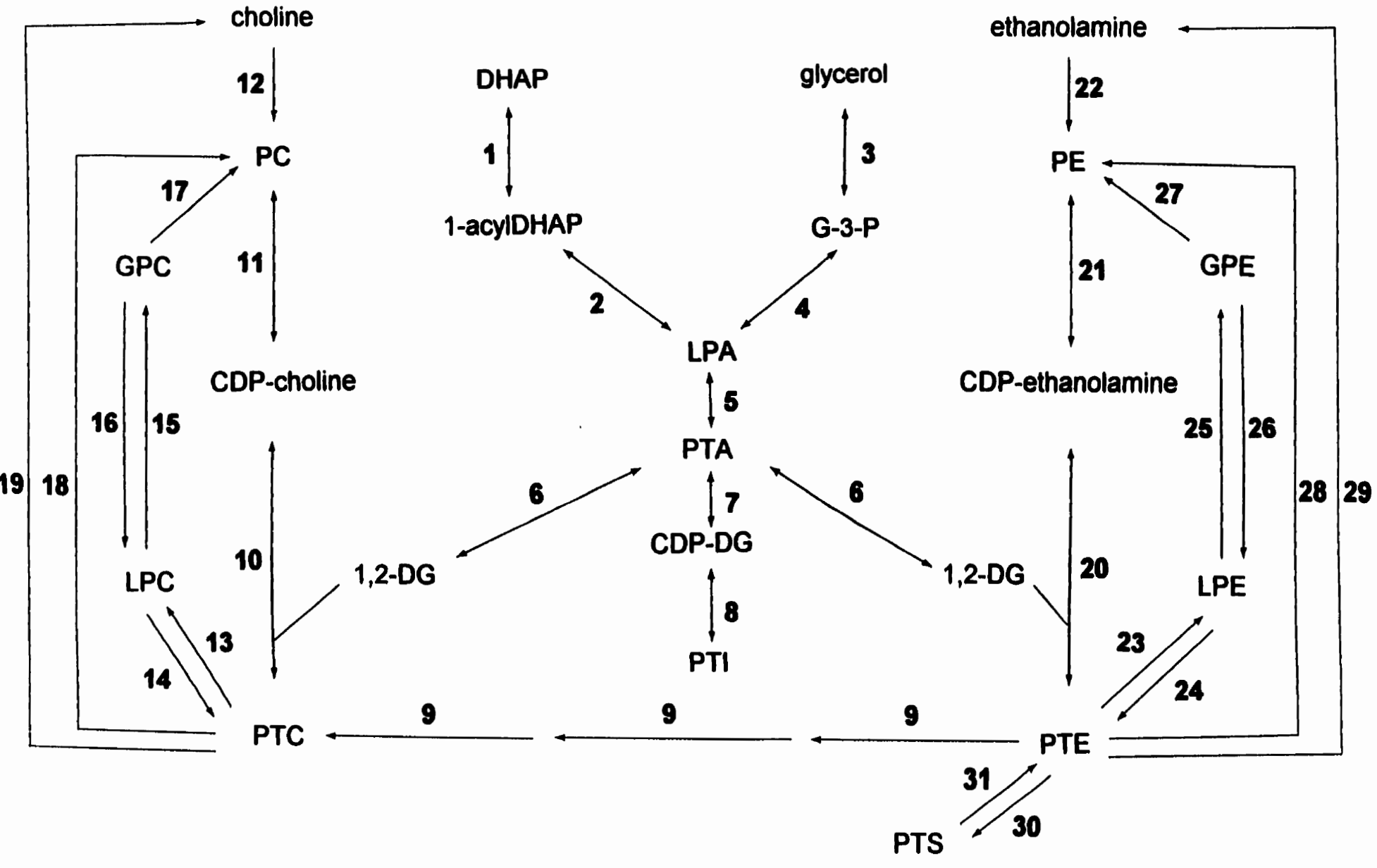
choline
12
PC
17
GPC
11
16
15
LPC
14
13
CDP-choline
10
19
18
DHAP
1
1-acylDHAP
2
glycerol
3
G-3-P
4
LPA
5
PTA
6
6
7
CDP-DG
8
PTI
1,2-DG
1,2-DG
ethanolamine
22
PE
27
21
GPE
CDP-ethanolamine
25
26
LPE
20
28
29
23
24
9
9
9
PTC
PTE
31
30
PTS

route of PTC synthesis and degradation in mammals is the CDP-choline pathway (Figure 5). In the synthesis process, choline is first phosphorylated to PC by choline kinase (12) followed by conversion of PC to CDP-choline via CTP:PC cytidylyltransferase (11), the rate limiting step in this pathway. CDP-choline:1,2-DG cholinephosphotransferase (10) then catalyzes the transfer of PC from CDP-choline to 1,2-DG, producing PTC. These reactions are all reversible and each step is catalyzed by the same enzyme in both synthetic and catabolic directions (Ansell and Spanner, 1982; Longmuir, 1987; Kuesel *et al.*, 1990; Mathews and van Holde, 1990). PTC can also be synthesized from GPC. Acyltransferases (16) catalyze the addition of a FA chain to either C_1 or C_2 of glycerol in GPC forming LPC. Another FA chain is then added to the remaining carbon of glycerol by acyl CoA:LPA acyltransferase (14). This pathway is reversible, involving phospholipase A_2 (13) in the conversion of PTC to LPC, followed by 2-LPC acylhydrolase (15) which converts LPC to GPC (Kuesel *et al.*, 1990; Voet and Voet, 1995). Choline and PC may also be liberated directly from PTC by the action of PTC phosphatidohydrolase (19) and PTC cholinephosphohydrolase (18), respectively. Besides the major CDP-choline pathway, there is also an alternate pathway for the biosynthesis of PTC (Figure 5). In this pathway, which is largely liver specific, PTE is converted to PTC by PTE *N*-methyltransferase (PEMT) (9). Two forms of this enzyme are known to exist: PEMT-1, localized on the cytosolic surface of the ER, and PEMT-2 which is located on a mitochondrial-associated membrane (Vance, 1990; Cui *et al.*, 1993). These enzymes catalyze the sequential addition of three methyl groups from *S*-adenosylmethionine to the nitrogen of the head group of PTE to produce PTC (Vance and Ridgeway, 1988; Cui *et al.*, 1993; Voet and Voet, 1995).

PTE, the second most abundant GPL, is also present in the plasma membrane along with membranes of all subcellular organelles. The

mitochondrial membranes, inner and outer, are particularly enriched with PTE (Longmuir, 1987). Analogous to the CDP-choline pathway of PTC synthesis, PTE is synthesized from ethanolamine via the CDP-ethanolamine pathway (Figure 5). Ethanolamine is converted to phosphoethanolamine (PE) by ethanolamine kinase (22). PE then forms CDP-ethanolamine in a reaction catalyzed by CTP:PE cytidylyltransferase (21); this is the rate limiting step in the CDP-ethanolamine pathway (Longmuir, 1987). CDP-ethanolamine:1,2-DG ethanolaminephosphotransferase (20) then catalyzes the transfer of PC from CDP-ethanolamine to 1,2-DG, forming PTE. As in the CDP-choline pathway, the enzymes involved in the CDP-ethanolamine pathway catalyze both the synthesis and degradation reactions of PTE (Longmuir, 1987; Kuesel *et al.*, 1990; Voet and Voet, 1995). PTE can also be synthesized from glycerophosphoethanolamine (GPE). In this reaction, GPE is converted to lysophosphatidylethanolamine (LPE) by acylation involving FA acyltransferases (26), followed by conversion to PTE via acyl-(2-acyl-*sn*-glycero-3-phospho)ethanolamine acyltransferase (24). PTE degradation via this LPE pathway requires deacylation to convert PTE to LPE and then to GPE (Ansell and Spanner, 1982; Kuesel *et al.*, 1990). Ethanolamine and PE can be released from PTE directly via PTE phosphatidohydrolase (29) and PTE ethanolaminephosphohydrolase (28), respectively (Mathews and van Holde, 1990). In addition, PTE and PTS are interconverted by PTE serine transferase (30) and PTS decarboxylase (31) (Mathews and van Holde, 1990; Voet and Voet, 1995). PTS is present predominantly in brain tissue and in the liver in the ER, golgi complex and plasma membrane (Longmuir, 1987).

Synthesis of PTI begins with PTA (Figure 5). Phosphatidate cytidylyltransferase converts PTA to CDP-DG, followed by addition of *myo*-inositol by CDP-DG-inositol phosphatidyltransferase to form PTI (Longmuir,

1987; Mathews and van Holde, 1990). This GPL, also present in the plasma membrane and membranes of all other subcellular organelles, accounts for only 5-10% of total hepatic phospholipids. Breakdown of PTI also produces phosphatidylinositol-4,5-bisphosphate, which in turn yields inositol-1,4,5-trisphosphate (IP_3), an important intracellular second messenger (Exton, 1988). IP_3 enters the cytosol, and 1,2-DG, the other product of phosphatidyl 4,5-bisphosphate breakdown, which may also act as an intracellular second messenger, remains in the cell membrane (Exton, 1988; Thomas and Gillham, 1989). IP_3 carries out its role as a second messenger by causing the rapid release of Ca^{2+} ions from components of the endoplasmic reticulum. This cytosolic Ca^{2+} binds to the protein calmodulin, causing the activation of protein kinases in the cell. These protein kinases in turn activate enzymes or other protein kinases, especially calmodulin-dependent protein kinase, which can inactivate enzymes such as glycogen synthase, pyruvate kinase, acetyl CoA carboxylase and ATP-citrate lyase, probably accounting for an inhibition of glycogen synthesis, glycolysis and lipogenesis (Exton, 1988). In addition, α-ketoglutarate dehydrogenase is also sensitive to Ca^{2+} levels, and is activated, along with isocitrate dehydrogenase, by increased Ca^{2+} levels in the hepatocyte. Activation of these enzymes could account for stimulation of the Kreb's cycle and increased β-oxidation of FAs (Exton, 1988).

Another important membrane component is cholesterol. It regulates membrane fluidity and serves as the immediate precursor for a number of essential vitamins, steroid hormones and bile acids (Turley and Dietschy, 1988; Voet and Voet, 1995). Cholesterol absorbed from dietary sources is transported in the blood in a lipoprotein complex called a chylomicron while cholesterol synthesized *de novo* in the liver is esterfied by acyl CoA:cholesterol acyl transferase into cholesterol esters which are carried by the blood to peripheral

tissues in the form of very low density lipoproteins (VLDLs). As TGs and other lipid molecules are removed from the VLDLs, they are sequentially transformed into intermediate density lipoproteins (IDLs) and then low density lipoproteins (LDLs) (Turly and Dietschy, 1988; Voet and Voet, 1995).

It is known that cestodes are incapable of *de novo* sterol and fatty acid synthesis and therefore depend on their hosts for lipids (Barrett, 1983). Host lipids are taken up by the parasite and modified according to the parasite's own cellular requirements. Lipids are not a source of energy for cestodes. Instead they use them in other ways such as incorporation into cell membranes, enzyme regulation and cell surface recognition and interaction (Smyth and McManus, 1989; McManus and Bryant, 1995). Continuous cell proliferation in adult and larval cestodes, including *E. multilocularis*, requires large amounts of lipids for membrane synthesis. As previously described (Novak *et al.*, 1995), by siphoning off glucose, *E. multilocularis* cysts induce starvation conditions in their hosts. Therefore, these parasite activities should also lower lipid reserves to compensate for reduced carbohydrate energy sources, and change lipid composition by oxidizing FA moieties for energy in the infected host. To gain more information about the effect of *E. multilocularis* on host lipid metabolism, the second part of my research was designed to study changes in the hepatic lipid composition. Using high field ^{1}H NMR, an excellent tool to analyze extracted mixtures of lipids from various tissues and organs (Cunnane, 1989; Sparling *et al.*, 1989; Sze and Jardetzky, 1990a; Casu *et al.*, 1991; Pollesello *et al.*, 1991; Pollesello *et al.*, 1993; Choi *et al.*, 1993; Adosraku *et al.*, 1994; Pollesello *et al.*, 1996), I identified and quantitatively analyzed various groups of lipids and phospholipids in the liver of uninfected and infected *M. unguiculatus*. Lipids in *E. multilocularis* cysts were also analyzed.

Materials and Methods

I. Carbohydrate metabolism

Infection

Thirty male jirds, *Meriones unguiculatus*, approximately 4 months old, were used in this experiment. Half of these were infected by an intraperitoneal injection of 0.5 ml of *Echinococcus multilocularis* cyst cell suspension each, prepared by following the method of Lubinsky (1960). The other 15 jirds served as uninfected controls. All animals were cared for and used in accordance with the principles of the Canadian Council on Animal Care, as stated in the "Guide to the Care and Use of Experimental Animals". On days 28, 29 and 30 post infection (p.i.), prior to the delivery of exogenous [2-^{13}C]acetate (99.5 atom % ^{13}C, MSD Isotopes), the animals were starved overnight (approximately 18 h). In the morning, they were anaesthetized with an intramuscular injection of sodium pentobarbital (60 mg/kg) (MTC Pharmaceuticals). Their abdomens were then opened, and 0.1 ml of a 26% by weight solution of [2-^{13}C]acetate (99.1 atom % ^{13}C; Isotec Inc.) in 0.85% NaCl saline was injected into the hepatic portal vein as a bolus injection using a 1 cc syringe over a period of about 2 minutes. Thirty minutes later, the liver, and parasite cyst biomass, free of host tissue, were removed, rinsed and frozen immediately in liquid nitrogen (N_2). The livers and cysts were then weighed and stored at -70°C until preparation of perchloric acid (PCA) (Fisher Scientific Ltd.) extracts. The uninfected control group was treated in the same manner. To ensure the metabolic rate of each animal was similar, all jirds were dissected between 9:00 am and 12 noon.

This experiment was repeated exactly as described above, except that in the second experiment, the livers and parasite cysts were removed 120 minutes post injection of [2-^{13}C]acetate solution into the hepatic portal vein of the host. In infected animals, all parasite cysts were, at this stage of infection, exohepatic and located in the paritoneal cavity.

Perchloric Acid Extracts

Each sample of frozen liver or cyst was pulverized in liquid N_2 using a precooled mortar and pestle. It was then transferred to a 50 ml homogenizing tube with 4 ml of cold 0.5 M PCA / g of tissue and homogenized in an ice bath. After homogenization, the sample suspension was centrifuged at 15000 rpm for 10 minutes at -2°C. The supernatant was decanted, its pH adjusted with potassium hydroxide (KOH) to between 7.1 and 7.4 and centrifuged again, under the above described conditions to remove any precipitated potassium perchlorate. Samples were then stored at -70°C until they were lyophilized. Following lyophilization, the freeze-dried residue of each sample was stirred with 1.3 ml of D_2O (99.9 atom % D, MSD Isotopes), and 0.2 ml of a solution of 0.0754 g sodium [2,2,3,3-$^2H_4$]-3-trimethylsilylpropionate (TSP) in 15 ml (17.2415 g) of D_2O, added as a chemical shift and intensity standard. After 2 h of stirring, the pH of each sample was adjusted to between 7.15 and 7.25, using sodium deuteroxide (NaOD). The samples were then centrifuged at 12000 rpm for 30 minutes at 5°C, and the supernatant transferred to a 5 mm NMR tube for analysis.

NMR Spectroscopy of Perchloric Acid Extracts

The ^{1}H spin echo NMR spectra of PCA extracts were acquired at 310 K (37°C) using a Bruker AMX-500 NMR spectrometer operating at 500.13 MHz for this nucleus. The spectra were ^{13}C decoupled using the GARP composite pulse decoupling routine (Shaka *et al.*, 1985). A spectral width of 6578.95 Hz, 16 K data points and a recycle time of 15.25 s were used in data accumulation. The number of scans used for liver and cyst samples was 192. Scans acquired with, and without, ^{13}C population inversion (Bendall *et al.*, 1981) were acquired alternatively in blocks of 16 scans and stored in separate computer memory locations. Inverting the ^{13}C puts attached protons 180° out of phase with respect to protons attached to ^{12}C and other nuclei. Consequently, resonances from protons attached to ^{13}C cancel when the spectra are added. Peak assignments were based on published data (Evanochko *et al.*, 1984; Gilroy *et al.*, 1988; Desmoulin *et al.*, 1990; Sze and Jardetzky, 1990b; Rafter *et al.*, 1991; Yacoe *et al.*, 1991), and the spectra of authentic compounds. The area under each peak was corrected for the number of contributing protons, as well as for the two anomers present in the case of glucose. In the case of citrate, two doublets make up the CH_2 resonance at 2.54 ppm. However, in spectra of cysts, where the citrate resonance was visible, only one of the two doublets could be cleanly integrated. As a consequence, the integral value obtained for the citrate CH_2 resonance was multiplied by two. Concentrations of metabolites present (in μmol / g of tissue) were calculated from integration data of metabolite peaks, relative to that of TSP, in the ^{12}C + ^{13}C spectra. The percent carbon-13 in metabolites was calculated using the ^{12}C + ^{13}C spectrum and the sum of the [^{12}C + ^{13}C] and [^{12}C - ^{13}C] spectra. Data obtained were statistically analyzed using an analysis of variance, (ANOVA), with $\alpha = 0.05$ deemed as significant.

II. Lipid metabolism

Infection

Thirty-three male *M. unguiculatus*, 6 months old, were used in this experiment. Eighteen of them were infected with 0.5 ml of *E. multilocularis* cyst cell suspension, as described above, while the other 15 served as uninfected controls. On days 35, 36 and 37 p.i., the animals were anaesthetized intramuscularly with sodium pentobarbital (60 mg/kg), their abdomens opened and the livers and parasite cysts removed, rinsed and frozen immediately in liquid N_2. Livers and cysts were then weighed and stored at -70°C until preparation of chloroform:methanol (C:M) extracts. To ensure the metabolic rate of each animal was similar, all animals were dissected between 9:00 am and 12 noon.

Chloroform:Methanol Extracts

Frozen livers and cysts were first pulverized in liquid N_2 using a mortar and pestle. Then the total lipids were extracted using a 2:1 (v/v) C:M mixture. The chloroform was HPLC grade from EM Industries (Merck) (CX1050-1); it is critical to use chloroform which does not contain ethanol and which has a low concentration of hydrocarbon stabilizer. The methanol was reagent grade from Mallinckrodt. Twenty ml of this solution was used per gram of sample, as suggested by Folch *et al.* (1957). The samples were homogenized using a Brinkman Polytron homogenizer, filtered through sintered glass and the filtrate collected. The residue was then resuspended in the same volume of 2:1 C:M

solution, re-homogenized and re-filtered. The first and second filtrates were combined and washed with one-quarter the total filtrate volume of 0.5 M potassium chloride (KCl) (Fisher Scientific) in a 1:1 (v/v) methanol:water solution. The phases were allowed to separate, and the top layer, containing water and methanol, was removed. The washing was repeated a second time, using the same volume of 0.5 M KCl solution. The bottom layer, containing chloroform and lipids, was transferred to a round-bottom flask and the chloroform removed under N_2(g), using a rotory evaporator. The residue was then resuspended in 5 ml of benzene (thiophene free, Fisher Scientific), to dry the sample by azeotropic distillation. The benzene and water solution was removed using a rotory evaporator. The resulting residue was resuspended in 5 ml of chloroform per 2.0 g of tissue, with a known amount of TMSS (tetrakis[trimethylsilyl]silane) (98%, Aldrich Chemical Co.) added as a chemical shift and intensity standard. Each sample was then centrifuged at 2500 rpm for 10 minutes. A 0.2 ml aliquot of the supernatant was removed, combined with 0.4 ml $CDCl_3$ (99.8 atom % D, CDN Isotopes) and 0.6 ml CD_3OD (99.8 atom % D, CDN Isotopes), and placed into a 5 mm NMR tube for proton NMR analysis. This ratio of total chloroform to CD_3OD was essential in placing the H_2O peak where it would not overlap lipid peaks at the temperature used for NMR.

NMR Spectroscopy of Chloroform:Methanol Extracts

Proton NMR spectra of C:M extracts were acquired at 300 K (27°C) using a Bruker AMX-500 NMR spectrometer operating at 500.13 MHz for this nucleus. Spectra were run locked on the CD_3 deuterons of CD_3OD. A spectral width of 4504.50 Hz, 32 K data points and a flip angle of 78° were used in data

acquisition. The recycle time was 10.24 s and each sample was scanned 160 times. The residual $CHCl_3$ peak was reduced by off resonance presaturation using a shaped gaussian 1024 pulse at 59 dB.

Spectral peaks were identified using published data (Sparling *et al.*, 1989; Sze and Jardetzky, 1990a; Casu *et al.*, 1991; Choi *et al.*, 1993; Adosraku *et al.*, 1994). The concentration of lipid components (μmol / g of tissue) was calculated from integration data of spectral peaks relative to TMSS. In this and subsequent calculations, integration values were corrected for the number of protons contributing to that resonance. Total fatty acid (FA) concentration was calculated from the combined integration values for the resonances of the ω-CH_3 of FA chains (δ = 0.87) and the ω-CH_3 β to a double bond in FA chains (δ = 0.95). In addition, FA chain composition was analyzed by comparing the individual FA components to total FAs. FA moieties were analyzed as follows:

Saturated FA components	Unsaturated FA components
$C\underline{H_2}CH_2COO$ (δ = 1.60) : total FA	$HC{=}CH(C\underline{H_2}HC{=}CH)_n$ (δ = 2.80) : total FA
$(C\underline{H_2})_n$ (δ = 1.30) : total FA	$C\underline{H_2}CH{=}CHHC{=}CHC\underline{H_2}$ (δ = 2.05) : total FA
$C\underline{H_2}COO$ (δ = 2.30) : total FA	$HC{=}CHCH_2C\underline{H_2}CH_2COO$ of arachidonic acid (δ = 1.65) : total FA
	$HC{=}CHC\underline{H_2}C\underline{H_2}COO$ of docosahexaenoic acid (δ = 2.40) : total FA
	$HC{=}CHC\underline{H_2}HC{=}CH$ of linoleic acid (δ = 2.75) : total FA

Note: in these and subsequent cases, underlined H's indicates the specific proton(s) of each component which was/were integrated.

The average number of double bonds per FA, or the degree of unsaturation (DU), and the average FA chain length were also calculated.

DU = $\underline{H}C=C\underline{H}$ (δ = 5.30) : total FA

Average FA Chain Length:

$1_a + 1_b + 2(DU) + (C\underline{H_2}CH_2COO$: total FA) + ($(CH_2)_n$: total FA) + ($C\underline{H_2}COO$: total FA) + ($HC=CH(C\underline{H_2}HC=CH)_n$: total FA) + ($C\underline{H_2}CH=CHHC=CHC\underline{H_2}$: total FA) + ($HC=CHCH_2C\underline{H_2}CH_2COO$ of arachidonic acid : total FA) + ($HC=CHC\underline{H_2}CH_2CH_2COO$ of arachidonic acid (δ = 2.10) : total FA) + ($HC=CHC\underline{H_2}C\underline{H_2}COO$ of docosahexaenoic acid : total FA) + ($HC=CHC\underline{H_2}HC=CH$ of linoleic acid : total FA)

where 1_a and 1_b are equal to one terminal methyl group (ω-CH_3) and one carbonyl group (C=O) per FA chain, respectively.

Data obtained were analyzed statistically using ANOVA. A value of α = 0.05 was deemed significant.

Results

I. Carbohydrate metabolism

A representative ^{13}C decoupled ^{1}H spin echo NMR spectrum of a PCA extract of liver from uninfected *Meriones unguiculatus*, removed 30 minutes post injection of [2-^{13}C]acetate is shown in Figure 6. Major well resolved resonances evaluated in this experiment were H_1 of glucose units having a (1-4) linkage in glycogen at 5.45 ppm; H_1 of α-glucose at 5.25 ppm; CH_2 of glycine at 3.56 ppm; $(CH_3)_3N$ of taurine at 3.42 ppm; $(CH_3)_3N$ of betaine/CH_2S of taurine at 3.26 ppm; $(CH_3)_3N$ of glycerophosphocholine (GPC) at 3.23 ppm; $(CH_3)_3N$ of phosphocholine (PC) at 3.22 ppm; $(CH_3)_3N$ of choline at 3.21 ppm; $(CH_3)_3N$ of acylcarnitine at 3.20 ppm; CH_3N of phosphocreatine/creatine (PCr/Cr) at 3.04 ppm; CH_2CH_2 of succinate at 2.41 ppm; CH_3 of acetate at 1.92 ppm; CH_3 of alanine at 1.47 ppm; CH_3 of lactate at 1.33 ppm and CH_2 of β-hydroxybutyrate (β-HB) at 1.18 ppm. The total concentrations, (labeled plus unlabeled), of these metabolites, in livers from uninfected and infected *M. unguiculatus*, are presented in Table 1. When compared to uninfected controls, the livers from infected animals contained less glycogen and glucose, but more glycine, PC, acylcarnitine, acetate and β-HB.

The ^{13}C decoupled ^{1}H spin echo NMR spectrum of a PCA extract of *E. multilocularis* cyst removed 30 minutes post injection of [2-^{13}C]acetate into the host, is shown in Figure 7. The cysts contained the same metabolites as host livers and in addition, one of the CH_2 doublets of citrate, that at 2.54 ppm, was clearly detectable. When the concentrations of these metabolites were compared to those of the host's liver it was found that the parasite had more

Figure 6

^{13}C decoupled ^{1}H spin echo NMR spectrum of a PCA extract of uninfected *M. unguiculatus* liver, 30 minutes after injection of [2-^{13}C]acetate

Peak assignments:

1	H_1 of glucose units having a 1-4 linkage in glycogen	9	$(CH_3)_3N$ of acylcarnitine
2	H_1 of α-glucose	10	CH_3N of PCr/Cr
3	CH_2 of glycine	11	CH_2CH_2 of succinate
4	$(CH_3)_3N$ of taurine	12	CH_3 of acetate
5	$(CH_3)_3N$ of betaine / (CH_2S) of taurine	13	CH_3 of alanine
6	$(CH_3)_3N$ of glycerophosphocholine (GPC)	14	CH_3 of lactate
7	$(CH_3)_3N$ of phosphocholine (PC)	15	CH_3 of β-hydroxybutyrate (β-HB)
8	$(CH_3)_3N$ of choline		

* indicates water

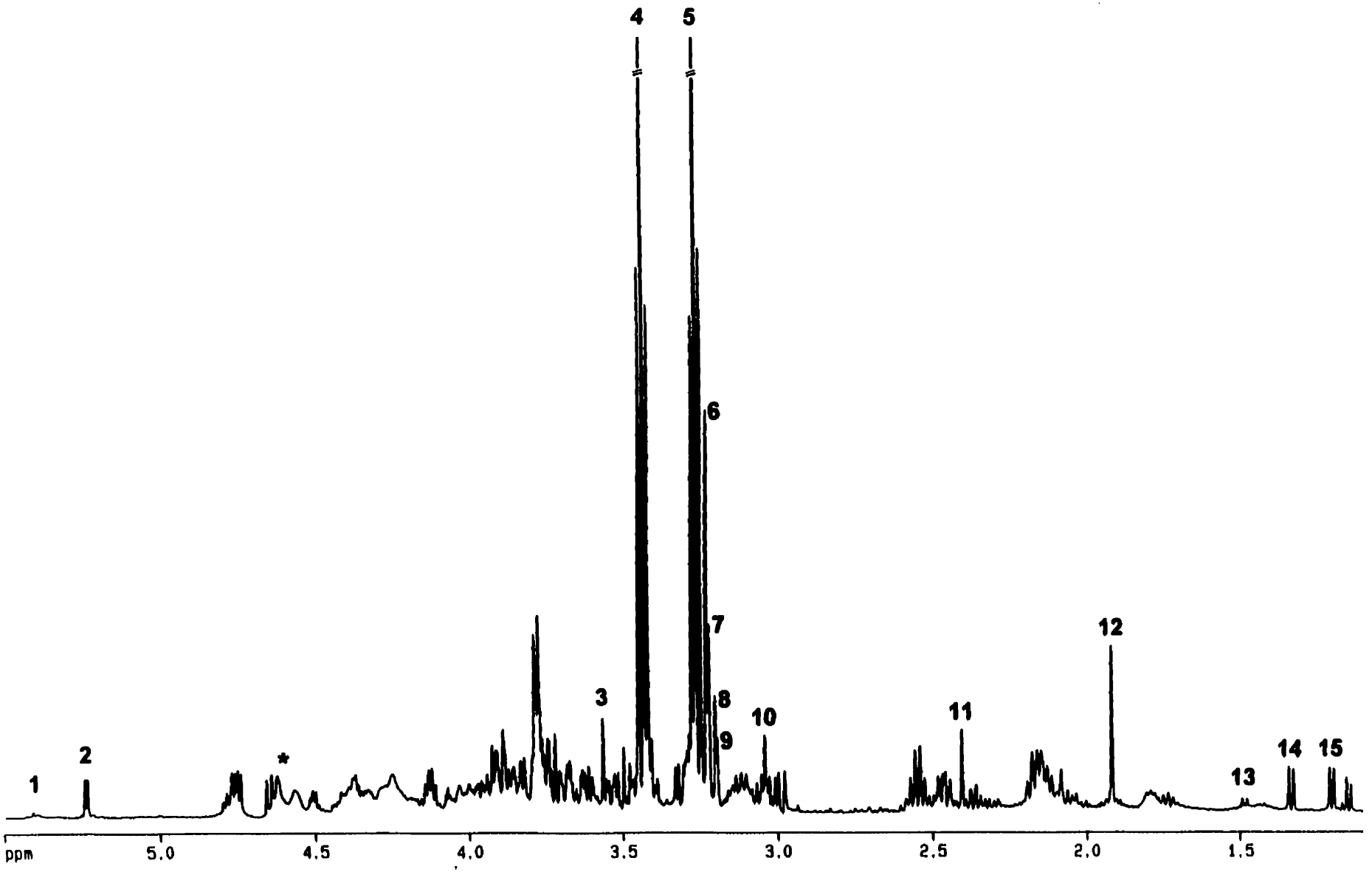
4
5
6
7
8
9
10
11
12
3
1
2
*
13
14
15
ppm
5.0
4.5
4.0
3.5
3.0
2.5
2.0
1.5

Table 1: Concentrations of metabolites from livers of uninfected and infected *Meriones unguiculatus*, and from *Echinococcus multilocularis* cysts, 30 minutes after introduction of [2-^{13}C]acetate into the host.

Metabolite	Concentration (mean ± S.D.) (μmol / g wet wt)		
	uninfected (n = 15)	infected (n = 15)	cyst[+] (n = 14)
Glycogen	1.12 ± 0.76[a]	0.32 ± 0.09[b]	1.14 ± 0.43*
Glucose	4.66 ± 1.11[a]	3.20 ± 1.02[b]	0.77 ± 0.43*
Glycine	0.69 ± 0.28[a]	1.11 ± 0.31[b]	0.47 ± 0.18*
Taurine	15.81 ± 2.78[a]	16.26 ± 2.35[a]	3.27 ± 1.14*
Betaine	0.44 ± 0.22[a]	0.48 ± 0.26[a]	0.42 ± 0.23
GPC	0.99 ± 0.29[a]	0.90 ± 0.40[a]	0.26 ± 0.08*
PC	0.08 ± 0.03[a]	0.26 ± 0.10[b]	0.14 ± 0.04*
Choline	0.07 ± 0.04[a]	0.11 ± 0.18[a]	0.08 ± 0.03
Acylcarnitine	0.03 ± 0.02[a]	0.06 ± 0.03[b]	0.01 ± 0.01*
PCr/Cr	0.31 ± 0.10[a]	0.35 ± 0.06[a]	0.43 ± 0.12
Citrate	-	-	1.08 ± 0.29
Succinate	0.40 ± 0.06[a]	0.50 ± 0.21[a]	1.06 ± 0.50*
Acetate	0.65 ± 0.35[a]	0.91 ± 0.31[b]	2.10 ± 0.25*
Alanine	0.10 ± 0.06[a]	0.26 ± 0.43[a]	1.91 ± 0.56*
Lactate	0.58 ± 0.33[a]	0.76 ± 0.74[a]	5.82 ± 0.86*
β-HB	0.57 ± 0.23[a]	0.88 ± 0.46[b]	0.58 ± 0.25*

[a,b]: different letters denote a significant difference between concentrations of metabolites in uninfected and infected groups, ($\alpha \leq 0.05$).

* indicates a significant difference between concentrations of metabolites in infected and cyst groups

[+] wet weight of cysts was, on average, 4.84 ± 3.55 g

Figure 7

^{13}C decoupled ^{1}H spin echo NMR spectrum of a PCA extract of *E. multilocularis* cyst, 30 minutes after injection of [2-^{13}C]acetate into the host

Peak assignments:

1	H_1 of glucose units having a 1-4 linkage in glycogen	9	$(CH_3)_3N$ of acylcarnitine
2	H_1 of α-glucose	10	CH_3N of PCr/Cr
3	CH_2 of glycine	11	CH_2 of citrate
4	$(CH_3)_3N$ of taurine	12	CH_2CH_2 of succinate
5	$(CH_3)_3N$ of betaine / (CH_2S) of taurine	13	CH_3 of acetate
6	$(CH_3)_3N$ of glycerophosphocholine (GPC)	14	CH_3 of alanine
7	$(CH_3)_3N$ of phosphocholine (PC)	15	CH_3 of lactate
8	$(CH_3)_3N$ of choline	16	CH_3 of β-hydroxybutyrate (β-HB)

* indicates water

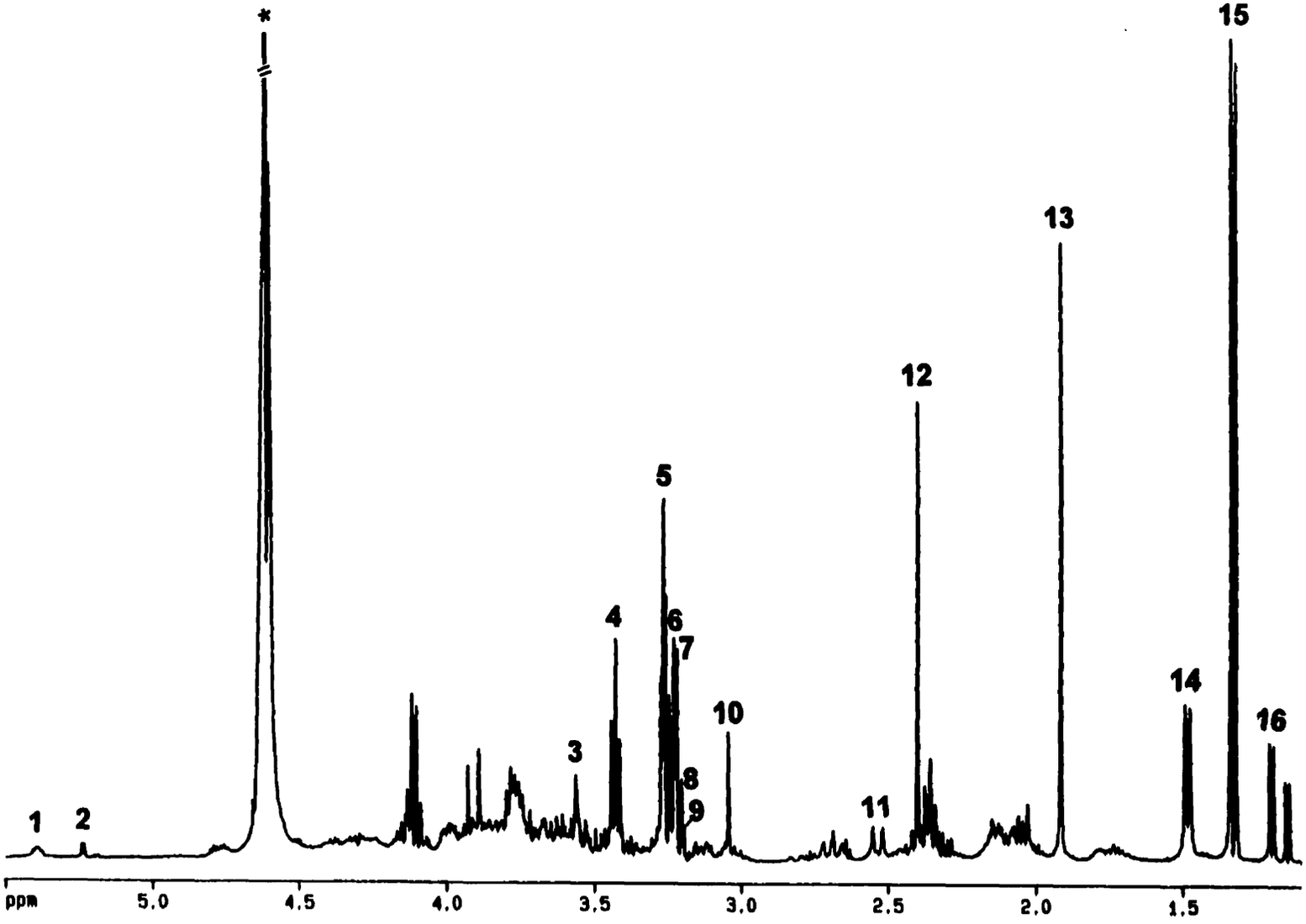
*
15
13
12
5
4
6
7
14
10
16
3
8
9
11
1
2
ppm
5.0
4.5
4.0
3.5
3.0
2.5
2.0
1.5

glycogen, succinate, acetate, alanine and lactate, but less glucose, glycine, taurine, GPC, PC, acylcarnitine and β-HB (Table 1).

The total concentrations of metabolites from livers of jirds which were collected 120 minutes post injection of [2-^{13}C]acetate are presented in Table 2. When compared to the uninfected controls, livers from infected *M. unguiculatus* had less glycogen and glucose, but more glycine, GPC, PC and acylcarnitine. *Echinococcus* cysts, removed 120 minutes after introduction of [2-^{13}C]acetate into the host, had higher concentrations of succinate, acetate, alanine and lactate but lower concentrations of glucose, glycine, taurine, betaine, GPC, PC, acylcarnitine and β-HB than the livers of infected jirds (Table 2).

The incorporation of ^{13}C from [2-^{13}C]acetate into hepatic and cyst metabolites, after 30 and 120 minutes, is presented in Table 3. Both the liver and the parasite contained label in glycogen, glucose, succinate, acetate, alanine, lactate and β-HB. In addition, *E. multilocularis* had label in citrate. After 30 minutes, livers from infected animals had a higher percentage of label in glycogen than those in the control group. However, for hepatic alanine and lactate, the percent carbon-13 was less in the infected group than in uninfected controls. In the parasite cysts, all metabolites, except for glucose and acetate, had less ^{13}C than the corresponding hepatic metabolites from infected jirds.

The percent ^{13}C in of metabolites from livers of uninfected and infected jirds in the 120 minute group did not differ statistically. Most of the label remaining in the liver was in acetate. In contrast, after 120 minutes, *E. multilocularis* cysts contained significantly more label in glycogen, glucose, succinate, acetate, alanine and lactate than corresponding hepatic metabolites.

When the flow of label from [2-^{13}C]acetate to hepatic and cyst metabolites was considered by comparing data at 30 and 120 minutes, it was found that, in general, the percent label in liver metabolites decreased, whereas that in cyst

Table 2: Concentrations of metabolites from livers of uninfected and infected *Meriones unguiculatus*, and from *Echinococcus multilocularis* cysts, 120 minutes after introduction of [2-^{13}C]acetate into the host.

Metabolite	Concentration (mean ± S.D.) (μmol / g wet wt)		
	uninfected (n = 14)	infected (n = 15)	cyst[+] (n = 15)
Glycogen	2.86 ± 1.95[a]	0.67 ± 0.74[b]	1.32 ± 0.43
Glucose	5.25 ± 0.98[a]	4.18 ± 1.38[b]	1.02 ± 0.45*
Glycine	0.35 ± 0.31[a]	1.11 ± 0.37[b]	0.22 ± 0.14*
Taurine	14.14 ± 3.63[a]	15.00 ± 1.79[a]	3.24 ± 0.42*
Betaine	0.68 ± 0.42[a]	0.53 ± 0.20[a]	0.33 ± 0.11*
GPC	0.47 ± 0.32[a]	1.04 ± 0.40[b]	0.22 ± 0.06*
PC	0.19 ± 0.13[a]	0.44 ± 0.27[b]	0.15 ± 0.05*
Choline	0.04 ± 0.04[a]	0.03 ± 0.02[a]	0.06 ± 0.04
Acylcarnitine	0.04 ± 0.03[a]	0.08 ± 0.04[b]	0.01 ± 0.01*
PCr/Cr	0.43 ± 0.29[a]	0.45 ± 0.18[a]	0.46 ± 0.08
Citrate	-	-	1.94 ± 0.60
Succinate	0.38 ± 0.08[a]	0.46 ± 0.10[a]	1.04 ± 0.33*
Acetate	0.32 ± 0.09[a]	0.22 ± 0.16[a]	1.41 ± 0.48*
Alanine	0.17 ± 0.25[a]	0.19 ± 0.15[a]	2.98 ± 0.87*
Lactate	0.90 ± 0.96[a]	0.74 ± 0.39[a]	8.58 ± 2.85*
β-HB	0.72 ± 0.38[a]	0.82 ± 0.36[a]	0.48 ± 0.22*

[a,b]: different letters denote a significant difference between concentrations of metabolites in uninfected and infected groups, ($\alpha \leq 0.05$).
*indicates a significant difference between concentrations of metabolites in infected and cyst groups.
[+] wet weight of cysts was, on average, 4.81 ± 1.37 g

Table 3: Percent carbon-13 in metabolites from livers of uninfected and infected *Meriones unguiculatus*, and from *Echinococcus multilocularis* cysts, after introduction of [2-^{13}C]acetate into the host.

Metabolite	Percent ^{13}C (mean ± S.D.)					
	30 minutes			120 minutes		
	uninfected (n = 15)	infected (n = 15)	cyst (n = 14)	uninfected (n = 14)	infected (n = 15)	cyst (n = 15)
Glycogen	1.67 ± 1.00^{a}	3.40 ± 2.77^{b}	1.70 ± 0.80*	1.60 ± 0.51^{a}	1.55 ± 0.31^{a+}	4.72 ± 1.60*$^{+}$
Glucose	3.62 ± 1.19^{a}	2.70 ± 1.09^{a}	2.31 ± 1.24	1.98 ± 0.85^{a+}	1.57 ± 0.26^{a+}	5.98 ± 2.72*$^{+}$
Citrate	-	-	2.93 ± 0.97	-	-	2.75 ± 0.76
Succinate	5.31 ± 2.16^{a}	5.91 ± 1.67^{a}	2.69 ± 0.94*	1.98 ± 0.63^{a+}	1.87 ± 0.87^{a+}	3.75 ± 1.26*$^{+}$
Acetate	24.75 ± 14.81^{a}	30.62 ± 14.14^{a}	38.35 ± 8.26*	4.83 ± 4.41^{a+}	3.22 ± 5.53^{a+}	14.52 ± 5.32*$^{+}$
Alanine	4.87 ± 3.55^{a}	3.07 ± 1.82^{b}	1.63 ± 0.80*	2.37 ± 1.02^{a+}	1.57 ± 0.41^{a+}	4.98 ± 1.73*$^{+}$
Lactate	3.90 ± 1.78^{a}	2.79 ± 0.82^{b}	1.64 ± 0.31*	1.97 ± 0.42^{a+}	1.62 ± 0.38^{a+}	3.54 ± 0.81*$^{+}$
β-HB	16.64 ± 3.78^{a}	15.22 ± 4.53^{a}	11.30 ± 3.53*	1.83 ± 0.76^{a+}	1.49 ± 0.33^{a+}	3.01 ± 1.03^{+}

^{a,b}: different letters denote a significant difference, ($\alpha \leq 0.05$), between percent ^{13}C in metabolites in uninfected and infected groups.

* denotes a significant difference, ($\alpha \leq 0.05$), in percent ^{13}C in metabolites between corresponding infected and cyst groups.

$^{+}$ indicates a significant difference, ($\alpha \leq 0.05$), between percent ^{13}C in metabolites in the 120 minute group, and the corresponding metabolite in the 30 minute group.

metabolites increased with time. In uninfected animals, less label was present after 120 minutes than after 30 minutes in all hepatic metabolites except glycogen, which contained a similar percentage of label as that from the 30 minute group. In livers from infected jirds, all metabolites including glycogen, contained less label two hours post injection of labeled acetate than those in the 30 minute group. In contrast, there was more label in cyst glycogen, glucose, succinate, alanine and lactate after 120 minutes than in corresponding metabolites of cysts in the 30 minute group. However, as in the liver, the percentage of label in cyst acetate and β-HB decreased with time. The percent ^{13}C in citrate remained unchanged.

II. Lipid metabolism

The ^{1}H NMR spectrum of a C:M extract of uninfected *M. unguiculatus* liver is shown in Figure 8. The following resonances were observed: peak 1, $\underline{H}C{=}C\underline{H}$ in fatty acid (FA) chains at 5.30 ppm; peak 2, $C_2\underline{H}$ in glycerol of glycerophospholipids (GPL) and triglycerides (TG) at 5.15 ppm; peak 3, $C_1\underline{H}$ in glycerol of GPL at 4.40 ppm; peak 4, $C_1\underline{H}$ in glycerol of TG at 4.32 ppm; peak 5, $OPO_2OC\underline{H}_2CH_2(CH_3)_3N^+$ in phosphatidylcholine (PTC) at 4.25 ppm; peak 6, $C_1\underline{H}$ in glycerol of PTC, phosphatidylethanolamine (PTE), phosphatidylinositol (PTI), TG and phosphatidylserine (PTS), and $C_1\underline{H}_2$ in glycerol of diacylglycerol (DG) at 4.15 ppm; peak 7, $C_3\underline{H}_2OPO_2O$ in glycerol of GPL at 3.98 ppm; peak 8, $C\underline{H}OP$ in the ring of PTI at 3.75 ppm; peak 9, $C\underline{H}_2(CH_3)_3N^+$ in PTC at 3.60 ppm; peak 10, $(C\underline{H}_3)_3N^+$ of PTC at 3.20 ppm; peak 11, $^+NH_3C\underline{H}_2$ in PTE at 3.10 ppm; peak 12, CH_2 between two double bonds in FA chains $(HC{=}CH(C\underline{H}_2HC{=}CH)_n)$ at 2.80 ppm; peak 13, CH_2 between two double bonds in FA chains

Figure 8

^{1}H NMR spectrum of a C:M extract of uninfected *Meriones unguiculatus* liver

Peak assignments:

1	$\underline{H}C{=}C\underline{H}$ in FA chains
2	$C_2\underline{H}$ in glycerol of GPL and TG
3	$C_1\underline{H}$ in glycerol of GPL
4	$C_1\underline{H}$ in glycerol of TG
5	$OPO_2OC\underline{H}_2CH_2(CH_3)_3N^+$ in PTC
6	$C_1\underline{H}$ in glycerol of PTC, PTE, PTI, TG and PTS; and $C_1\underline{H}_2$ in glycerol of DG
7	$C_3\underline{H}_2OPO_2O$ in glycerol of GPL
8	$C\underline{H}OP$ in the ring of PTI
9	$C\underline{H}_2(CH_3)_3N^+$ in PTC
10	$(C\underline{H}_3)_3N^+$ of PTC
11	$^+NH_3C\underline{H}_2$ in PTE
12	$HC{=}CHC\underline{H}_2CH{=}CH$ in FA chains
13	$HC{=}CHC\underline{H}_2CH{=}CH$ in FA chains of linoleic acid
14	$HC{=}CHC\underline{H}_2C\underline{H}_2COO$ in FA chains of docosahexaenoic acid
15	$C\underline{H}_2COO$ in FA chains
16	$HC{=}CHC\underline{H}_2CH_2CH_2COO$ in FA chains of arachidonic acid
17	$C\underline{H}_2HC{=}CHHC{=}CHC\underline{H}_2$ in FA chains
18	$HC{=}CHCH_2C\underline{H}_2CH_2COO$ in FA chains of arachidonic acid
19	$C\underline{H}_2CH_2COO$ in FA chains
20	$(C\underline{H}_2)_n$ of FA chains
21	$HC{=}CHCH_2C\underline{H}_3$ in FA chains
22	ω-$C\underline{H}_3$ of FA chains
23	$C_{18}\underline{H}_3$ in CTL
*1	indicates water
*2	indicates methanol

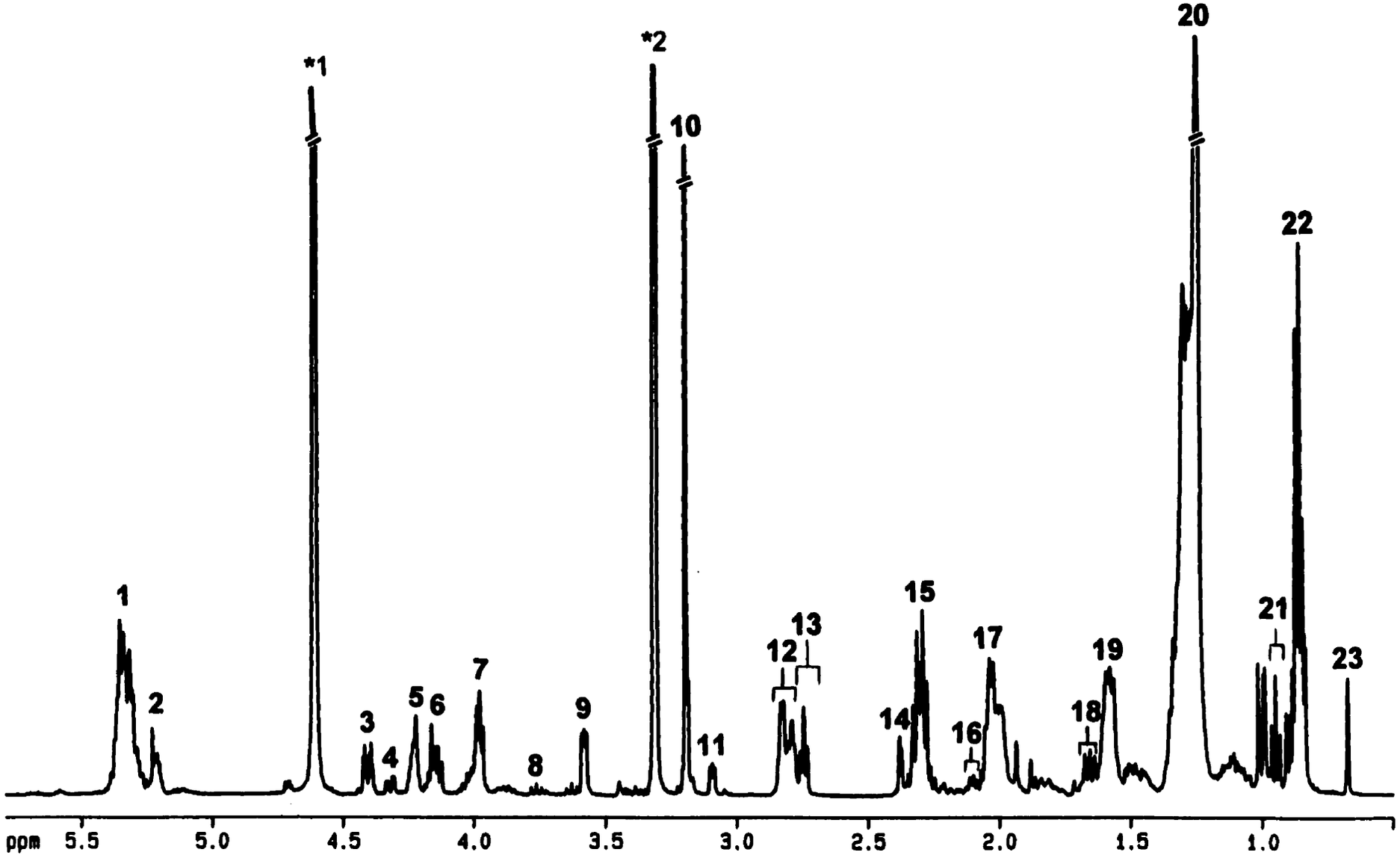
*1
*2
20
10
22
1
15
21
13
12
17
19
23
2
3
5
6
7
9
14
16
18
4
8
11
ppm 5.5
5.0
4.5
4.0
3.5
3.0
2.5
2.0
1.5
1.0

(HC=CHC$\underline{H_2}$HC=CH) of linoleic acid at 2.75 ppm; peak 14, CH_2CH_2 α to a double bond and α to C=O, respectively (HC=CHC$\underline{H_2}$C$\underline{H_2}$COO) in FA chains of 4,7,10,13,16,19-docosahexaenoic acid at 2.40 ppm; peak 15, CH_2 α to C=O in FA chains (C$\underline{H_2}$COO) at 2.30 ppm; peak 16, CH_2 α to a double bond and γ to C=O in FA chains (HC=CHC$\underline{H_2}CH_2CH_2$COO) of arachidonic acid, at 2.10 ppm; peak 17, CH_2 α to a double bond in FA chains (C$\underline{H_2}$HC=CHHC=CHC$\underline{H_2}$) at 2.05 ppm; peak 18, CH_2 β to a double bond and β to C=O in FA chains (HC=CHCH_2C$\underline{H_2}CH_2$COO) of arachidonic acid at 1.65 ppm; peak 19, CH_2 β to C=O in FA chains (C$\underline{H_2}CH_2$COO) at 1.60 ppm; peak 20, (C$\underline{H_2}$)$_n$ of FA chains at 1.30 ppm; peak 21, ω-CH_3 β to a double bond in FA chains (HC=CHCH_2C$\underline{H_3}$) at 0.95 ppm; peak 22, ω-C$\underline{H_3}$ of FA chains at 0.87 ppm; and peak 23, $C_{18}\underline{H_3}$ in cholesterol (CTL) at 0.67 ppm. Peaks 2, 3, 5, 6, 9 and 16 were not required for calculations. Concentrations of TG, GPL, PTI, PTC, PTE, FA and CTL (μmol / g wet weight) are presented in Table 4. When compared to uninfected controls, livers from infected jirds had less total GPL, PTI, PTC and CTL, but more PTE. The ratio of saturated and unsaturated FA components to total hepatic FA, the degree of unsaturation of FA chains and the average FA chain length were also analyzed. As results in Table 5 show, there was no change in ratios of saturated FA between the groups. However, there were changes in unsaturated FA moieties. In livers from infected jirds, the ratios of the C$\underline{H_2}$CH=CHHC=CHC$\underline{H_2}$ moiety, HC=CHCH_2C$\underline{H_2}CH_2$COO of arachidonic acid and HC=CHC$\underline{H_2}$HC=CH of linoleic acid to total FA were higher than those in the corresponding control group. The infection did not alter the degree of unsaturation or average chain length of hepatic FA.

A ^{1}H NMR spectrum of a C:M extract of *E. multilocularis* cyst is shown in Figure 9. In cyst spectra, the same resonances as in spectra of *M. unguiculatus* liver were present, except for the absence of a detectable peak for PTI at 3.75

Table 4: Concentrations of lipid from livers of uninfected and infected *Meriones unguiculatus* and from *Echinococcus multilocularis* cysts

Lipid	Concentration (mean ± S.D.) (μmol / g wet weight)		
	uninfected (n = 15)	infected (n = 18)	cysts+ (n = 18)
Total TG	5.63 ± 2.37[a]	6.26 ± 5.66[a]	5.38 ± 8.37
Total GPL	34.99 ± 2.84[a]	31.97 ± 4.79[b]	6.94 ± 1.69*
PTI	4.50 ± 0.88[a]	2.65 ± 0.68[b]	NM
PTC	21.52 ± 1.42[a]	19.21 ± 2.16[b]	4.68 ± 1.13*
PTE	7.42 ± 0.60[a]	8.27 ± 1.16[b]	1.22 ± 0.63*
Total FA	114.02 ± 8.69[a]	102.86 ± 17.75[a]	42.80 ± 26.80*
CTL	8.57 ± 0.97[a]	6.93 ± 0.99[b]	4.72 ± 0.69*

[a,b]: different letters denote a significant difference, ($\alpha \leq 0.05$), between concentrations of lipid in uninfected and infected groups.

* indicates a statistically significant difference, ($\alpha \leq 0.05$), between concentrations of lipid in cyst and infected groups.

NM = not measureable

Abbreviations: TG, triacylglycerols; GPL, glycerophospholipids; PTI, phosphatidylinositol; PTC, phosphatidylinositol; PTE, phosphatidylethanolamine; FA, fatty acid; and CTL, cholesterol.

+ wet weight of cysts was, on average, 10.64 ± 5.00 g

Table 5: Analysis of fatty acid components in livers from uninfected and infected *Meriones unguiculatus* and from *Echinococcus multilocularis* cysts

Fatty acid component	Ratio of individual FA component : total FA (mean ± S.D.)		
	Uninfected	Infected	Cysts
Saturated fatty acid components			
$C\underline{H_2}CH_2COO$	0.87 ± 0.04[a]	0.85 ± 0.06[a]	0.72 ± 0.09*
$(C\underline{H_2})_n$	8.11 ± 0.27[a]	8.36 ± 0.61[a]	7.91 ± 0.41*
$CH_2C\underline{OO}$	0.81 ± 0.03[a]	0.82 ± 0.07[a]	0.60 ± 0.10*
Unsaturated fatty acid components			
$HC{=}CH(C\underline{H_2}HC{=}CH)_n$	0.59 ± 0.05[a]	0.59 ± 0.06[a]	0.25 ± 0.09*
$C\underline{H_2}CH{=}CHHC{=}CHC\underline{H_2}$	0.54 ± 0.05[a]	0.60 ± 0.06[b]	0.39 ± 0.05*
$CH{=}CHCH_2C\underline{H_2}CH_2COO$ of arachidonic acid	0.14 ± 0.03[a]	0.18 ± 0.03[b]	0.12 ± 0.04*

continued ...

CH=CHC$\underline{H}_2$C$\underline{H}_2$COO of docosahexaenoic acid	0.05 ± 0.01[a]	0.06 ± 0.01[a]	0.02 ± 0.01*
CH=CHC$\underline{H}_2$CH=CH of linoleic acid	0.18 ± 0.02[a]	0.21 ± 0.02[b]	0.14 ± 0.02*
		Degree of Unsaturation	
$\underline{H}$C=C$\underline{H}$	1.20 ± 0.04[a]	1.23 ± 0.09[a]	0.80 ± 0.10*
		Average chain length	
	15.76 ± 0.31[a]	16.18 ± 0.89[a]	13.75 ± 0.58*

[a,b]: different letters denote a significant difference, ($\alpha \leq 0.05$), between ratios of fatty acid components in uninfected and infected groups.

* indicates a significant difference, ($\alpha \leq 0.05$), between ratios of fatty acid components in cyst and infected groups.

Figure 9

^{1}H NMR spectrum of a C:M extract of *Echinococcus multilocularis* cyst

Peak assignments:

1	$\underline{H}C=C\underline{H}$ in FA chains
2	$C_2\underline{H}$ in glycerol of GPL and TG
3	$C_1\underline{H}$ in glycerol of GPL
4	$C_1\underline{H}$ in glycerol of TG
5	$OPO_2OC\underline{H}_2CH_2(CH_3)_3N^+$ in PTC
6	$C_1\underline{H}$ in glycerol of PTC, PTE, PTI, TG and PTS; and $C_1\underline{H}_2$ in glycerol of DG
7	$C_3\underline{H}_2OPO_2O$ in glycerol of GPL
9	$C\underline{H}_2(CH_3)_3N^+$ in PTC
10	$(C\underline{H}_3)_3N^+$ of PTC
11	$^+NH_3C\underline{H}_2$ in PTE
12	$HC=CHC\underline{H}_2CH=CH$ in FA chains
13	$HC=CHC\underline{H}_2CH=CH$ in FA chains of linoleic acid
14	$HC=CHC\underline{H}_2C\underline{H}_2COO$ in FA chains of docosahexaenoic acid
15	$C\underline{H}_2COO$ in FA chains
16	$HC=CHC\underline{H}_2CH_2CH_2COO$ in FA chains of arachidonic acid
17	$C\underline{H}_2HC=CHHC=CHC\underline{H}_2$ in FA chains
19	$C\underline{H}_2CH_2COO$ in FA chains
20	$(C\underline{H}_2)_n$ of FA chains
21	$HC=CHCH_2C\underline{H}_3$ in FA chains
22	ω-$C\underline{H}_3$ of FA chains
23	$C_{18}\underline{H}_3$ in CTL
*1	indicates water
*2	indicates methanol

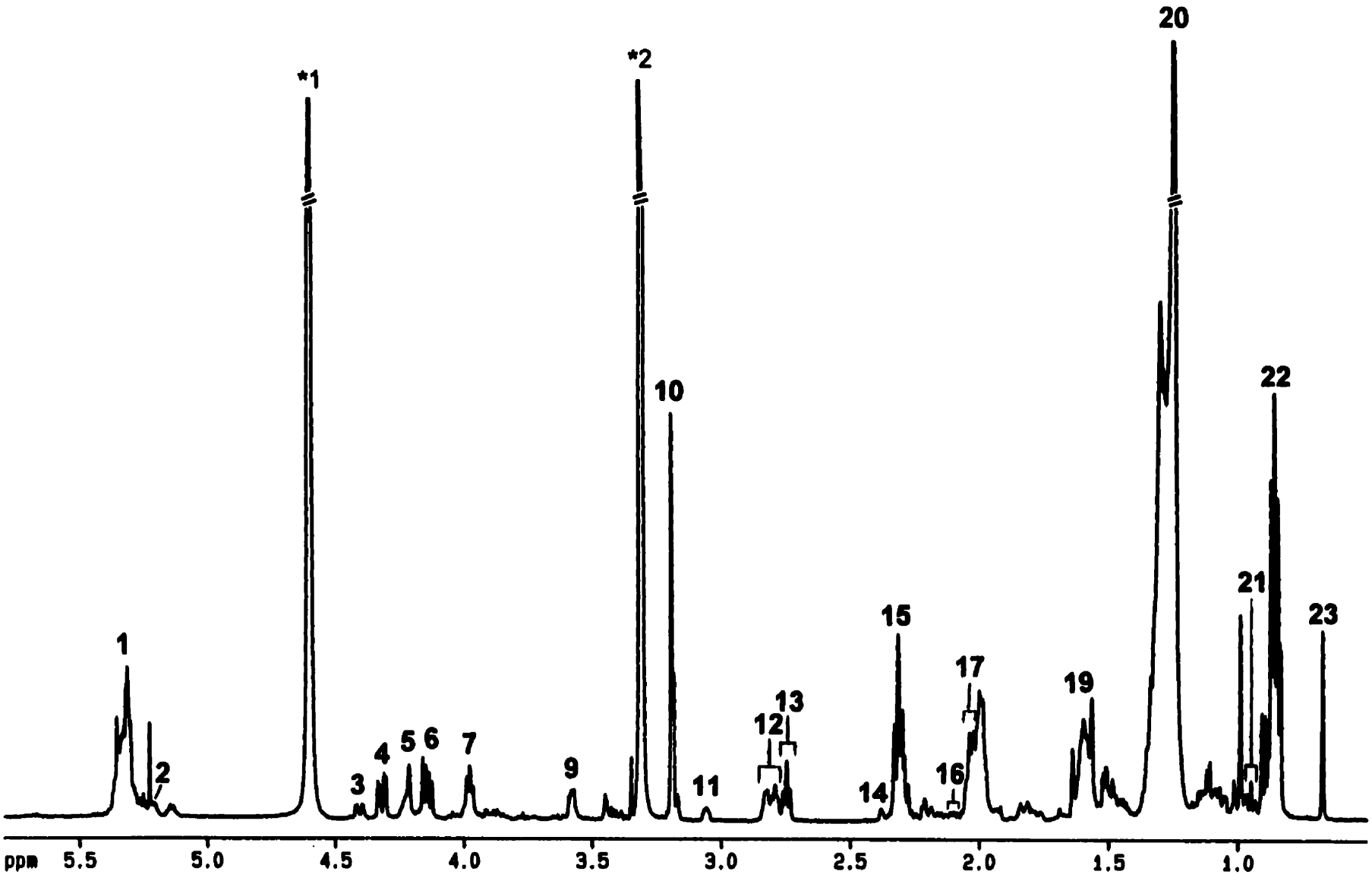
*1
*2
20
10
22
1
2
3
4
5
6
7
9
11
12
13
14
15
16
17
19
21
23
ppm
5.5
5.0
4.5
4.0
3.5
3.0
2.5
2.0
1.5
1.0

ppm (peak 8), and for arachidonic acid at 1.65 ppm (peak 18). In general, the concentrations of lipid in the cysts were lower than those in the livers (Table 4). When the same FA moieties as in the liver were analyzed for cysts, it was found that in cysts on average, all saturated and unsaturated FA components had lower ratios (Table 5). Furthermore, the degree of unsaturation of FA chains and the average FA chain length were also lower than those in the liver.

Discussion

I. Carbohydrate metabolism

Detection of carbon-13 beyond natural abundance in ^1H spin echo NMR spectra of PCA extracts of livers from uninfected and infected *M. unguiculatus* provides solid evidence that exogenous [2-^{13}C]acetate was metabolized in host biochemical pathways. Labeled glucose found in jird liver could only be synthesized via entry of exogenous acetate into the Kreb's cycle followed by use of labeled intermediate metabolites in gluconeogenesis. Entry of labeled acetate into host metabolism and subsequent flow of carbon-13 atoms through Kreb's cycle intermediates is presented in Figure 10. Acetyl CoA, labeled at carbon-2 from exogenous [2-^{13}C]acetate, enters the Kreb's cycle via condensation with unlabeled oxaloacetate to form citrate labeled at carbon-4. Although citrate is a symmetrical molecule, it is known that carbon-2 of acetate becomes carbon-4 of citrate, due to stereospecific catalysis by citrate synthase (Voet and Voet, 1995). The label remains at carbon-4 in isocitrate and α-ketoglutarate, even though these reactions are reversible. Carbon-1 of α-ketoglutarate is lost as CO_2 due to decarboxylation by α-ketoglutarate dehydrogenase. Thus, the carbon-13 label from [2-^{13}C]acetate is now located at carbon-3 of succinyl CoA (Cohen and Bergman, 1994). Loss of CoA from succinyl CoA generates succinate labeled at carbon-2 or -3. Although carbon-2 of acetate has become carbon-3 of succinate in a given orientation, the succinate molecule has the opportunity to reorient itself once released from succinyl CoA synthetase. In this opposite orientation, carbon-13 label will now appear to be at carbon-2. Therefore, although only one carbon atom in the succinate molecule is labeled during the first turn of the Kreb's cycle, it is

Figure 10

The fate of carbon-13 label from [2-^{13}C]acetate in intermediates of the Kreb's cycle

Carbon-13 label from [2-^{13}C]acetate enters the Kreb's cycle as [2-^{13}C]acetyl CoA. This acetyl CoA condenses with oxaloacetate initiating the first turn of the cycle.

• indicates the position of ^{13}C label during the first turn of the Kreb's cycle. At malate, multiple carbons with label indicators represent only the possible position of carbon-13 label and not multiple labeled carbon atoms. Thus, only 1 carbon atom in malate and oxaloacetate will be labeled from [2-^{13}C]acetate on the first turn of the Kreb's cycle.

^ indicates the possible location of ^{13}C during the second turn of the Kreb's cycle. Once again, label will be located at only one of the carbon atoms indicated by ^. Therefore, two carbon atoms in Kreb's cycle intermediates may be labeled during the second turn, one represented by * and one by ^.

~ indicates possible position of ^{13}C during the third turn of the Kreb's cycle. Thus, three atoms may be labeled during the third turn, one represented by *, one by ^ and one by ~. If labeled intermediates remain in the mitochondria and continue to participate in the Kreb's cycle, subsequent turns could result in further scrambling of label and increased label at neighboring carbon-13 atoms.

Enzymes of the Kreb's cycle include:

1, acetyl CoA synthase; 1a, acetyl CoA hydrolase; 2, citrate synthase; 3, aconitase; 4, isocitrate dehydrogenase; 5, α-ketoglutarate dehydrogenase; 6, succinyl CoA synthetase; 7, succinate dehydrogenase; 8, fumarase; 9, malate dehydrogenase.

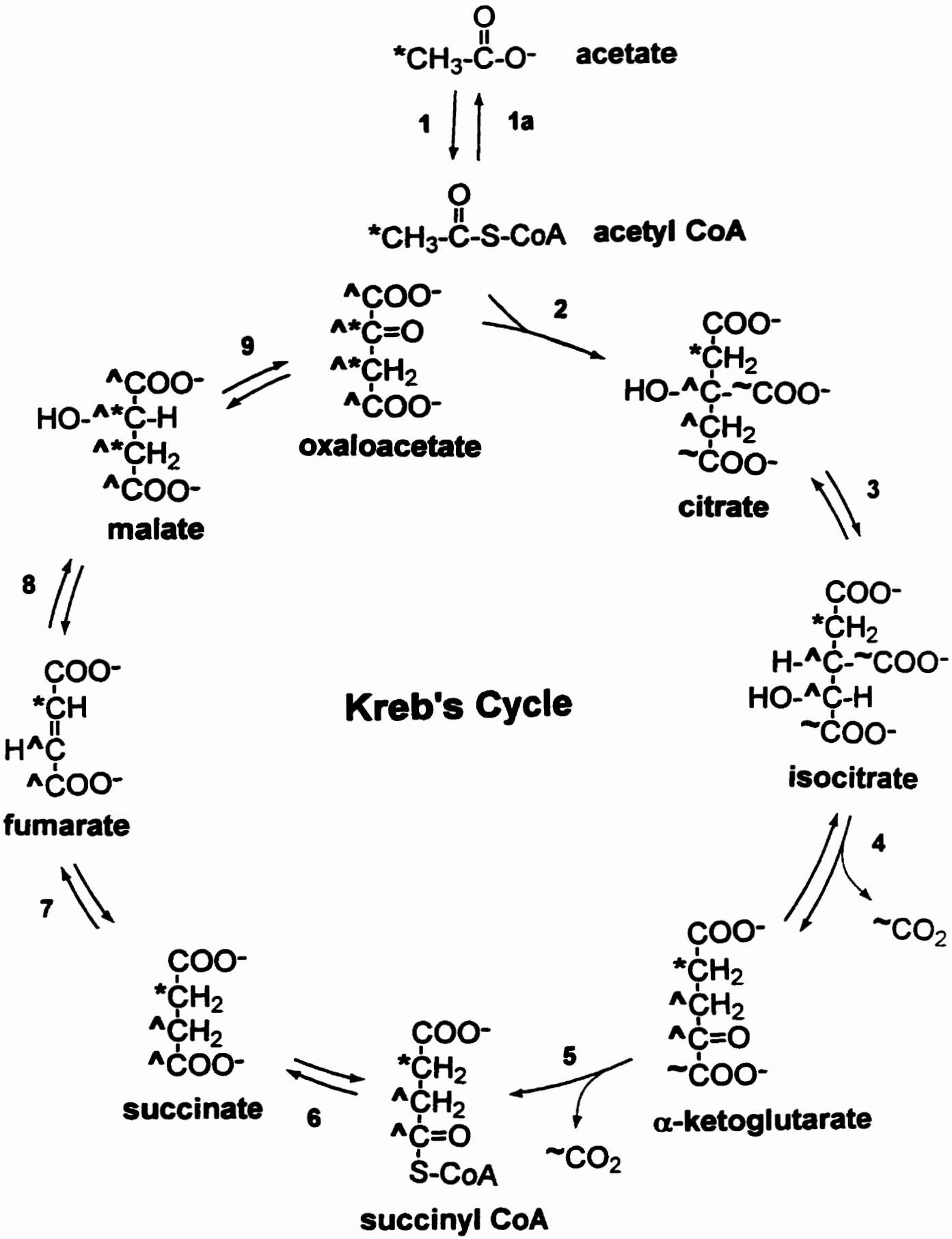
acetate
1
1a
acetyl CoA
2
oxaloacetate
citrate
3
isocitrate
4
~CO2
α-ketoglutarate
5
~CO2
6
succinyl CoA
succinate
7
fumarate
8
malate
9
Kreb's Cycle

generally accepted that the position of the labeled atom is randomized, and may be located at either carbon-2 or -3. Although some evidence of conservation of orientation in the succinate molecule is provided by Sherry *et al.* (1994) who studied ^{13}C NMR of rat hearts perfused with [2-^{13}C]acetate, this phenomenon was observed only during the first 10-15 minutes of perfusion at 37°C. It is still unclear whether or not orientation of succinate is conserved, or whether contributions from other pathways are involved. As such, the generally accepted assumption of randomization of label at succinate in the Kreb's cycle has been employed here. Succinate and fumarate, which are both symmetrical, are thus labeled at either carbon-2 or -3. When fumarate is converted to malate, water is added across the double bond. This results in two possible, and unequivalent, malate isotopomers, labeled at either carbon-2 or -3. Oxaloacetate, also labeled at either carbon-2 or -3, is then generated from malate by malate dehydrogenase.

At this point, both malate and oxaloacetate, labeled at carbon-2 or carbon-3, may either exit the cycle and the mitochondrion as malate or PEP, or continue on in the cycle initiating another turn. In the latter, the oxaloacetate will react with another molecule of acetyl CoA labeled at carbon-2. Acetyl CoA entering the Kreb's cycle is initially assumed to be labeled at carbon-2 due to the large influx of exogenous [2-^{13}C]acetate. Therefore, citrate formed during the second turn of the Kreb's cycle will be labeled at carbon-4, from exogenous acetate, and at either carbon-3 or carbon-2 from labeled oxaloacetate (Badar-Goffer *et al.*, 1990; Sonnewald *et al.*, 1993). As the second turn of the cycle continues, there is further randomization of label at malate, with the possible formation of three different malate isotopomers. Now, should the malate and oxaloacetate remain in the mitochondrion and participate in a third turn of the Kreb's cycle, the carbon-13 label may be lost as carbon dioxide at the isocitrate

to α-ketoglutarate step and at the α-ketoglutarate to succinyl CoA step. First, carbon-6, the carboxyl group attached to carbon-3 of isocitrate, will be lost as carbon dioxide, followed by the carboxyl group at carbon-1 of α-ketoglutarate. These reactions, involving aconitase and isocitrate dehydrogenase are also reversible, although metabolite orientation is conserved (Mathews and van Holde, 1990; Des Rosiers *et al.*, 1994; 1995; Fernandez and Des Rosiers, 1995).

When labeled malate exits the mitochondrion, it can participate in gluconeogenesis. Through the action of cytosolic malate dehydrogenase, malate is first converted to oxaloacetate which, in turn, is converted to PEP by phosphoenolpyruvate carboxykinase (PEPCK). This metabolite will be labeled at carbon-2 or carbon-3 if it is a product of the first turn of the Kreb's cycle (Figure 11). PEP then forms 2-phosphoglycerate, in a reaction catalyzed by enolase, followed by conversion to 3-phosphoglycerate via phosphoglycerate mutase. 1,3-Bisphosphoglycerate (1,3-BPG), formed from 3-phosphoglycerate by phosphoglycerate kinase will also be labeled at carbon-2 or -3. Further randomization of label results when 1,3-BPG is converted to glyceraldehyde-3-phosphate (GAP) by GAP dehydrogenase. This is because GAP, labeled at either carbon-2 or -3 is then interconverted with dihydroxyacetone phosphate (DHAP), as in glycolysis, by triose phosphate isomerase. Formation of fructose-1,6-bisphosphate (F-1,6-BP), catalyzed by adolase, requires one molecule of GAP and one molecule of DHAP. It is possible that each of these required precursors may be labeled at either carbon-2 or carbon-3, resulting in isotopomers of F-1,6-BP labeled at either carbon-1 or -2, and carbon-5 or -6. This F-1,6-BP is then converted via fructose-1,6-bisphosphatase to fructose-6-phosphate (F-6-P) followed by conversion to glucose-6-phosphate (G-6-P) by phosphoglucose isomerase, each isomer being labeled at either carbon-1 or -2

Figure 11

The fate of carbon-13 label from [2-^{13}C]acetate in metabolites of gluconeogenesis

Following entry of acetyl CoA into the Kreb's cycle, carbon-13 labeled malate may exit the mitochondrion. Once in the cytosol, it is converted to oxaloacetate and then participates in gluconeogenesis.

* indicates the position of carbon-13 label.

Enzymes include:

1, cytosolic malate dehydrogenase; 2, PEPCK; 3, enolase; 4, phosphoglycerate mutase; 5, phosphoglycerate kinase; 6, GAP dehydrogenase; 7, triose phosphate isomerase; 8, aldolase; 9, fructose 1,6-bisphosphatase; 10, phosphoglucose isomerase; 11, glucose-6-phosphatase.

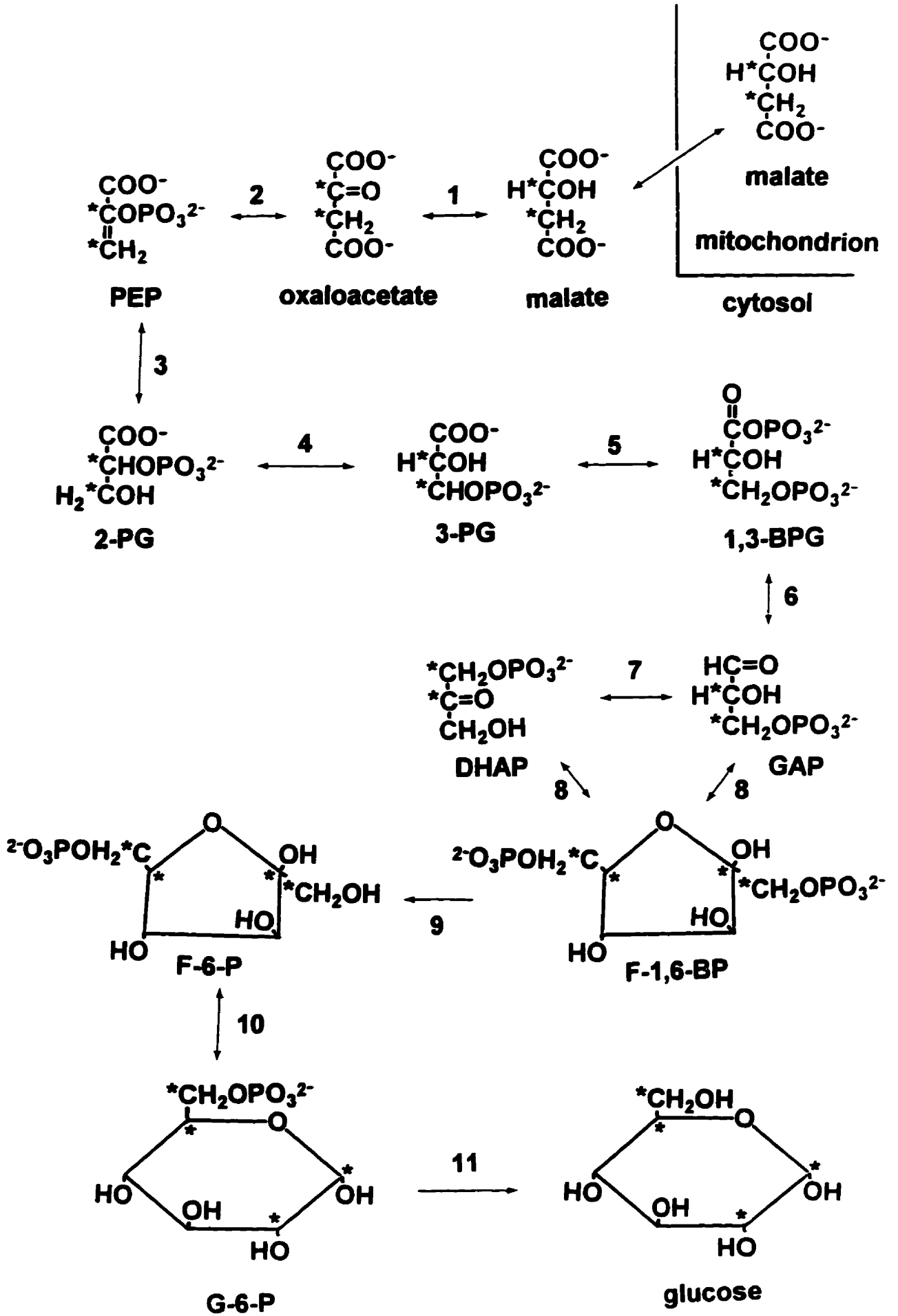
malate
mitochondrion
cytosol
PEP
oxaloacetate
malate
2
1
3
2-PG
3-PG
1,3-BPG
4
5
6
DHAP
GAP
7
8
8
F-6-P
F-1,6-BP
9
10
G-6-P
glucose
11

and carbon-5 or -6. Glucose is then formed from G-6-P via glucose-6-phosphatase. Several isotopomers of glucose are possible, with carbon-13 label located at either carbon-1 or -2, and carbon-5 or -6. With successive turns of the Kreb's cycle, randomization of label in glucose is increased. However, to explore the labeling patterns of glucose from [2-^{13}C]acetate in more detail, ^{13}C NMR would have to be employed.

Glucose synthesized by the infected host had three fates. In the liver, some of it was stored in glycogen and some could have been used in catabolic processes, as suggested by the presence of label in lactate and alanine. However, some of the labeled glucose was also found in the parasite. This indicates that *E. multilocularis* siphoned off labeled glucose produced by the host, as carbon-13 could only end up in the glucose molecule through entry of [2-^{13}C]acetate in to the Kreb's cycle followed by subsequent participation of labeled metabolites in gluconeogenesis. As cestodes do not have a complete Kreb's cycle (Smyth and McManus, 1989), it is unlikely that the parasite could incorporate labeled atoms from acetate into glucose. Further, there is also no convincing evidence of gluconeogenesis in these organisms except from the level of fumarate (Blackburn *et al.*, 1986). Thus, the presence of labeled glucose in *Echinococcus* cysts and the decrease in the amount of this carbohydrate in livers of infected jirds demonstrates competition between the host and parasite for the product which was synthesized in gluconeogenic pathways of the host. Although, 30 minutes into the experiment, some of the labeled glucose was used in host glycogenesis, the total amount of hepatic glycogen was significantly lower in infected jirds than in controls. Thus, as in previous studies (Novak *et al.*, 1993; 1995), the depletion of glucose and glycogen in livers of infected jirds again illustrates that *E. multilocularis* induces a starvation effect in its host.

Carbon-13 enrichment of most hepatic metabolites decreased with time. The results indicate that at the end of two hours, most of the labeled acetate and labeled metabolites were processed in host biochemical pathways and/or distributed to the extrahepatic tissues. Also, some of the carbon-13 labeled compounds, namely glucose, acetate and β-HB, were taken up by the cysts. My method of detection only allowed quantitative analysis of label at C_1 of glucose. A scheme for its catabolism in *E. multilocularis* to the labeled end products lactate, alanine, succinate and acetate is outlined in Figure 12. First, in the cytosol, [1-^{13}C]glucose is metabolized via glycolysis to PEP labeled at carbon-3. PEP is converted by PEPCK to [3-^{13}C]oxaloacetate or to pyruvate, also labeled at carbon-3, by pyruvate kinase. The pyruvate is then either reduced to [3-^{13}C]lactate by lactate dehydrogenase, transaminated to [3-^{13}C]alanine by a transaminase. Malate dehydrogenase catalyzes the reaction of [3-^{13}C]oxaloacetate to [3-^{13}C]malate which is further metabolized in the mitochondria. There, malate is either converted by malic enzyme to [3-^{13}C]pyruvate, by fumarase to fumarate labeled at carbon-2, or by malate dehydrogenase to [3-^{13}C]oxaloacetate. Labeled pyruvate, converted initially to [2-^{13}C]acetyl CoA by the pyruvate dehydrogenase complex, then becomes [2-^{13}C]acetate. Fumarate, produced from labeled malate forms succinate, labeled at carbon-2, via fumarate reductase. The ^{13}C labeled metabolic end products lactate, alanine, succinate and acetate were then excreted into the host.

Recent experiments in our lab with the tetrathyridia of the cestode *Mesocestoides vogae* revealed that mitochondrial oxaloacetate, formed from malate via malate dehydrogenase, can, with the help of citrate synthase, combine with acetyl CoA to form citrate (Payette, 1996). This TCA cycle intermediate is then also excreted as demonstrated by the presence of the citrate resonance in ^{1}H NMR spectra of culture media in which tetrathyridia were

Figure 12

Metabolism of labeled glucose in *Echinococcus multilocularis* cysts.

• indicates carbon-13 label. Glucose taken from the host is labeled at carbon-1. This glucose is then used in parasite metabolic pathways to produce energy for the cyst.

Enzymes include:

1, glycolysis; 2, pyruvate kinase; 3, lactate dehydrogenase; 4, transaminase; 5, PEPCK; 6, cytosolic malate dehydrogenase; 7, cytosolic malic enzyme; 8, mitochondrial malic enzyme; 9, fumarase; 10, fumarate reductase; 11, pyruvate dehydrogenase complex; 12; mitochondrial malate dehydrogenase; 13, citrate synthase; 14, not known; E, metabolite is excreted

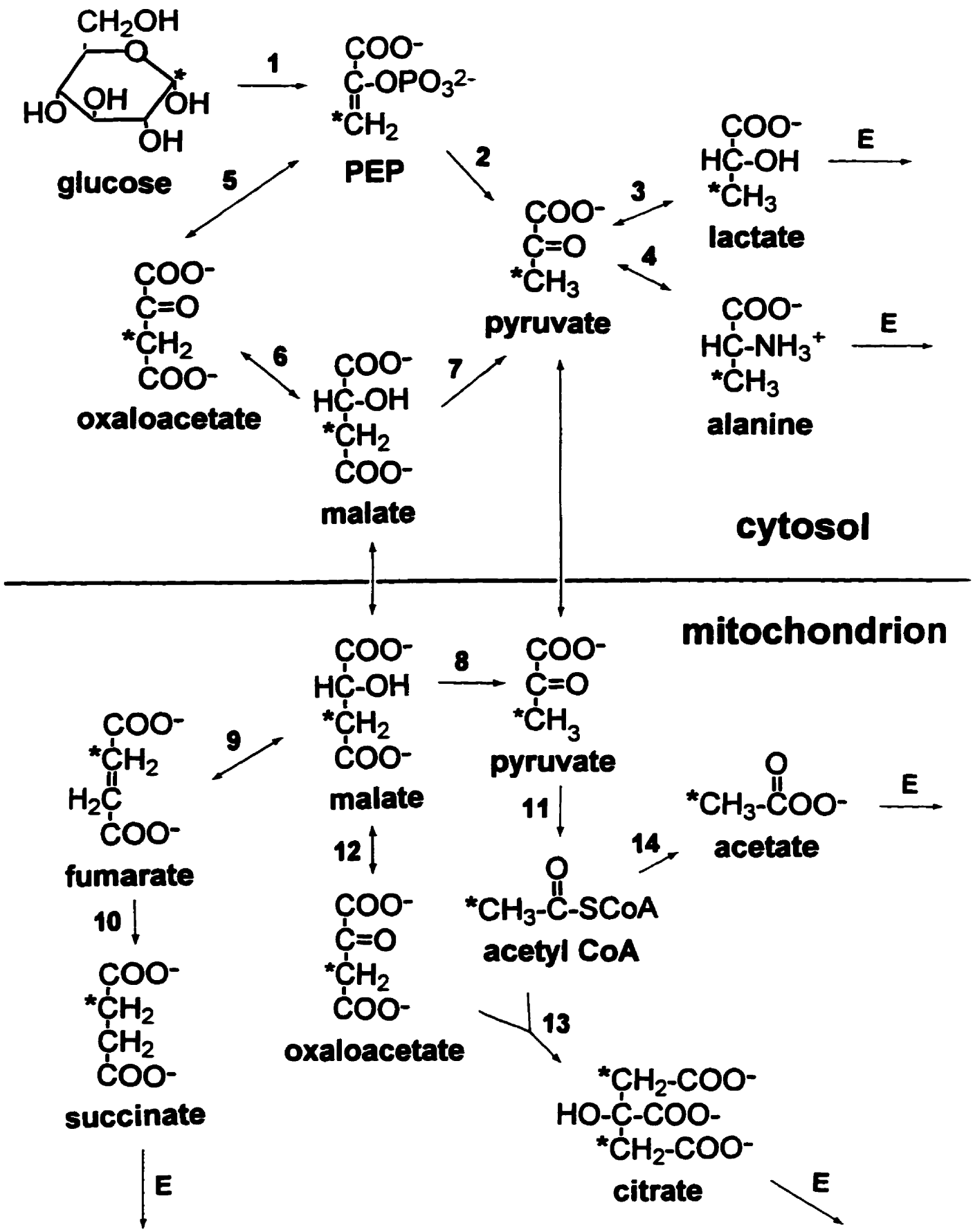
glucose
1
PEP
2
pyruvate
3
lactate
E
4
5
oxaloacetate
6
malate
7
alanine
E
cytosol
mitochondrion
8
pyruvate
9
fumarate
malate
10
succinate
E
11
12
oxaloacetate
13
14
acetyl CoA
acetate
E
citrate
E

incubated. Payette's experiments showed that in *Mesocestoides*, the Kreb's cycle is not functioning completely and that some of the intermediates which are produced cannot be utilized and are therefore excreted. Similarly, results of the present study suggest that only part of the Kreb's cycle is operational to a significant extent in the mitochondria of *E. multilocularis*. Detection of citrate, labeled at carbon-2, in tissues of this parasite indicates citrate synthase activity. Indeed, citrate synthase and other Kreb's cycle enzymes were found in *E. multilocularis* cysts (McManus and Bryant, 1995). The build up of citrate to a level that can be readily detected by NMR, with no evidence for subsequent metabolites, is consistent with greater activity of citrate synthase than of the enzymes in the following steps.

As discussed above, acetate produced by the parasite from [1-^{13}C]glucose becomes labeled at carbon-2. However, it seems unlikely that the high level of ^{13}C enrichment of acetate observed in *E. multilocularis* cysts could have been produced solely by catabolism of labeled glucose. Novak *et al.* (1992) found that the concentration of acetate in intraperitoneal cysts from unstarved jirds was lower than that of lactate, alanine and succinate, suggesting that conversion of glucose to acetate proceeds more slowly than to the other metabolites. Therefore, it seems that the majority of labeled acetate found in *E. multilocularis* was the result of direct uptake by the parasite. The percent ^{13}C in acetate decreased on going from the 30 minute to the 120 minute experiment.

A similar reduction in carbon-13 label with time was observed for β-HB in livers of infected jirds and *E. multilocularis* cysts. This ketone body was most likely taken up from the host rather than synthesized *de novo* by the cysts. It is known that cestodes do not possess a pathway for β-oxidation of FA chains (Smyth and McManus, 1989), which is the usual source of acetyl CoA for ketone body synthesis in mammals. Also, the enzyme HMG CoA synthase is required

for ketone body synthesis (Murray *et al.*, 1988). While present in the liver of the host, it is not known whether this enzyme is present in *E. multilocularis* cysts. Even if the parasite could synthesize β-HB, this ketone body, along with the labeled metabolic excretory end products lactate, alanine, succinate and acetate, cannot be utilized by the cysts in known biochemical pathways due to an incomplete Kreb's cycle and non-functional gluconeogenic pathway. Thus, the labeled β-HB in *E. multilocularis* cysts was most likely of host origin.

As acetate is used in host metabolic pathways, it is highly probable that acetate of parasite origin is disposed of in biochemical pathways of the host. Although lactate, alanine and succinate had to be excreted by *Echinococcus* into the host, there was no difference in the concentration of these metabolites between livers of uninfected and infected jirds. That would mean, in order for the concentrations to be the same, lactate, alanine and succinate would have to be metabolized, in infected animals, at a greater rate. Increased gluconeogenesis has been previously described for cancer cells which behave much like parasites in terms of metabolic interaction with their host (Dills Jr., 1993). The accumulation of the tumor metabolic end product lactate in the host is not observed because host gluconeogenesis accelerates, using this tumor-produced metabolite as a substrate, in proportion to the rate of tumor glycolysis. Indeed, gluconeogenesis is known to increase with increasing precursor supply (Alberti *et al.*, 1992). Therefore, if in the present experiments, more lactate and alanine were utilized in the liver of infected hosts, this could account for the unchanged concentration, and lower percent enrichment of these metabolites after 30 minutes. Similarly, there was no observable change in the amount of hepatic succinate in infected jirds. This could also be a result of increased utilization of this metabolite in livers of infected hosts. However, unlike lactate and alanine, the percent ^{13}C in hepatic succinate in uninfected and infected

hosts did not differ. Since [2-^{13}C]acetate must be metabolized via the Kreb's cycle, all Kreb's cycle intermediates, including succinate, should therefore have a constant influx of carbon-13 label. Thus, in the infected host, ^{13}C enrichment of succinate seems to reflect a balance between metabolism of this and other Kreb's cycle intermediates with the influx of carbon-13 label from [2-^{13}C]acetate.

After 30 minutes, the total concentration of hepatic acetate, labeled and unlabeled, was higher in infected hosts. This increase in the amount of acetate suggests that further metabolic alterations have occurred in the infected host. It is known that acetate enters into mammalian biochemical pathways by conversion to acetyl CoA via acetyl CoA synthase (Crabtree *et al.*, 1990). It seems likely that in the infected host there will be a higher concentration of acetyl CoA due to greater β-oxidation of FAs. In turn, a higher concentration of acetyl CoA would inhibit more the reaction of acetate to form acetyl CoA in this readily reversible reaction.

In the liver, at 30 and 120 minutes post-injection, the majority of the carbon-13 label was present in acetate. There was no difference in the percent ^{13}C of hepatic acetate between uninfected and infected hosts. This label was most likely due to residual exogenous [2-^{13}C]acetate and, in the infected host, also due to contribution of labeled acetate produced and excreted by the parasite. In addition, some of the [2-^{13}C]acetate was carried by blood to *E. multilocularis* cysts and since the parasite cannot metabolize this compound, it eventually had to be returned to and recycled by the host.

Metabolism of acetate in the host was not carried out solely by direct oxidation in the Kreb's cycle. The relatively high carbon-13 enrichment of β-HB in both uninfected and infected hosts after 30 minutes suggests that a large amount of exogenous acetate was initially diverted to ketone body synthesis. Indeed, more β-HB was produced in infected animals than in the controls. This

result is in contrast with that of Novak *et al.* (1995) who found a decrease in hepatic β-HB in *E. multilocularis*-infected jirds when exogenous glucose was administered in a bolus injection. Under those experimental conditions, β-oxidation of FAs would have been the primary source of acetate and acetyl CoA for ketogenesis (Guyton, 1991), and the host was probably using β-HB faster than acetate could be liberated from FAs. Similarly, Corbin *et al.* (1996) suggested that an observed decrease in hepatic β-HB in mice infected with cysticerci of *Taenia crassiceps* could be due to an increased demand for FA by the parasite or that more β-HB had been used by the host to compensate for energy stolen by the parasite. In this experiment, labeled acetate could have been diverted to ketogenesis as an alternate means of metabolizing excess acetyl CoA. Indeed, when the amount of acetyl CoA exceeds that of oxaloacetate, the accumulating acetyl CoA is directed toward ketone body synthesis (Orten and Neuhaus, 1982). This increase in β-HB in infected animals was most likely due to the extra starvation induced by the parasite. However, after 120 minutes, all labeled β-HB left the liver and there was no difference in the concentration of hepatic β-HB between uninfected and infected jirds. It seems that with time, as the excess acetate was metabolized, less of it was available for ketogenesis and more β-HB was released into circulation for further utilization.

The metabolism of hepatic PC, acylcarnitine and glycine was also affected by *E. multilocularis* infection as the concentrations of these metabolites were increased in infected jirds for both the 30 and 120 minute experiments. PC is formed in the cytosol by phosphorylation of choline via choline kinase (Mathews and van Holde, 1990). It is a precursor in the synthesis of PTC, the most common membrane phospholipid (Ansell and Spanner, 1982; Bhamidipati and Hamilton, 1993). PTC is predominantly synthesized by the CDP-choline

pathway (Figure 13). PC is converted to CDP-choline via CTP:PC cytidylyltransferase (6) followed by transfer of the PC component to 1,2-DG, catalyzed by CDP-choline:1,2-DG cholinephosphotransferase (5). The reaction catalyzed by CTP:PC cytidylyltransferase (6) is the rate limiting step in PTC synthesis due to the limited availability of CTP (Ansell and Spanner, 1982; Kuesel *et al.*, 1990; Mathews and van Holde, 1990). In their work with human tumor cells, Kuesel *et al.* (1990) suggested that increased PC levels may result from saturation of the rate limiting enzyme CTP:PC cytidylyltransferase (6) in the CDP-choline pathway. When the enzyme CTP:PC cytidylyltransferase (6) is saturated, PC may not be used as quickly as it is produced and therefore accumulates. Also, the reactions of the CDP-choline pathway are reversible, utilizing the same enzymes in both the synthesis and degradation reactions (Ansell and Spanner, 1982; Kuesel *et al.*, 1990). Thus, increased degradation of PTC to PC in response to a greater requirement for FA oxidation in the nutrient-depleted infected host may also contribute to saturation of the enzyme CTP:PC cytidylyltransferase (6). Further, as indicated in Figure 13, specific hydrolysis of PTC by phospholipase C (4) releases additional PC, which could also contribute to an increase in the concentration of this metabolite (Kuesel *et al.*, 1990; Ferretti *et al.*, 1993).

Livers of infected jirds removed after 120 minutes also contained more glycerophosphocholine (GPC). GPC is another product of PTC breakdown (Figure 13). Hydrolysis of PTC by phospholipase A_2 (2) liberates the FA from C_2 of the glycerol backbone of the phospholipid, creating lysophosphatidylcholine (LPC) (Voet and Voet, 1995). This LPC can be further hydrolyzed, releasing another FA moiety, to form GPC. A greater rate of PTC breakdown by phospholipase A_2 (2) would lead to an increase in the amount of hepatic GPC.

Figure 13

Pathways of phosphatidylcholine synthesis in mammals

Enzymes include:

1, phosphatidylcholine phosphatidylhydrolase; 2, phospholipase A_2; 2a, acyl CoA:2-acyl-sn-glycero-3-phosphocholine acyltransferase; 3, 2-lysophosphatidylcholine acylhydrolase; 3a, acyltransferase; 4, phospholipase C; 5, CDP-choline:1,2-DG cholinephsophotransferase; 6, CTP:PC cytidylyltransferase; 7, choline kinase.

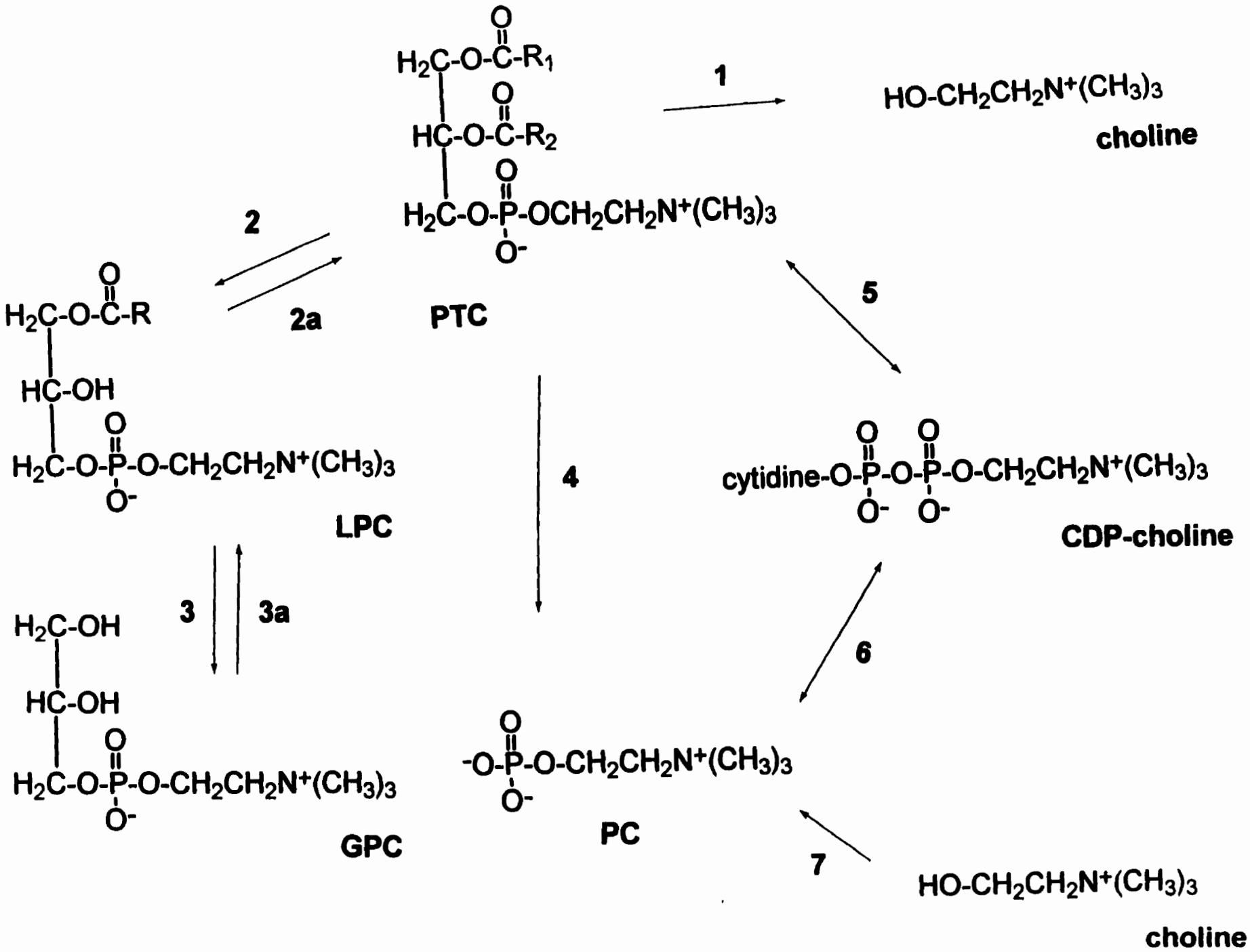
1
HO-CH2CH2N+(CH3)3
choline
2
2a
PTC
5
LPC
4
cytidine-O-P-O-P-O-CH2CH2N+(CH3)3
CDP-choline
3
3a
6
PC
7
HO-CH2CH2N+(CH3)3
choline
GPC

However, as an elevated amount of this hepatic phosphomonoester was detected only in the 120 minute group, it is possible that an increase in hepatic GPC was the direct result of a severe starvation effect. When, at the time of dissection, the animal body mass was corrected for the parasite cyst mass, those in the 120 minute group lost 14.15% in body mass whereas those in the 30 minute group lost only 0.09% of their body mass. Thus, in the more starved host, greater amounts of PTC was probably broken down via the LPC pathway, in addition to the CDP-choline pathway and phospholipase C, in response to increased energy demands of the parasitized hosts.

In order for FAs to be used in energy generating pathways, they must be first taken up by the cells and activated in the cytosol to fatty acyl CoA via acyl CoA synthase. This fatty acyl CoA is then transferred to a fatty-acyl carrier, carnitine, in a reaction catalyzed by carnitine palmitoyltransferase I located on the external surface of the outer mitochondrial membrane. The resulting acylcarnitine can then cross the mitochondrial membrane in exchange for free carnitine, which is liberated from acylcarnitine in the mitochondria. During this process, the FA moiety is released in a reaction catalyzed by carnitine palmitoyltransferase II located on the matrix side of the inner membrane of the mitochondria. The FA may then participate in β-oxidation, which is known to increase under starvation conditions (Mathews and van Holde, 1990; Voet and Voet, 1995). Since β-oxidation of FAs depends on the availability of carnitine (Bremer, 1983), altered carnitine metabolism would affect energy generation from this source. Krahenbuhl and Reichen (1997) detected altered carnitine metabolism in livers of patients with alcohol-induced cirrhosis. These patients had higher hepatic acylcarnitine levels, which were attributed to increased carnitine biosynthesis. Additionally, Brady and Brady (1987) found that the activity and synthesis of the enzyme carnitine palmitoyltransferase increased

during starvation, when the insulin/glucagon ratio was low. Thus, it is possible that similar changes occurred in the liver of *E. multilocularis*-infected hosts. Increased carnitine biosynthesis along with higher carnitine palmitoyltransferase activity lead to increased production of hepatic acylcarnitine which would allow more FAs to be transported into the mitochondria to undergo β-oxidation.

Livers of infected jirds also contained more glycine. The levels of this amino acid were previously found to be increased in livers of hosts infected with the cestodes *Mesocestoides vogae* (Blackburn *et al.*, 1993b) and *Taenia crassiceps* (Corbin *et al.*, 1996). Glutathione (GSH), composed of the three amino acid residues glutamine, cystine and glycine, protects against oxidative stress induced by peroxidation and free radicals, and also assists in detoxification of drugs or other xenobiotics (Mathews and van Holde, 1990; Churchill *et al.*, 1995). Under fasting conditions, hepatic GSH levels are reduced (Hum *et al.*, 1991). Therefore, it is possible that less glycine was used in GSH synthesis in the *E. multilocularis*-infected host resulting in a greater amount of free glycine. In addition, glycine is involved in bile acid formation. The bile acid glycocholate is formed when cholic acid conjugates with glycine (Mathews and van Holde, 1990). Clearly, if less of this amino acid would be utilized in the conjugation process of bile acid formation in the infected host, higher glycine levels should be present. Since bile acid synthesis involves cholesterol, the reduced amount of this sterol in livers of infected jirds may cause an increase in glycine. Also, during fasting an increase in protein breakdown takes place (Hellerstein and Munro, 1988). The release of amino acids from protein degradation could also account for some of the increase in glycine in the parasitized host. Finally, the concentration of hepatic glycine may have been affected by increased glycerophospholipid (GPL) breakdown. There were fewer GPLs in livers of infected jirds. Two of these GPLs,

phosphatidylethanolamine (PTE) and phosphatidylserine (PTS) are interconverted by PTE serine transferase. When PTS is converted to PTE, serine is released. This serine can then react to form glycine via serine hydroxymethyl transferase (Mathews and van Holde, 1990; Thureen *et al.*, 1995; Voet and Voet, 1995). Indeed, the livers of infected jirds contained more PTE along with a higher concentration of glycine. This suggests that synthesis of PTE via PTE serine transferase could be increased in infected jirds.

II. Lipid metabolism

As cestodes cannot synthesize FA and sterols *de novo*, considerable lipid material must be obtained from the host (Barrett, 1983). FAs and glycerol of host origin are used by the cyst in the formation of PTC, PTE, PTS, LPC and PTI (Smyth and McManus, 1989; McManus and Bryant, 1995). Predominant FAs in *E. multilocularis* are saturated palmitic and stearic, and the unsaturated oleic and linoleic acids (McManus and Bryant, 1995). Since cestodes cannot desaturate preformed FAs, modification of these moieties is restricted to elongation by sequential addition of acetyl CoA to the FA chain via an unknown mechanism (Smyth and McManus, 1989). Cholesterol (CTL), an important membrane component and the dominant sterol in cestodes, must be taken up from the host in its entirety (Smyth and McManus, 1989; McManus and Bryant, 1995). In the present work, resonances of total GPLs, PTC, PTE, and CTL were detected in ^{1}H NMR spectra of *E. multilocularis* cysts. This indicates that precursors such as glycerol, FAs and phosphate head groups or their components must have been taken from the host and assembled into GPLs by the cyst.

As the parasite grows, greater amounts of GPLs are required for continued membrane synthesis. This competition between host and parasite for GPL precursors results, as shown in the present experiment, in a decrease in total hepatic GPLs which is mainly due to a decrease in PTC and PTI. It is also possible that other changes such as modification of enzyme activities in biosynthetic pathways of GPLs leads to the reduction of some GPLs and accumulation of others. At present, the enzymatic mechanisms which regulate these alterations are not fully understood. However, one condition which has been implicated in having a profound effect of the activity of various enzymes involved in GPL metabolism is pH. Kuesel *et al.* (1990) found that acidification of the medium in the range of pH 6 to 7 led to modified activities of enzymes in the CDP-choline and CDP-ethanolamine pathways of GPL biosynthesis in cultured tumor cells. Since the activity of the enzyme CDP-choline:1,2-DG cholinephosphotransferase is optimal at a pH of 8.0 to 8.5 (Pelech and Vance, 1984), Kuesel *et al.* (1990) suggested that lower pH may cause a decrease in the activity of this enzyme. This would lead to a reduction in the amount of PTC produced by the CDP-choline pathway. The normal cytosolic pH of hepatocytes was measured at 7.18 for rats (Durand *et al.*, 1993) and 7.16 for mice (Lee *et al.*, 1988). As such, it stands to reason that CDP-choline:1,2-DG cholinephosphotransferase is not operating under peak conditions in the normal mammalian liver. Thus, under conditions of lower pH, this enzyme may become the second rate limiting step in the CDP-choline pathway (Kuesel *et al.*, 1990). A low pH was detected, using ^{31}P *in vivo* NMR, in livers of mice infected with the cestode *Hymenolepis microstoma* (Blackburn *et al.*, 1993a). The acidic condition of the liver was attributed to the production of metabolic end products by the parasite and their subsequent excretion into the host. Therefore, it is possible that a similar hepatic acidosis may also exist in *M. unguiculatus*

infected with *E. multilocularis*. This then could lead to reduction in the activity of CDP-choline:1,2-DG cholinephosphotransferase and thereby reduced biosynthesis of PTC.

Synthesis of PTI requires glycerol and FAs, as does PTC and other GPLs. Thus, it is possible that reduced availability of these precursors in the host due to uptake of them by the parasite could result in a decrease in hepatic PTI. Furthermore, breakdown of PTI in response to hormonal stimuli produces inositol-1,4,5-trisphosphate (IP_3), an important intracellular second messenger (Exton, 1988; Mathews and van Holde, 1990). Therefore, stimulation of hepatocytes by hormones such as glucagon could contribute to increased PTI degradation in infected jirds. Release of the second messenger, IP_3, from PTI by glucagon causes Ca^{2+} ions to be released from the ER, resulting in an increase in Ca^{2+} concentration (Grollman, 1988; Exton, 1988). Ca^{2+} ions target two important hepatic enzymes. These are phosphorylase *b* kinase, which activates phosphorylase leading to the breakdown of glycogen and release of glucose, and type II calmodulin-dependent protein kinase, which inactivates glycogen synthase and pyruvate kinase inhibiting glycogen synthesis and glycolysis, respectively (Exton, 1988). Accelerated hepatic glycogenolysis has been demonstrated in jirds infected with *E. multilocularis* by Novak *et al.* (1995) and in the present experiments. Therefore, an elevation in glucagon levels in response to parasite-induced starvation could occur and cause a rise in the second messenger IP_3 and a decrease in hepatic PTI.

In contrast to reduced PTC and PTI, the amount of PTE increased in livers of infected hosts. The increase in this GPL again suggests a parasite induced modification in PTE biosynthetic pathways. As discussed above for the CDP-choline pathway, enzyme activity in the analogous CDP-ethanolamine pathway of PTE production (Figure 5) could also be modified by a lower pH.

When the pH was lowered from 7.2 to 6.0, Kuesel *et al.* (1990) found differing amounts of phosphomonoester intermediates in the CDP-ethanolamine pathway compared to those in the CDP-choline pathway in cancer cells. This suggested a reciprocal enzymatic activity between these two synthetic routes which caused a shift in the balance from choline- to ethanolamine-containing membrane GPLs. Thus, a similar situation may exist for livers of *E. multilocularis*-infected jirds as a consequence of possible acidosis induced by the parasite. However, further research is necessary to determine if the increase in PTE in livers of *E. multilocularis*-infected jirds was indeed due to a pH-induced alteration, or if other, at present unknown mechanisms are involved. Also, PTE can normally be converted to PTC by a series of three sequential methylation reactions catalyzed by the enzyme PEMT-2 (Figure 5), which exhibits high levels of activity only in the liver (Vance and Ridgeway, 1988). Although not the main pathway of PTC synthesis, sequential methylation of PTE accounts for 20 to 40% of PTC biosynthesis in the liver (Ansell and Spanner, 1982). Expression of PEMT-2 has been shown to reduce the rate of tumor and hepatic cell division and growth (Cui *et al.*, 1994), and decrease the activity of CTP:PC cytidylyltransferase, the rate limiting step in PTC synthesis via the CDP-choline pathway (Cui *et al.*, 1995). However, it is possible that activity of this enzyme may be reduced under the current experimental conditions. Since the optimal pH for PEMT-2 in rat liver was measured at 9.2, and that in mouse liver at 8.8 (Vance and Ridgeway, 1988), the activity of this enzyme could be affected by lower pH. Such a reduction in PEMT-2 activity could then result in decreased PTC synthesis from PTE, and therefore subsequent accumulation of PTE. In addition, hepatocytes treated with glucagon demonstrated a small reduction in PTC synthesis from methylation of PTE (Vance and Ridgeway, 1988). Glucagon release is stimulated by low blood glucose and serves to increase hepatic glycogenolysis

under these conditions (Mathews and van Holde, 1990). As previous workers (Novak *et al.*, 1989) and the present study have revealed that hosts infected with this parasite become hypoglycemic, the possibility also exists that glucagon was involved in modification of hepatic PEMT-2 activity. Finally, PTE and PTS can be interconverted in a base exchange reaction catalyzed by PTE serine transferase (Mathews and van Holde, 1990). Conversion of PTS to PTE releases serine which can then be converted to glycine via serine hydroxymethyl transferase (Mathews and van Holde, 1990; Thureen *et al.*, 1995; Voet and Voet, 1995). Since an increase in hepatic glycine along with more PTE was observed in the present experiment, it is possible that the activity of PTE serine transferase in *E. multilocularis*-infected jirds was increased.

In addition to PTC and PTI, the concentration of CTL was also decreased in livers of infected jirds. During starvation, CTL synthesis is inhibited (Pallardo and Williamson, 1989). *De novo* CTL synthesis in the liver begins with the reaction between acetyl CoA and acetoacetyl CoA via 3-hydroxy-3-methylglutaryl CoA synthase (HMG CoA synthase) producing HMG CoA which is converted to mevalonate via HMG CoA reductase. HMG CoA is also a precursor of the ketone bodies acetoacetate and β-HB. Since fasting decreases the activity of HMG CoA reductase, the rate limiting enzyme in CTL synthesis (Lehninger, 1975; Voet and Voet, 1995), it is possible that more HMG CoA was used by the infected host in ketogenesis than in CTL synthesis. Also, the contribution of the parasite to the depletion of hepatic CTL must be considered. As *E. multilocularis* cannot synthesize it *de novo*, all CTL present in the cysts had to be obtained from the host.

Cestodes also cannot synthesize FAs *de novo* (Barrett, 1983). Thus, all FAs detected in ^{1}H NMR spectra of *E. multilocularis* cysts must have been initially of host origin. These moieties were either taken up from the host in their

entirety or were formed by the parasite from host FAs via chain elongation. However, even though the parasite had to siphon off FAs from its environment, there was no statistically significant difference in the total amount of FAs between livers of uninfected and infected hosts. Differences in the ratios of FA components to the total amount of FAs between livers of uninfected and infected hosts are due to an alteration in the relative amounts of the individual FA moiety. When the ratio of each FA component to the total amount of FA in each group was compared, no difference was found in the ratios of hepatic saturated FA moieties. However, the relative amount of some unsaturated FA components in the liver was altered in response to *E. multilocularis* infection; ratios were higher for linoleic and arachidonic acids, and the conjugated diene moiety $C\underline{H_2}CH{=}CHHC{=}CHC\underline{H_2}$.

Linoleic acid ($18{:}2^{\Delta 9,12}$) is predominantly acquired from the diet (Hagmann and Keppler, 1988; Mathews and van Holde, 1990). Although linoleic acid can be synthesized *de novo* or through modification of existing FAs, through desaturation followed by chain elongation (Longmuir, 1987; Mathews and van Holde, 1990), this synthetic pathway represents only a minor contribution compared to dietary intake (Hagmann and Keppler, 1988; Mathews and van Holde, 1990). Both uninfected and infected hosts in this experiment were fed *ad libitum*. Thus, it is possible that infected hosts ate more and somehow retained a greater amount of linoleic acid from their diet, accounting for the higher proportion of this FA present in livers of infected jirds. Also, more linoleic acid, along with other FAs, could have been liberated from TGs in extrahepatic locations, such as adipose tissue, in response to an increased requirement for FAs in the starved host. In any case, the greater proportion of linoleic acid in livers of infected hosts suggests that less of this FA was used in β-oxidation relative to other FAs. This possible preferential utilization of some FAs for

energy generation and selective retention of others requires further investigation.

Interestingly, linoleic acid is also a precursor of arachidonic acid ($20:4^{\Delta5,8,11,14}$). First, a third double bond is introduced into linoleic acid at position 6 by a Δ^6 desaturase enzyme forming γ-linolenic acid ($18:3^{\Delta6,9,12}$), followed by elongation to homo-γ-linolenic acid ($20:3^{\Delta8,11,14}$). A Δ^5 desaturase enzyme then introduces another double bond at position 5 forming arachidonic acid (Longmuir, 1987). Chen and Cunnane (1992) and Andriamampandry *et al.* (1996) observed selective retention of arachidonic acid in livers of starved rats. These researchers suggested that certain FAs may be retained relative to others, rather than undergo oxidation to produce energy, in an effort to prevent deficiency in essential hepatic FAs under conditions of increased lipid utilization. Unfortunately, the mechanisms involved in selective retention and utilization of FAs under conditions of increased lipid breakdown and oxidation are not yet completely understood (Andriamampandry *et al.*, 1996). At present, it can only be hypothesized that the process of selective FA retention could be the cause of the increased proportion of arachidonic acid observed in livers of infected jirds.

Arachidonic acid is the precursor not only of various phospholipids, but also of biologically important compounds known as the eicosanoids (Hagmann and Keppler, 1988). These include prostaglandins (PGs), thromboxanes (TXs) and leukotrienes (LTs) which have roles in inflammatory response, pain and fever production, regulation of blood pressure, induction of blood clotting and control of reproductive functions (Hagmann and Keppler, 1988; Tao *et al.*, 1989; Voet and Voet, 1995; Woldseth *et al.*, 1995; Pageaux *et al.*, 1996). Several authors have reported increased eicosanoid production in host cells in response to parasitic infections (Belley and Chadee, 1995). LTs, especially, might play a role in host inflammatory response to *E. multilocularis* infection, as their function

includes stimulation of eosinophils, macrophages, monocytes and T-lymphocytes as well as augmentation of natural cytotoxic cell activities and T-lymphocyte proliferation (Hagmann and Keppler, 1988). Indeed, cell mediated host response to *E. multilocularis* infection includes an influx of macrophages and eosinophils, along with T- and B-lymphocytes to affected regions (Devouge and Ali-Khan, 1984; Gottstein, 1993). Arachidonic acid used in intracellular eicosanoid synthesis is liberated from C_2 of PTC by phospholipase A_2 and from PTI via phospholipase C and DG lipase (Mathews and van Holde, 1990; Belley and Chadee, 1995). PGs and TXs are formed from arachidonic acid by the action of cyclooxygenase/prostaglandin G/H synthase while LT synthesis is initiated via 5-lipoxygenase (Belley and Chadee, 1995 and references therein). These researchers also established that production of eicosanoids is not restricted to mammals, as many parasites also produce and excrete these lipid mediators. PGE_2, the most extensively studied PG, is produced from arachidonic acid, and is excreted into the host. There, it supresses the host immune response by inhibiting macrophage functions, T-lymphocyte proliferation and B-lymphocyte responsiveness. Larval *E. multilocularis* is known to be immunosupressive, successfully overcoming the immune defenses of its host (Rakha *et al.*, 1991; Gottstein *et al.*, 1993). As the eicosanoid PGE_2 has the same initial structure, beginning from the carboxyl end, as does arachidonic acid (i.e.: $CH{=}CHCH_2CH_2CH_2COO$), the possibility exists that this PG is produced and excreted by *E. multilocularis* and contributes, together with eicosanoids of host origin, to the NMR resonance used for quantitative analysis arachidonic acid in livers of infected jirds. Further investigation is required, however, to determine if, indeed, any eicosanoids contribute to the arachidonic acid resonance in ^1H NMR spectra.

The ratio of the conjugated diene moiety ($\underline{H_2}CHC=CHHC=CHC\underline{H_2}$) to total FA chains was also higher in livers of infected jirds. The formation of conjugated dienes represents the first step in peroxidation of FAs (Krajcovicova-Kudlackova and Ozdin, 1995; Benzie, 1996). Peroxidation is initiated by free radicals, defined as any species with unpaired electrons, such as the superoxide radical ($O_2\cdot^-$), the hydroxyl radical ($\cdot OH$), the hydroperoxyl radical ($HO_2\cdot$), nitric oxide ($\cdot NO$) and oxygen (O_2). Generally, free radicals are produced as a consequence of normal aerobic metabolism but they also accumulate at sites of cell injury caused by inflammation or post-ischaemic reperfusion (Benzie, 1996). These free radicals can attack an unsaturated FA, removing one hydrogen from an α-methylene group (Figure 14). This results in an extremely unstable carbon-centered radical, which can either undergo a bond rearrangement, forming a more stable conjugated diene moiety, or react with an $O_2(g)$ molecule to form a peroxyl radical. The peroxyl radical can then remove a hydrogen atom from another unsaturated FA to form a lipid hydroperoxide and another carbon-centered radical in a self-propagating process. Protective factors such as oxidase enzymes and antioxidants, or free radical scavengers, break the free radical chain reaction, limiting free radical damage (Mathews and van Holde, 1990; Benzie, 1996). Should peroxidation be allowed to continue, structure and function of FAs, and thereby membranes, will be irreparably damaged (Benzie, 1996). As previously described, host response to *E. multilocularis* infection involves inflammation. Because free radicals can be generated at sites of inflammation causing subsequent peroxidation of lipids (Bryant and Behm, 1989; Benzie, 1996), this action could result in the increase in the relative amount of conjugated diene moieties observed in the present experiment. Also, Rojas *et al.* (1993) found that under conditions of carbohydrate restriction, lipid sensitivity to peroxidation is increased. As *E. multilocularis* infection decreases the

Figure 14

Peroxidation of fatty acids

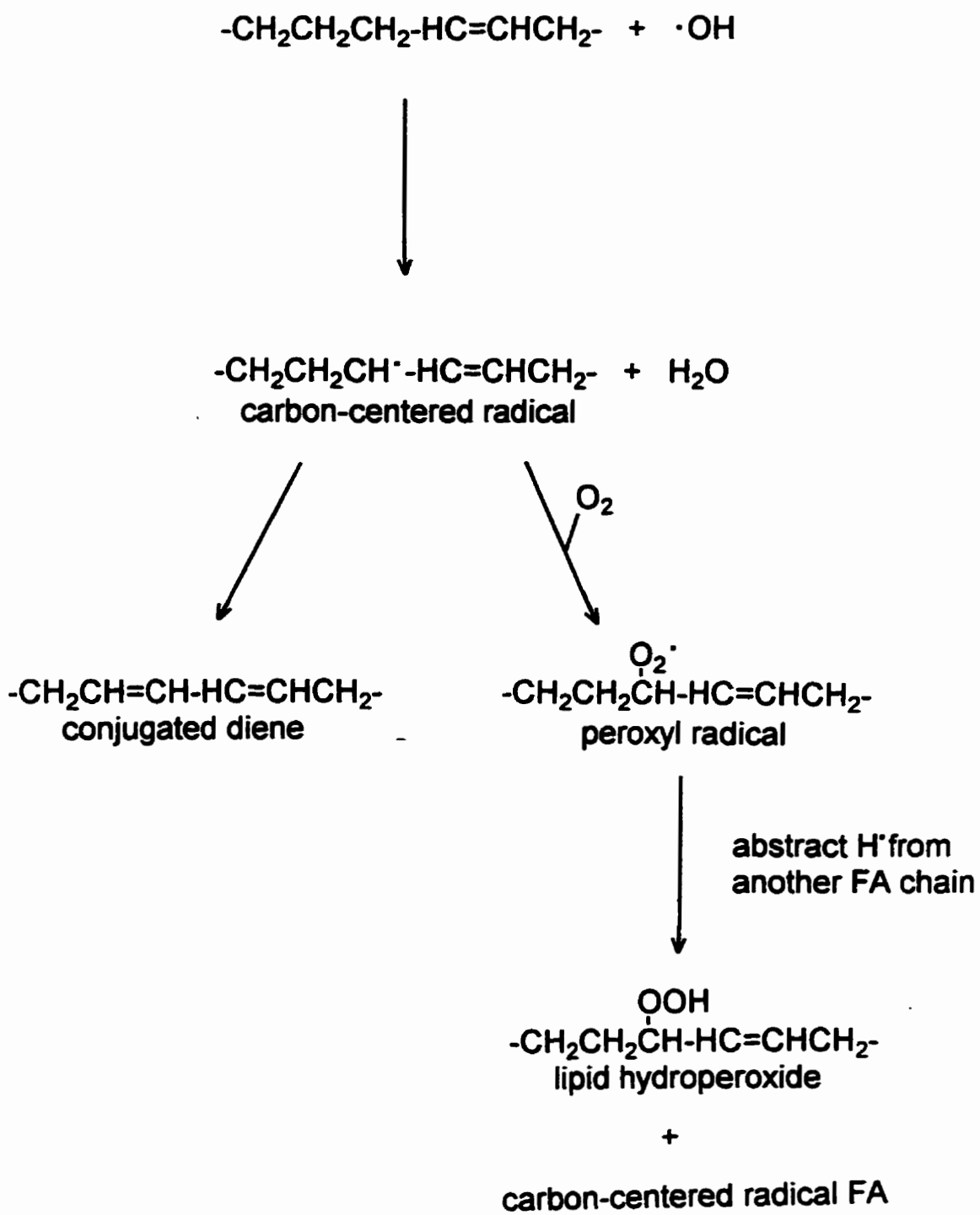
-CH2CH2CH2-HC=CHCH2- + ·OH
-CH2CH2CH·-HC=CHCH2- + H2O
carbon-centered radical
O2
-CH2CH=CH-HC=CHCH2-
conjugated diene
O2·
-CH2CH2CH-HC=CHCH2-
peroxyl radical
abstract H·from
another FA chain
OOH
-CH2CH2CH-HC=CHCH2-
lipid hydroperoxide
+
carbon-centered radical FA

availability of carbohydrates to the host, this deficiency might lead to increased FA peroxidation. Thus, an increase in peroxidation of FAs could be the mechanism responsible for the increase in the proportion of conjugated dienes in livers of infected jirds. Obligate endoparasites such as *E. multilocularis* metacestodes are continuously exposed to oxygen-derived radicals from their host, and to a lesser extent, their own metabolism (Bryant and Behm,1989). Therefore conjugated dienes found in cyst tissue may have either been taken up from the host or be a result of FA peroxidation by radicals in the parasite itself.

Further differences between host and parasite lipid composition are illustrated by a lower degree of unsaturation and shorter average chain length in *E. multilocularis* cysts. While, on average, there were 1.23 double bonds per hepatic FA chain in infected hosts, those from the parasite contained only 0.80. This dissimilarity may be due to the inability of cestodes to desaturate preformed FA chains. The average chain length in cysts was 13.75 carbons long while that in host livers was 16.18. Limited information about lipid composition in helminths disclosed that in *E. multilocularis* metacestodes, major FAs in both neutral and phospholipids were the saturated palmitic (16:0) and stearic (18:0), and the unsaturated oleic ($18:1^{\Delta 9}$) and linoleic ($18:2^{\Delta 9,12}$) acids (Smyth and McManus, 1989; McManus and Bryant, 1995). Persat *et al.* (1990a) reported that the monohexosylceramide fraction of membrane glycosphingolipids (GSLs), isolated from *E. multilocularis* metacestodes were specific to this parasite only. These GSLs contained FA moieties ranging from 16 to 30 carbons long, with palmitic (16:0), cerotic (26:0) and stearic (18:0) acids predominating (Persat *et al.*, 1990b). Palmitic and stearic acids are also common in the liver and in addition this organ is also rich in oleic ($18:1^{\Delta 9}$), arachidonic ($20:4^{\Delta 5,8,11,14}$) and docosahexaenoic ($22:6^{\Delta 4,7,10,13,16,19}$) acids (Marsh, 1990; Mathews and van Holde, 1990). It can be seen that the above information cannot be compared

directly to data obtained in this study. In ^{1}H NMR spectra of livers and cysts, separate analysis of individual free FAs and those in TGs, GPLs and GSLs was not possible as the resonances contained contributions from all of these. The work of Persat, described above, and the present study indicate that, on average, the length of the FA chains in *E. multilocularis* cysts is shorter than that in GSLs. The host-parasite differences in average FA chain length, and also in the degree of unsaturation, may be a consequence of a requirement for distinct membrane FA composition in the cyst compared to the host in order to accommodate the various functions of parasite membranes. The vesicular cyst wall of *E. multilocularis* participates in keeping the metacestode alive in a hostile environment by protecting it from the host immune response, and also takes up all nutrients from the host (Smyth and McManus, 1989). Further research is required to determine the composition of FAs in TGs, GPLs and GSLs in *E. multilocularis* cysts.

III. Future Research

In order to further knowledge on the *M. unguiculatus*/*E. multilocularis* host/parasite relationship, additional research is needed. For example, the present experiments did not show specifically that acetate of parasite origin was used in host gluconeogenesis, but rather that acetate can participate in this pathway. To determine if parasitic acetate is used in host metabolism, carbon-13 labeled acetate should be injected *in vivo* directly into the parasite cysts and the metabolism of this labeled compound then traced in the liver. Also, blood could be removed and analyzed to determine how much of the labeled tracer, along with labeled products, is circulated throughout the body. Use of carbon-13

NMR, in addition to ^{1}H spin echo NMR, would be beneficial in obtaining a more detailed analysis of ^{13}C labeled metabolites.

Although [2-^{13}C]acetate is not considered to be a substrate for gluconeogenesis, the present experiments showed that atoms from this metabolite were incorporated into glucose. However, to follow this information further, it would be interesting to determine how much acetate is used in gluconeogenesis when another alternate substrate is also provided. Lactate is considered to be a major gluconeogenic substrate, entering the gluconeogenesis pathway through conversion to pyruvate via lactate dehydrogenase. Conversion of lactate to glucose proceeds by a more direct route than that of acetate. Thus, the labeling patterns of glucose from lactate and acetate should be different. Lactate labeled at carbon-3 would label glucose at C_1, C_2, C_5 and C_6 due to randomization at the triose phosphate level in gluconeogenesis and at the fumarate to malate step. Label from [2-^{13}C]acetate would be randomized at the same points and could occur at C_1 through C_6 of glucose, depending on how many turns of the Kreb's cycle the oxaloacetate had participated in before exiting the mitochondrion. Thus, comparison of labeling patterns in glucose, should provide information on gluconeogenic substrate selection in the liver of the infected host. In order to obtain information on labeling patterns in glucose, ^{13}C NMR should be used.

It would also be interesting to determine if *E. multilocularis* cysts are capable of gluconeogenesis from the level of DHAP and GAP. To do this, labeled glycerol should be used. This metabolite is converted to glycerol-3-phosphate (G-3-P) by glycerol kinase followed by dehydrogenation to DHAP. Detection of labeled intermediates in cysts incubated in medium containing labeled glycerol would provide evidence for further metabolism of this substrate, and the presence of labeled glucose would show that gluconeogenesis was

taking place. Labeled glycerol could also be injected into the parasite *in vivo*. This experiment would provide additional information on the dynamic relationship between *M. unguiculatus* and *E. multilocularis* with respect to parasite glycerol metabolism. This would clarify whether any of the labeled glucose observed in the cysts in the present experiments was really of host or of parasite origin.

Further investigation into lipid metabolism of the infected host is also required. First, classes of phospholipids such as GPLs and GSLs could be separated. Determination of FA composition within each of these classes may require an alternate method of examination. For example, gas chromatography should be used to observe differences in the relative amounts of saturated FAs. This would provide additional information on how each class of lipids contributes to the overall chain length of FAs. Also, GPLs such as PTC, PTE, PTI and PTS could be separated from the crude C:M liver extracts from uninfected and infected hosts. Once separated, analysis of these groups using ^{1}H NMR spectroscopy would give more information on the FA composition of each group, and how the composition of FAs changes relative to the type of GPL. In addition, hepatocytes from uninfected and infected hosts could be incubated with ^{13}C-labeled FAs. These could include palmitic, stearic, linoleic or arachidonic acid. The use of both saturated and unsaturated FAs would provide information on selective FA uptake under starved and fed conditions, in livers of infected and uninfected hosts, respectively. Moreover, this experiment could demonstrate preferential utilization of different FAs, saturated (palmitic and stearic) versus unsaturated (linoleic and arachidonic), in β-oxidation. To obtain the most information from this study, carbon-13 NMR spectroscopy should be used to determine positioning of labeled carbon-atoms within FA moieties in

conjunction with ^{1}H spin echo NMR spectroscopy to follow labeled carbon atoms from FAs through β-oxidation and into host energy metabolism.

In addition, the contribution of eicosanoids to the resonance of arachidonic acid ($HC{=}CHCH_2C\underline{H_2}CH_2COO$) in ^{1}H NMR spectra should be determined. This could be accomplished through analysis of ^{1}H NMR spectra of PGs and TXs which contain the same initial structure from the carboxyl group as does arachidonic acid. Since eicosanoids of both host and parasite origin may contribute to the resonance of arachidonic acid, this FA, labeled with ^{13}C, could be fed to uninfected and *E. multilocularis*-infected jirds. Subsequent isolation of PGs and their analysis using ^{13}C NMR would indicate if any of the labeled arachidonic acid had been used in PG synthesis. Also, the presence of ^{13}C label in PGs from *E. multilocularis* cysts could be examined to determine if labeled arachidonic acid was used in eicosanoid synthesis by the parasite. Finally, to determine if PGs of parasite origin are excreted into the host, *E. multilocularis* cyst cells could be incubated in a medium enriched with ^{13}C-labeled arachidonic acid. Analysis of PGs in cyst cells and the culture medium would determine if these eicosanoids were synthesized from exogenous arachidonic acid and subsequently excreted into the environment by the parasite.

References

Adosraku, R.K., Choi, G.T.Y., Constantinou-Kokotos, V., Anderson, M.M. and Gibbons, W.A., 1994. NMR lipid profiles of cells, tissues and body fluids: proton NMR analysis of human erythrocyte lipids. *J. Lip. Res.*, **35**: 1925-1931.

Alberti, K.G.M.M., Taylor, A.R. and Johnston, D.G., 1992. Carbohydrate metabolism in liver disease. In: Wright's liver and biliary disease, 3rd ed., vol. 1. Eds: G.H. Millwars-Sadler, R.Wright and M.J.P. Arthur. W.B. Saunders Co., Toronto.

Alberts, B., Vray, D., Lewis, J., Raff, M., Roberts, K. and Watson, J.D., 1989. Molecular Biology of the Cell, 2nd edition. Garland Publishing, Inc., New York.

Ali-Khan, Z. and Siboo, R., 1980. Pathogenesis and host response in subcutaneous alveolar hydatidosis. I. Histogenesis of alveolar cyst and quantitative analysis of the inflammatory infiltrates. *Zeitschrift Parasitenkunde*, **62**: 241.

Ali-Khan, Z., Siboo, R., Gomersall, M. and Faucher, M., 1983. Cytosolic events and the possible role of germinal cells in metastasis in chronic alveolar hydatidosis. *Ann. Trop. Med. Parasitol.*, **77**: 497-512.

Alkarmi, T. and Behbehani, K., 1989. *Echinococcus multilocularis*: Inhibition of murine neutrophil and macrophage chemotaxis. *Exp. Parasitol.*, **69**: 16-22.

Ammann, R. and Eckert, J., 1995. Clinical diagnosis and treatment of Echinococcosis in humans. In: *Echinococcus* and hydatid disease. Ed. R.C.A. Thompson and A.J. Lymbery. CAB International, Wallingford, U.K, pp. 1-50.

Andriamampandry, M.D., Bnouham, M., Michard, D., Gutbier, G., Maho, Y.L. and Leray, C., 1996. Food deprivation modifies fatty acid partitioning and β-oxidation capacity in rat liver. *J. Nutr.*, **126**: 2020-2027.

Ansell, G.B. and Spanner, S., 1982. Phosphatidylserine, phosphatidylethanolamine and phosphatidylcholine. In: Phospholipids. Eds. J.N. Hawthorne and G.B. Ansell, Elsevier Biomedical Press, New York.

Badar-Goffer, R.S., Bachelard, H.S. and Morris, P.G., 1990. Cerebral metabolism of acetate and glucose studied by ^{13}C-n.m.r. spectroscopy. *Biochem. J.*, **266**:133-139.

Barrett, J., 1983. Lipid metabolism. In: Biology of Eucestoda. Ed.: Arme, C. and Pappas, P.W., vol.2. Academic Press, London.

Bartel, M.H., Seesee, F.M. and Worley, D.E., 1992. Comparison of Montana and Alaska isolates of *Echinococcus multilocularis* in gerbils with observations on the cyst growth, hook characteristics, and host response. *J. Parasitol.*, **78(3)**: 529-532.

Belley, A. and Chadee, K., 1995. Eicosanoid production by parasites: from pathogenesis to immunomodulation? *Parasitol. Today*, **11(9)**: 327-334.

Bendall, M.R., Pegg, D.T., Doddrell, D.M. and Field, J., 1981. NMR of protons coupled to ^{13}C nuclei only. *J. Am. Chem. Soc.*, **103**: 934-936.

Benzie, I.F.F., 1996. Lipid peroxidation: a review of causes, consequences, measurements and dietary influences. *Int. J. Food Sci. Nutr.*, **47**: 233-261.

Bhamidipati, S.P. and Hamilton, J.A., 1993. NMR studies of phospholipase C hydrolysis of phosphatidylcholine in model membranes. *J. Biol. Chem.*, **268(4)**: 2431-2434.

Blackburn, B.J., Hutton, H.M., Novak, M. and Evans, W.S., 1986. *Hymenolepis diminuta*: nuclear magnetic resonance analysis of the excretory products resulting from the metabolism of D-[$^{13}C_6$]glucose. *Exp. Parasitol.*, **62**: 381-388.

Blackburn, B.J., Buist, R.J., Hudspeth, C. and Novak, M., 1993a. Phosphorus metabolites of liver from mice infected with *Hymenolepis microstoma*. *Int. J. Parasitol.*, **23(1)**: 95-103.

Blackburn, B.J., Hudspeth, C. and Novak, M., 1993b. Proton nuclear magnetic resonance analysis of liver metabolites from mice infected with *Mesocestoides vogae*. *Int. J. Parasitol.*, **23(7)**: 953-957.

Brady, P.S. and Brady, L.J., 1987. Hepatic carnitine palmitoyltransferase turnover and translation rates in fed, starved, streptozotocin-diabetic and diethylhexyl phthalate-treated rats. *Biochem. J.*, **246**: 641-646.

Bremer, J., 1983. Carnitine: metabolism and functions. *Physiol. Rev.*, **63**: 1420-1480.

Bryant, C. and Behm, C., 1989. Biochemical adaptation in parasites. Chapman and Hall, New York.

Casu, M., Anderson, G.J., Choi, G. and Gibbons, W.A., 1991. NMR lipid profiles of cells, tissues and body fluids. *Mag. Reson. Chem.*, **29**: 594-602.

Chen, Z.Y. and Cunnane, S.C., 1992. Preferential retention of linoleic acid-enriched triacylglycerols in liver and serum during fasting. *Am. J. Physiol.*, **263**: R233-R239.

Choi, G.T.Y., Casu. M. and Gibbons, W.A., 1993. N.m.r. lipid profiles of cells, tissues and body fluids. *Biochem.*, **290**: 717-721.

Churchill, T.A., Green, C.J. and Fuller, B.J., 1995. Protective proterties of amino acids in liver preservation: effects of glycine and a combination of amino acids on anaerobic metabolism and energetics. *J. Hepatol.*, **23**: 720-726.

Cohen, D.M. and Bergman, R.N., 1994. Prediction of positional isotopomers of the citric acid cycle: the syntactic approach. *Am. J. Physiol.*, **266(29)**: E341-E350.

Cook, B.R., 1991. *Echinococcus multilocularis* infestation acquired in the UK. *Lancet*, **337**: 560-561.

Corbin, I., Blackburn, B.J., Wolowiec, T., and Novak, M., 1996. Metabolic profile of the liver of mice infected with cysticerci of *Taenia crassiceps*. *Parasitol. Res.*, **82**: 273-275.

Crabtree, B., Gordon, M.-J. and Christie, S.L., 1990. Measurement of the rates of acetyl-CoA hydrolysis and synthesis from acetate in rat hepatocytes and the role of these fluxes in substrate cycling. *Biochem. J.*, **270**: 219-225.

Craig, P.S., Deshan, L., Macpherson, C.N.L., Dazhong, S., Reynolds, D., Barnish, G., Gottstein, B. and Zhirong, W., 1992. A large focus of alveolar echinococcosis in central China. *Lancet*, **340**: 826-831.

Cui, Z., Vance, J.E., Chen, M.H., Voelker, D.R. and Vance, D.E., 1993. Cloning and expression of a novel phosphatidylethanolamine *N*-methyltransferase. *J. Biol. Chem.*, **268(22)**: 16655-16663.

Cui, Z., Houweling, M. and Vance, D.E., 1994. Supression of rat hepatoma cell growth by expression of phosphatidylethanolamine *N*-methyltransferase-2. *J. Biol. Chem.*, **269(40)**: 24531-24533.

Cui, Z., Houweling, M. and Vance, D.E., 1995. Expression of phosphatidylethanolamine *N*-methyltransferase-2 in McArdle RH-7777 hepatoma cells inhibits the CDP-choline pathway for phosphatidylcholine biosynthesis via decreased gene expression of CTP:phosphocholine cytidylyltransferase. *Biochem. J.*, **312**: 939-945.

Cunnane, S.C., 1989. Application of NMR spectroscopy to the study of lipid metabolism and composition. *Nutr.*, **5(4)**: 271-273.

Deblock, S., Prost, C., Walbam, S. and Petavy, A.F., 1989. *Echinococcus multilocularis*: a rare cestode of the domestic cat in France. *Int. J. Parasitol.*, **19(6)**: 687-688.

Derome, A.E., 1987. Modern NMR techniques for chemistry research. Pergamon Press, Toronto.

Desmoulin, F., Confort-Gouny, S., Masson, S., Bernard, M., Doddrell, D.M. and Cozzone, P.J., 1990. Application of reverse-DEPT polarization transfer pulse sequence to study the metabolism of carbon-13-labeled substrates in perfused organs by ^{1}H NMR spectroscopy. *Magn. Reson. Med.*, **15**: 456-461.

Des Rosiers, C., Fernandez, C.A., France, D. and Brunengraber, H., 1994. Reversibility of the mitochondrial isocitrate dehydrogenase reaction in the perfused rat liver. *J. Biol. Chem.*, **269(44)**: 27179-27182.

Des Rosiers, C., Di Donato, L., Comte, B., Laplante, A., Marcoux, C., France, D., Fernandez, C.A. and Brunengraber, H., 1995. Isotopomer analysis of citric acid cycle and gluconeogenesis in rat liver. *J. Biol. Chem.*, **270(17)**: 10027-10036.

Devouge, M. and Ali-Khan, Z., 1984. Intraperitoneal murine alveolar hydatidosis: relationship between the size of the larval cyst mass, immigrant inflammatory cells, splenomegaly and thymus involution. *Tropenmed. Parasit.*, **34**: 15-20.

Dills Jr., W.L., 1993. Nutritional and physiological consequences of tumour glycolysis. *Parasitol.*, 107: S177-S186.

Durand, T., Gallis, J.-L., Masson, S., Cozzone, P.J. and Canioni, P., 1993. pH regulation in perfused rat liver: respective role of Na^+-H^+ exchanger and Na^+-HCO_3^- cotransport. *Am. J. Physiol.*, **265**: G43-G50.

Ersahin, Y., Mutluer, S. and Guzelbag, E., 1993. Intracranial hydatid cysts in children. *Neurosurg.*, **33(2)**: 219-224.

Erzurumlu, K., Ozdemir, M., Mihmanli, M. and Cevikbas, U., 1995. The effect of intraoperative Mebendazole-Albendazole applications of the hepatobiliary system. *Eur. Surg. Res.*, **27**: 340-345.

Evanochko, W.T., Sakai, T.T., Thian, C. N., Krishna, N.R., Kim, H.D., Zeidler, R.B., Ghanta, V.K., Brockman, R.W., Schiffer, L.M., Braunschweiger, P.G. and Glickson, J.D., 1984. NMR study of *in vivo* RIF-1 tumors. *Biochim. Biophys. Acta.*, **805**: 104-116.

Exton, J.H., 1988. Role of inositol trisphosphate and diacylglycerol in the regulation of liver function. In: The liver: biology and pathobiology, second edition. Eds. I.M. Arias, W.B. Jakoby, H. Popper, D. Schachter and D.A. Shafritz. Raven Press, New York.

Fernandez, C.A. and Des Rosiers, C., 1995. Modeling of liver citric acid cycle and gluconeogenesis based on ^{13}C mass isotopomer distribution analysis of intermediates. *J. Biol. Chem.*, **270(17)**: 10037-10042.

Ferretti, A., Podo, F., Carpinelli, G., Chen, L., Borghi, P. and Masella, R., 1993. Detection of neutral active phosphatidylcholine-specific phospholipase C in friend leukemia cells before and after erythroid differentiation. *Anticancer. Res.*, **13**: 2309-2317.

Folch, J., Lees, M. and Sloane Stanley, G.H., 1957. A simple method for the isolation and purification of total lipides from animal tissues. *J. Biol. Chem.*, **226**: 497-509.

Fujioka, Y., Aoki, S., Sato, N. and Uchino, J., 1993. Pathology. In: Alveolar Echinococcus of the Liver. Eds.: J. Uchino and N. Sato, Hokkaido University School of Medicine, Sapporo, Japan.

Gilroy, F.V., Edwards, M.R., Norton, R.S. and Sullivan, W.J.C., 1988. Metabolic studies of the protozoan parasite, *Crithidia luciliae*, using proton nuclear magnetic resonance spectroscopy. *Mol. Biochem. Parasitol.*, **31**: 107-116.

Gottstein, B., 1993. *Echinococcus multilocularis* infection: Immunology and immunodiagnosis. *Adv. Parasitol.*, **31**: 321-380.

Gottstein, B., Tschudi, K., Eckert, J. and Ammann, R., 1989. Em2-ELISA for the follow-up of alveolar echinococcosis after complete surgical resection of liver lesions. *Trans. Royal Soc. Trop. Med. Hyg.*, **83**: 389-393.

Grollman, E.F., 1988. Calcium signals in the liver. In: The liver: biology and pathobiology, 2nd edition. Eds. I.M. Arias, W.B. Jakoby, H. Popper, D. Schachter and D.A. Shafritz, Raven Press, New York.

Guyton, A.C., 1991. Textbook of Medical Physiology, 8th edition. Ed. A.C.Guyton. W.B. Saunders Co., Philadelphia.

Hagmann, W. and Keppler, D., 1988. Leukotrienes and other eicosanoids in liver pathophysiology. In: The liver: biology and pathobiology, 2nd edition. Eds. I.M. Arias, W.B. Jakoby, H. Popper, D. Schachter and D.A. Shafritz, Raven Press, New York.

Hahn, E.L., 1950. Spin echoes. *Phys. Rev.*, **80**: 580-590.

Hellerstein, M.K. and Munro, H.N., 1988. Interaction of liver and muscle in the regulation of metabolism in response to nutritional and other factors. In: The liver: biology and pathobiology, 2nd edition. Eds. I.M. Arias, W.B. Jakoby, H. Popper, D. Schachter and D.A. shafritz, Raven Press, New York.

Hum, S., Robitaille, L. and Hoffer, L.J., 1991. Plasma glutathione turnover in the rat: effect of fasting and buthionine sulfoximine. *Can. J. Physiol. Pharmacol.*, **69**: 581-587.

Kamya, M. and Sato, H., 1990. Complete life cycle of the canid tapeworm *Echinococcus multilocularis*, in laboratory rodents. *FASEB J.*, **4**: 3334-3339.

Karlsson, N., Fellenius, E. and Kiessling, K.-H., 1975. The metabolism of acetate in the perfused hind-quarter of the rat. *Acta Physiol. Scand.*, **93**: 391-400.

Kasai, Y., Koshino, I., Kawanishi, N., Salamoto, H., Sasaki, E. and Kumagai, M., 1980. Alveolar echinococcosis of the liver. *Ann. Surg.*, **191(2)**: 145-152.

Kizaki, T., Kobayashi, S., Ogasawara, K., Day, N.K., Good, R.A. and Onoe, K., 1991. Immune suppression induced by protoscoleces of *Echinococcus multilocularis* in mice. *J. Immunol.*, **147(5)**: 1659-1666.

Kohler, P., 1985. The strategies of energy conservation in helminths. *Molec. Biochem. Parasitol.*, **17**: 1-18.

Krahenbuhl, S. and Reichen, J., 1997. Carnitine metabolism in patients with chronic liver disease. *Hepatol.*, **25(1)**: 148-153.

Krajcovicova-Kudlackova, M. and Ozdin, L., 1995. Effect of fatty acid composition, cadmium and vitamin E intake on prooxidative-antioxidative state of rat liver. *Vet. Med. - Czech.*, **40(9)**: 293-298.

Kumagai, M., 1993. Immunodiagnosis. In: Alveolar Echinococcus of the Liver. Eds.: J. Uchino and N. Sato, Hokkaido University School of Medicine, Sapporo, Japan.

Kuesel, A.C., Graschew, G., Hull, W.E., Lorenz, W. and Thielmann, H.W., 1990. ^{31}P NMR studies of cultured human tumor cells. Influence of pH on phospholipid metabolite levels and the detection of cytidine 5'-diphosphate choline. *NMR. Biomed.*, **3(2)**: 78-88.

Leduq, R. and Gabrion, C., 1992. Developmental changes of *Echinococcus multilocularis* metacestodes revealed by tegumental ultrastructure and lectin-binding sites. *Parasitol.*, **104**: 129-141.

Lee, R.G., Clouse, M.E. and Lanir, A., 1988. Liver adenosine triphosphate and pH in fasted and well-fed mice after infusion of adenine nucleotide precursors. *Liver*, **8**: 337-343.

Lee, G.W., Lee, K.A. and Davidson, W.R., 1993. Evaluation of fox-chasing enclosures as sites of potential introduction and establishment of *Echinococcus multilocularis*. *J. Wildlife Diseases*, **29(3)**: 498-501.

Lehninger, A.L., 1975. Biochemistry. Worth Publishers Inc., New York.

Liebfritz, D., 1996. An introduction to the potential of ^{1}H-, ^{31}P- and ^{13}C-NMR-spectroscopy. *Anticancer Res.*, **16**: 1317-1324.

Longmuir, K.J., 1987. Biosynthesis and distribution of lipids. *Cur. Topics Membr. Transp.*, **29**: 129-174.

Lubinsky, G., 1960. The maintenance of *Echinococcus multilocularis* without the definitive host. *Can. J. Zool.*, **38**: 149-151.

Lukashenko, N.P., 1971. Problems of epidemiology and prophylaxis of alveococcosis (Multilocular Echinococcosis): A general review - with particular reference to the U.S.S.R. *Int. J. Parasitol.*, **1**: 125-134.

Lundquist, F., 1962. Production and utilization of free acetate in man. *Nature*, **193**: 579-580.

Malloy, C.R., Sherry, A.D. and Jeffrey, F.M.H., 1988. Evaluation of carbon flux and substrate selection through alternate pathways involving the citric acid cycle of the heart. *J. Biol. Chem.*, **263(15)**: 6964-6971.

Marsh, D., 1990. CRC handbook of lipid bilayers. CRC Press, Florida.

Mathews, C.K. and van Holde, K.E., 1990. Biochemistry. Benjamin/Cummings Publishing Co., California.

McManus, D.P. and Smyth, J.D.,1982. Intermediary carbohydrate metabolism in protoscoleces of *Echinococcus granulosus* (horse and sheep strains) and *E. multilocularis*. *Parasitol.*, **84**: 351-366.

McManus, D.P. and Bryant, C., 1995. Biochemistry, physiology and molecular biology of *Echinococcus*. In: *Echinococcus* and hydatid disease. Ed. R.C.A. Thompson and A.J. Lymbery. CAB International, Wallingford, U.K.

Miskovitz, P.F. and Javitt, N.B., 1980. Leukopenia associated with mebendazole therapy of hydatid disease. *Am. J. Trop. Med. Hyg.*, **29(6)**: 1356-1358.

Modha, A., Novak, M. and Blackburn, B.J., 1997. Treatment of experimental alveolar echinococcosis with albendazole: a ^{1}H NMR spectroscopic study. *Can. J. Zool.*, **75**: 198-204.

Morris, D.L. and Smith P.G., 1987. Albendazole in hydatid disease - hepatocellular toxicity. *Trans. Royal Soc. Trop. Med. Hyg.*, **81**: 343-344.

Murray, R.K., Granner, D.K., Mayes, P.A. and Rodwell, V.W., 1988. Harper's biochemistry, 21st edition. Appleton and Lange, Conneciticut.

Novak, M., Marat, K., Johnson, L. and Blackburn, B.J., 1989. ^{1}H and ^{13}C N.M.R. studies of serum from normal and *Echinococcus multilocularis* infected jirds. *Int. J. Parasitol.*, **19(4)**: 395-400.

Novak, M., Hameed, N., Buist, R. and Blackburn, B.J., 1992. Metabolites of alveolar *Echinococcus* as determined by [^{31}P]- and [^{1}H]-nuclear magnetic resonance spectroscopy. *Parasitol. Res.*, **78**: 665-670.

Novak, M., Modha, A. and Blackburn, B., 1993. Metabolic alterations in organs of *Meriones unguiculatus* infected with *Echinococcus multilocularis*. *Comp. Biochem. Physiol.*, **105B(3/4)**: 517-521.

Novak, M., Modha, A., Lee, J., Buist, R. and Blackburn, B., 1995. Metabolism of D-[1-^{13}C]glucose in livers of *Meriones unguiculatus* infected with *Echinococcus multilocularis*. *Can. J. Zool.*, **73**: 58-66.

Ogasawara, K., Matsuoka, S., Sato, N., Nakajima, Y. and Uchino, J., 1993. Image diagnosis. In: Alveolar Echinococcus of the Liver. Eds.: J. Uchino and N. Sato, Hokkaido University School of Medicine, Sapporo, Japan.

Ohbayashi, M., 1993. Parasitology. In: Alveolar Echinococcus of the Liver. Eds.: J. Uchino and N. Sato, Hokkaido University School of Medicine, Sapporo, Japan.

Okamoto, M., Fujita, O., Arikawa, J., Kurosawa, T., Oku, Y. and Kamiya, M., 1992. Natural *Echinococcus multilocularis* infection in a norway rat, *Rattus norvegicus*, in southern Hokkaido, Japan. *Int. J. Parasitol.*, **22(5)**: 681-684.

Orten, J.M. and Neuhaus, O.W., 1982. Human biochemistry, 10th edition. The C.V. Mosby Co., Missouri.

Pageaux, J.-F., Bechoun, S., Bonnot, G., Fayard, J.-M., Cohen, H., Lagarde, M. and Laugier, C., 1996. Biogenesis and metabolic fate of docosahexaenoic and arachidonic acids in rat uterine stromal cells in culture. *Arch. Biochem. Biophys.*, **327(1)**: 142-150.

Pallardo, F.V. and Williamson, D.H., 1989. Comparison of the flux of carbon to hepatic glycogen deposition and fatty acid and cholesterol synthesis on refeeding rats fed *ad libitum* or meal-fed rats with a chow-diet meal. *Biochem. J.*, **257**: 607-610.

Payette, J., 1996. Nuclear magnetic resonance (NMR) analysis of metabolites excreted by *Mesocestoides vogae* after exposure to oxaloacetate. Undergraduate thesis.

Pelech, S.L. and Vance, D.E., 1984. Regulation of phosphatidylcholine biosynthesis. *Biochim. Biophys. Acta*, **779**: 217-251.

Persat, F., Bouhours, J.-F., Mojon, M. and Petavy, A.-F., 1990a. Glycosphingolipids of *Echinococcus multilocularis* metacestodes. *Molec. Biochem. Parasitol.*, **38**: 97-104.

Persat, F., Bourhours, J.-F., Mojon, M. and Petavy, A.-F., 1990b. Analysis of the monohexosylceramide fraction of *Echinococcus multilocularis* metacestodes. *Molec. Biochem. Parasitol.*, **41**: 1-6.

Petavy, A.F., Deblock, S. and Walbaum, S., 1990. The house mouse: a potential intermediate host for *Echinococcus multilocularis* in France. *Trans. Royal Soc. Trop. Med. Hyg.*, **84**: 571-572.

Petersen, K.F. and Grunnet, N, 1993. Gluconeogenesis in hepatocytes determined with [2-^{13}C]acetate and quantitative ^{13}C NMR spectroscopy. *Int. J. Biochem.*, **25(1)**: 1-5.

Pethick, D.W., Lindsay, D.B., Barker, P.J. and Northrop, A.J., 1981. Acetate supply and utilization by the tissues of sheep *in vivo*. *Br. J. Nutr.*, **46**: 97-110.

Petroff, O.A.C., 1988. Biological ^{1}H NMR spectroscopy. *Comp. Biochem. Physiol.*, **90B**: 249-260.

Playford, M.C., Ooi, H.K., Oku, Y. and Kamiya, M., 1992. Secondary *Echinococcus multilocularis* infection in severe combined immunodeficient (SCID) mide: biphasic growth of the larval cyst mass. *Int. J. Parasitol.*, **22(7)**: 975-982.

Playford, M.C., Ooi, H.K., Oku, Y. and Kamiya, M., 1993. Immunology: Rodent intermediate host models for alveolar echinococcosis: biology and immunology. In: Alveolar Echinococcus of the Liver. Eds.: J. Uchino and N. Sato, Hokkaido University School of Medicine, Sapporo, Japan.

Pollesello, P., Eriksson, O., Kvam, B.J., Paoletti, S. and Saris, N-E.L., 1991. ^{1}H-NMR studies of lipid extracts of rat liver mitochondria. *Biochem. Biophys. Res. Comm.*, **179(2)**: 904-911.

Pollesello, P., Masutti, F., Croce, L.S., Toffanin, R., Eriksson, O., Paoletti, S., Hockerstedt, K. and Tiribelli, C., 1993. ^{1}H NMR spectroscopic studies of lipid extracts from human fatty liver. *Biochem. Biophys. Res. Comm.*, **192(3)**: 1217-1222.

Pollesello, P., Eriksson, O. and Hockerstedt, K., 1996. Analysis of total lipid extracts from human liver by ^{13}C and ^{1}H nuclear magnetic resonance spectroscopy. Anal. Biochem., 236: 41-48.

Prescott, L.M. and Campbell, J.W., 1965. Phosphoenolpyruvate carboxylase activity and glycogenesis in the flatworm, *Hymenolepis diminuta*. *Biochem. Physiol.*, **14**: 491-551.

Rafter, J.E.M., Bates, T.E., Bell, J.D. and Iles, R.A., 1991. Metabolites in the developing rat liver - a proton nuclear magnetic resonance spectroscopic study. *Biochim. Biophys. Acta.*, **1074**: 263-269.

Rakha, N.K., Dixon, J.B., Carter, S.D., Craig, P.S., Jenkins, P. and Folkard, S., 1991. *Echinococcus multilocularis* antigens modify accessory cell function of macrophages. *Immunol.*, **74**: 652-656.

Rausch, R.L. and Wilson, J.F., 1973. Rearing of the adult *Echinococcus multilocularis*, Leuckart, 1863, from sterile larvae from man. *Am. J. Trop. Med. Hyg.*, **22**: 357-360.

Rausch, R.L., Wilson, J.F., McMahon, B.J. and O'gorman, M.A., 1986. Consequences of continuous mebendazole therapy in alveolar hydatid disease - with a summary of a ten-year clinical trial. *Ann. Trop. Med. Parasitol.*, **80(4)**: 403-419.

Rausch, R. L., Wilson, J.F. and Schantz, P.M., 1990. A programme to reduce the risk of infection by *Echinococcus multilocularis*: the use of praziquantel to control the cestode in a village in the hyperendemic region of Alaska. *Ann. Trop. Med. Parasitol.*, **84(3)**: 239-250.

Rolin, S., Souhaili-El Amri, H., Batt, A., Levy, N., Bagrel, D., and Siest, G., 1989. Study of the *in vitro* bioactivation of albendazole in human liver microsomes and hepatoma cell lines. *Cell Biol. Toxic.*, **5(1)**: 1-14.

Rojas, C., Cadenas, S., Perez-Campo, R., Lopez-Torres, M., Pamplona, R., Prat, J. and Barja, G., 1993. Relationship between lipid peroxidation, fatty acid composition and ascorbic acid in the liver during carbohydrate and caloric restriction in mice. *Arch. Biochem. Biophys.*, **306(1)**: 59-64.

Sato, N., Aoki, S., Matsushita, M. and Uchino, J., 1993a. Clinical Features. In: Alveolar Echinococcus of the Liver. Eds.: J. Uchino and N. Sato, Hokkaido University School of Medicine, Sapporo, Japan.

Sato, N., Uchino, J. and Suzuki, K., 1993b. Chemotherapy. In: Alveolar Echinococcus of the Liver. Eds.: J. Uchino and N. Sato, Hokkaido University School of Medicine, Sapporo, Japan.

Schantz, P.M., 1993. *Echinococcus multilocularis* in North America. In: Alveolar Echinococcus of the Liver. Eds.: J. Uchino and N. Sato, Hokkaido University School of Medicine, Sapporo, Japan.

Schmidt, G.D. and Roberts, L.S., 1989. Foundations of Parasitology, 4th edition. Times Mirror/Mosby College Publishing, Missouri.

Shaka, A.J., Barker, P.B. and Freeman, R., 1985. Computer-optimized decoupling scheme for wideband applications and low-level operation. *J. Magn. Res.*, **64**: 547-552.

Sherry, A.D., Sugmei, B., Miller, B., Cottam, G.L., Gavva, S., Jones, J.G. and Malloy, C.R., 1994. Orientation-conserved transfer of symmetric Kreb's cycle intermediates in mammalian tissue. *Biochem.*, **33**: 6268-6275.

Smyth, J.D. and McManus, D.P., 1989. The physiology and biochemistry of cestodes. Cambridge University Press, New York.

Sonnewald, U., Westergaard, N., Hassel, B., Muller, T.B., Unsgard, G., Fonnum, F., Hertz, L., Schousboe, A. and Petersen, S.B., 1993. NMR spectroscopic studies of ^{13}C acetate and ^{13}C glucose metabolism in neocortical astrocytes: evidence for mitochondrial heterogeneity. *Dev. Neurosci.*, **15**: 351-358.

Sparling, M.L., Zidovetzki, R., Muller, L. and Chan, S.I., 1989. Analysis of membrane lipids by 500 MHz ^{1}H NMR. *Anal. Biochem.*, **178**: 67-76.

Stehr-Green, J.K., Stehr-Green, P.A., Schantz, P.M., Wilson, J.F. and Lanier, A., 1988. Risk factors for infection with *Echinococcus multilocularis* in Alaska. *Am. J. Trop. Med. Hyg.*, **38(2)**: 380-385.

Storandt, S.T. and Kazacos, K.R., 1993. *Echinococcus multilocularis* identified in Indiana, Ohio, and east-central Illinois. *J. Parasitol.*, **79(2)**: 301-305.

Sze, D.Y. and Jardetzky, O., 1990a. Characterization of lipid composition in stimulated human lymphocytes by ^{1}H NMR. *Biochim. Biophys. Acta*, **1054**: 198-206.

Sze, D.Y. and Jardetzky, O., 1990b. Determination of metabolite and nucleotide concentrations in proliferating lymphocytes by ^{1}H-NMR of acid extracts. *Biochim. Biophys. Acta*, **1054**: 181-197.

Tao, W., Moliski, T.F.P. and Sha'afi, R.I., 1989. Arachidonic acid release in rabbit neutrophils. *Biochem. J.*, **257**: 633-637.

Taneja, K., Gothi, R., Kumar, K., Jain, S. and Mani, R.K., 1990. Peritoneal *Echinococcus multilocularis* infection: CT appearance. *J. Comput. Assist. Tomogr.*, **14(3)**: 493-494.

Thompson, R.C.A., 1986. Biology and systematics of *Echinococcus*. In: The biology of *Echinococcus* and hydatid disease. Ed. R.C.A. Thompson. George Allen and Unwin, London, 1986, pp. 5-43.

Thompson, R.C.A., 1995. Biology and systematics of *Echinococcus*. In: *Echinococcus* and hydatid disease. Ed. R.C.A. Thompson and A.J. Lymbery. CAB International, Wallingford, U.K, pp. 1-50.

Thureen, P.J., Markewicz, M.R., Battaglia, F.C., Tjoa, S. and Fennessey, P.V., 1995. Pathways of serine and glycine metabolism in primary culture of ovine fetal hepatocytes. *Ped. Res.*, 38(5): 775-781.

Tornieporth, N.G. and Disko, R., 1994. Alveolar hydatid disease (*Echinococcus multilocularis*) - review and update. *Prog. Clin. Parasitol.*, **4**: 55-76.

Treves, S. and Ali-Khan, Z., 1984. Characterisation of the inflammatory cells in progressing tumor-like alveolar hydatid cysts: Kinetics and composition of inflammatory infiltrates. *Tropenmed. Parasitol.*, **35**, 183.

Turly, S.D. and Dietschy, J.M., 1988. The metabolism and excretion of cholesterol by the liver. In: The liver: Biology and pathobiology. Eds. I.M. Arias, W.B. Jakoby, H. Popper, D. Schachter and D.A. Shafritz, Raven Press, New York.

Uchino, J. and Sato, N, 1993. Prognosis. In: Alveolar Echinococcus of the Liver. Eds.: J. Uchino and N. Sato, Hokkaido University School of Medicine, Sapporo, Japan.

Uchino, J., Sato., N., Nakajima, Y., Matasushita, M., Takahashi, M. and Une, Y., 1993. Treatment. In: Alveolar Echinococcus of the Liver. Eds.: J. Uchino and N. Sato, Hokkaido University School of Medicine, Sapporo, Japan.

Vance, D.E. and Ridgeway, N.D., 1988. The methylation of phosphatidylethanolamine. *Prog. Lipid Res.*, **27**: 61-79.

Vance, J.E., 1990. Phospholipid synthesis in a membrane fraction associated with mitochondria. *J. Biol. Chem.*, **13**: 7248-7256.

Voet, D. and Voet, J., 1995. Biochemistry, 2nd edition. John Wiley and Sons, Inc., New York.

Vuitton, D., Bresson, H.S., Lenys, D., Flausse, F., Liance, M., Wattre, P., Miguet, J. and Capron, A., 1988. IgE dependent humoral immune response in *Echinococcus multilocularis* infection: circulating and basophil bound specific IgE against *Echinococcus* antigens in patients with alveolar echinococcosis. *Clin. Exp. Immunol.*, **78**: 67-74.

Wilson, J.F. and Rausch, R.L., 1980. Alveolar hydatid disease - a review of clinical features of *Echinococcus multilocularis* infection in Alaskan Eskimos. *Am. J. Trop. Med. Hyg.*, **29(6)**: 1340-1355.

Wilson, J.F., Rausch, R.L., McMahon, B.J. and Schantz, P.M., 1992. Parasiticidal effect of chemotherapy in alveolar hydatid disease: Review of experience with mebendazole and albendazole in Alaskan Eskimos. *Clin. Inf. Dis.*, **15**: 234-249.

Woldseth, B., Lund, A.M., Tverdal, S., Christensen, E. and Christophersen, B.O., 1995. Phospholipid molecular species with eicosapentaenoic acid (20:5(n-3)) are less stable than species with arachidonic acid (20:4(n-6)) in isolated rat liver cells. *Scand. J. Clin. Lab. Invest.*, **55**: 513-522.

Yacoe, M.E., Sommer, G. and Peehl, D., 1991. *In vitro* proton spectroscopy of normal and abnormal prostate. *Magn. Reson. Med.*, **19**: 429-438.